Re-use of laundry rinsing water by low cost adsorption technology

Re-use of Laundry Rinsing Water by low cost Adsorption Technology

Natasja Schouten

Graduation committee

Chairman	prof. dr. P.J. Lemstra	Eindhoven University of Technology
Promotor	prof. dr. ir. A.B. de Haan	Eindhoven University of Technology
Assistant promoter	dr. ir. A.G.J. van der Ham	University of Twente
Committee members	prof. dr. ir. P.J.A.M. Kerkhof	Eindhoven University of Technology
	prof. dr. ir. W.H. Rulkens	Wageningen University
	prof. dr. ir. G.L. Amy	Delft University of Technology
	dr. ing. Ph.C. van der Hoeven	Unilever Research & Development, Vlaardingen
	dr. H.A. Romijn	Eindhoven University of Technology

Re-use of Laundry Rinsing Water by low cost Adsorption Technology
N. Schouten
ISBN: 978-90-386-1494-6
A catalogue record is available from the Eindhoven University of Technology Library.

Cover design by Karen Visser

Printed by PrintPartners Ipskamp, Enschede

Re-use of Laundry Rinsing Water by low cost Adsorption Technology

PROEFSCHRIFT

ter verkrijging van de graad van doctor aan de
Technische Universiteit Eindhoven, op gezag van de
Rector Magnificus, prof.dr.ir. C.J. van Duijn, voor een
commissie aangewezen door het College voor
Promoties in het openbaar te verdedigen
op donderdag 5 februari 2009 om 16.00 uur

door

Natasja Schouten

geboren te Amsterdam

Dit proefschrift is goedgekeurd door de promotor:

prof.dr.ir. A.B. de Haan

Copromotor:
dr.ir. A.G.J. van der Ham

"In search of the answers to questions unknown,
to be part of the movement and part of the growing
part of beginning to understand"

Calypso by John Denver

Voor mijn ouders en zusje

Table of contents

Re-use of Laundry Rinsing Water by low cost Adsorption Technology

Summary

Shortage of water is a growing global problem. One way of dealing with this problem is the development of technologies for wastewater clean-up and re-use. Laundry accounts often for more than half of the daily domestic water consumption in countries like India. The major part of laundry water is rinsing water. Laundry rinsing water is relatively clean and therefore highly suitable for clean-up and re-use. The objective of this thesis is to design a rinsing water recycler (RWR) for low cost decentral recycling of laundry rinsing water. To design a RWR with an optimal performance, criteria were determined that needed to be fulfilled: removal of the main components from rinsing water, household scale, low cost, no power source needed, easy to use, portable, safe, attractive to culture, no recycling of the adsorbent and low amount of waste.

The application of adsorption technology for clean-up of laundry rinsing water offers high potential. It can be low cost, applied in small devices, no power is necessary and is therefore suitable for use on low-income household scale. The project started with the removal of the main component in laundry rinsing water, namely the anionic surfactant, linear alkyl benzene sulfonate (LAS).

Selection of the adsorbent is of main importance, because it determines the adsorption capacity and by that the operation cost of the RWR, the size of the RWR and the amount of waste. Furthermore, the adsorbent should be safe to use and safe to discharge in the environment. A selection of potential adsorbents with different surfactant adsorption mechanisms was investigated. The surface charge of adsorbents was found to be the most important parameter to obtain a high adsorption capacity. A positive surface interacts with the negative head group of LAS molecules and results in a high adsorption capacity. Non-ionic interactions, such as hydrophobic interactions between LAS and activated carbons, result in a lower adsorption capacity. Negatively charged materials do not adsorb LAS at all. The adsorbents were compared by LAS adsorption capacity and cost. Layered double hydroxide (LDH) was found to be very promising because of the high adsorption capacity and activated carbons (AC) were suitable because of their relatively low cost. Based on the type of material no safety or environmental issues are expected when both adsorbents are used and disposed.

The LAS adsorption capacity of LDH is very promising and therefore the process parameters of the LDH production (co-precipitation method) on the LDH structure, stability and LAS adsorption capacity were investigated. The highest adsorption capacity was obtained for calcinated LDH with a M^{2+}/M^{3+} ratio of 1 and 2 because of the high charge density at these ratios. LDH can be applied in a small device for re-use laundry rinsing water for short term use only. LDH aggregates are instable and the adsorption capacity of anionic surfactants reduces dramatically after prolonged use and storage in aqueous surroundings. This is probably caused by the rearrangement of the nano size crystallites of which a LDH aggregate consists. The crystallites slip past

each other and form a denser structure restricting the access of the surfactant molecules.

The RWR operating time depends on the adsorption kinetics. The LAS adsorption rate on activated carbon and LDH was investigated with the zero length column (ZLC) method. The influence of pre-treatment of the adsorbent, flow rate, particle size and initial LAS concentration on the adsorption rate were investigated. The experimental results were described with several models to determine the rate limiting step and accompanying parameters. The adsorption of LAS onto granular activated carbon (Norit GAC-1240) was well described by the selected adsorption model. The effective diffusion coefficient of LAS onto GAC-1240 is $1.3 \cdot 10^{-10} \pm 0.2 \cdot 10^{-10}$ m^2/s and does not change with particle size of GAC-1240 or initial LAS concentration. The adsorption of LAS onto LDH was not well described by the adsorption model or the ion exchange model. The LAS adsorption rate follows a first order decline. This cannot be caused by chemisorption because the adsorbent particle size influences the LAS adsorption rate. Surfactant molecules form a double layer or bilayer on oppositely charged surfaces resulting in a film layer resistance. A double layer model resulted in a good description of the experimental results for LAS adsorption onto LDH. The resistance of LAS adsorption onto LDH was found to be situated completely in the double layer outside the particle. The double layer mass transfer coefficient is $7 \cdot 10^{-5} \pm 2 \cdot 10^{-5}$ m/s.

LAS is not the only contaminant in laundry rinsing water. Other contaminates present in laundry rinsing water could influence the LAS adsorption. Sodium triphosphate (STP), sodium carbonate (Na_2CO_3) and sodium chloride (NaCl) present in laundry rinsing water were investigated for their influence on the LAS adsorption capacity and LAS adsorption rate onto GAC-1240 and LDH. There is no large effect of STP, Na_2CO_3 and NaCl on the adsorption capacity of LAS onto GAC-1240 and LDH. STP, Na_2CO_3 and NaCl increased the LAS adsorption rate onto GAC-1240. This is caused by an increase in ionic strength that enhances LAS adsorption. For LDH, NaCl increased the LAS adsorption rate also by increasing the ionic strength. Both STP and Na_2CO_3 decrease the LAS adsorption rate. CO_3^{2-} and STP compete with LAS for the adsorption onto LDH. However, in time LAS expels CO_3^{2-} and STP from the LDH structure.

The application of a suitable adsorbent in the RWR is most practical in a column operation. The main reason is the high adsorption capacity of the bed since it is in equilibrium with the influent concentration rather than the effluent concentration. Small column experiments were performed to investigate the adsorption of LAS onto GAC-1240 in a column application. The column is designed for a long term operation and therefore LDH is not investigated. The influence of flow rate, bed height, initial LAS concentration, external mass transfer and flow direction on the breakthrough curve was investigated. In parallel a mathematical model was developed that described the experimental results well. The main deviation between the model and experimental results is caused by neglecting the effect of the particle size distribution of the adsorbent. The model assumes one particle size, where in practice the adsorbent consists of particles ranging from 315 to 500 μm. The model is used to design a

column for the rinsing water recycler (RWR) to treat 25 litres of laundry rinsing water per day during an extended period. This resulted in two designs; a column (Diameter=0.06 m; Heigth=0.18 m) with a flow rate of 50 ml/min and with a flow rate of 100 ml/min. The adsorbent cost of both columns is around $12-15 per year.

Three prototypes of the RWR were developed for the clean-up of laundry rinsing water. Two prototypes consist of GAC-1240 in a column operation: the bucket-to-bucket and siphon. The third prototype, the permeable bag, is designed for short term operation and instantly cleans the laundry rinsing water during rinsing. The permeable bag was tested with a LAS solution and GAC-1240 or LDH. The amount of GAC-1240 and LDH to clean one litre of rinsing water was high, which makes the cost and amount of waste too high, therefore the permeable bag is disregarded. The two prototypes consisting of the column operation were tested with model rinsing water. Model rinsing water contains a high concentration of particulate soil that does not settle and easily clogs filters and columns. Therefore, an additional step, coagulation was introduced to remove the particulate soil. The combination of coagulation and adsorption in the RWRs is very effective in removing LAS, STP, perfumes and model soil. The bucket-to-bucket and siphon prototypes meet all the initially determined criteria and were exposed to early consumer tests.

The RWR prototypes were discussed in two consumer groups and successfully tested by four individual consumers in Phulera, Rajasthan, India. The flow rate is an important point for improvement according to the consumers. This can be improved by increasing the diameter of the column or by increasing the LAS adsorption rate by decreasing the particle size of the adsorbent. The consumers are interested in using and purchasing the prototypes because they are easy to use, small and clean the rinsing water to a satisfactory quality to reuse it for other household applications.

Hergebruik van spoelwater gebruikt voor het wassen van kleren met behulp van goedkope adsorptie technologie

Samenvatting

Tekort aan water is een wereldwijd probleem dat met de toenemende bevolkingsgroei steeds groter wordt. Een oplossing kan worden gevonden in het ontwikkelen van een technologie voor het schoonmaken van afvalwater, zodat het afvalwater kan worden hergebruikt. In India wordt meer dan de helft van de dagelijkse hoeveelheid water gebruikt voor het wassen van kleren. Het grootste gedeelte van dit water wordt gebruikt voor het uitspoelen van kleren. Het spoelwater is ongeveer 25 liter per dag en is relatief schoon, daarom is het zeer geschikt om schoon te maken en te hergebruiken. Het doel van dit proefschrift is het ontwerpen van een 'spoelwater hergebruiker' (in het Engels een 'rinsing water recycler' (RWR)). Om een zo optimaal mogelijk ontwerp te maken zijn er een aantal criteria gesteld waaraan de RWR moet voldoen. Deze criteria zijn: verwijderen van de belangrijkste componenten uit het spoelwater, kleine schaal (één huishouden), goedkoop, geen gebruik van elektriciteit, gebruikersgemakkelijk, draagbaar, veilig, aangepast aan de cultuur van de gebruiker, geen hergebruik van de adsorbentia en weinig afval.

Adsorptie heeft veel potentie als technologie voor het schoonmaken van spoelwater. Adsorbentia kunnen goedkoop worden gemaakt, adsorptie kan worden toegepast op kleine schaal en er is geen elektriciteit voor nodig. Het project is gestart met het verwijderen van de belangrijkste component in spoelwater, namelijk de anionische surfactant; lineair alkyl benzeen sulfonaat (LAS).

Het selecteren van een geschikte adsorbent is van groot belang. Er wordt gezocht naar een materiaal met een hoge adsorptie capaciteit en daarmee worden de kosten, de grootte van de RWR en de hoeveelheid afval bepaald. Verder moet het adsorbent veilig zijn in gebruik en na gebruik (als afval). Adsorbentia zijn geselecteerd op verschillende adsorptiemechanismen van de anionische surfactant. De belangrijkste parameter voor een hoge adsorptie capaciteit bleek de lading van het oppervlak. Het positief geladen oppervlak heeft een interactie met de negatief geladen kop van de LAS moleculen en dit resulteert in een bilaag van LAS moleculen en daarmee een hoge adsorptie capaciteit. Ongeladen interacties, zoals hydrofobe interacties tussen LAS staart en actieve kolen, resulteren in een lagere adsorptie capaciteit. Negatief geladen oppervlaken vertonen geen adsorptie capaciteit. De adsorptie capaciteit en kosten zijn vervolgens vergeleken en daaruit volgde dat layered double hydroxide (LDH) en actieve kolen veelbelovende adsorbentia zijn. LDH heeft een zeer hoge adsorptie capaciteit en actieve kolen zijn relatief goedkoop. Er worden geen veiligheidskwesties verwacht bij het gebruik van deze adsorbentia.

De LAS adsorptie capaciteit van LDH is zeer hoog, daarom is de LDH productie onderzocht om de LDH structuur, LAS adsorptie capaciteit en LDH stabiliteit verder te verbeteren. LDH wordt geproduceerd met de co-precipitatie methode en de invloed van verschillende procesparameters is onderzocht. De hoogste adsorptie capaciteit is

behaald voor gecalcineerde LDH met een M^{2+}/M^{3+} ratio van 1 en 2, deze ratios bevatten de hoogste ladingsdichtheid. Het toepassen van LDH in de RWR is alleen mogelijk voor korte gebruikstijden. LDH bestaat uit aggregaten die instabiel zijn in water. De aggregaten bestaan uit kristallieten en deze schuiven langs elkaar heen en vormen een dichte structuur. De surfactant moleculen kunnen niet meer doordringen in de structuur en daardoor wordt de LAS adsorptie capaciteit verlaagd.

De gebruikstijd van de RWR wordt bepaald door de LAS adsorptie snelheid. De LAS adsorptie snelheid op actieve kool en LDH is onderzocht met de 'zero length column' (ZLC) methode. De invloed van adsorbent voorbehandeling, stroomsnelheid, deeltjesgrootte en initiële LAS concentratie is onderzocht. Verschillende wiskundige modellen zijn gebruikt om de experimentele resultaten te beschrijven en om de snelheidsbepalende stap te bepalen. De adsorptie snelheid van LAS op actief kool granulaten (GAC-1240) wordt het best beschreven met het adsorptie model. De effectieve diffusie coëfficiënt is $1.3 \cdot 10^{-10} \pm 0.2 \cdot 10^{-10}$ m^2/s en wordt niet beïnvloed door de deeltjesgrootte of de initiële LAS concentratie. De adsorptie van LAS op LDH wordt niet goed beschreven door het adsorptie model of het ion uitwisselingsmodel. De experimentele resultaten volgen een eerste orde afname. Deze eerste orde afname kan niet worden veroorzaakt door chemisorptie, omdat er een invloed van deeltjesgrootte op de LAS adsorptie snelheid is gevonden. Surfactant moleculen kunnen een dubbel laag of bilaag vormen op een oppervlak met tegenovergestelde lading. Dit resulteert in een film laag weerstand. Het dubbel laag model geeft een goede beschrijving van de experimentele resultaten van LDH. De weerstand van de LAS adsorptie is volledig gesitueerd in de dubbel laag aan de buitenkant van het deeltje. De dubbel laag coëfficiënt is $7 \cdot 10^{-5} \pm 2 \cdot 10^{-5}$ m/s.

LAS is niet de enige verontreiniging in spoelwater. Andere verontreinigingen kunnen de LAS adsorptie beïnvloeden. Natrium trifosfaat (STP), natrium carbonaat (Na_2CO_3) en natrium chloride (NaCl) zijn aanwezig in spoelwater en hun invloed op de LAS adsorptie capaciteit en adsorptie snelheid is onderzocht voor GAC-1240 en LDH. Er is geen grote invloed van de verschillende componenten gevonden op de LAS adsorptie capaciteit voor GAC-1240 en LDH. De LAS adsorptie snelheid op GAC-1240 werd verhoogd door de aanwezigheid van de componenten, die de ionische sterkte van de oplossing verhogen. De LAS adsorptie snelheid op LDH werd verhoogd door de aanwezigheid van NaCl en dit werd ook veroorzaakt doordat de ionische sterkte werd verhoogd. STP en CO_3^{2-} verlagen de LAS adsorptie snelheid omdat ze met LAS concurreren voor adsorptie. Na langere tijden worden STP en CO_3^{2-} uit de LDH structuur verdreven door de LAS moleculen.

Het gebruik van de adsorbentia in de RWR is het meest praktisch als kolom operatie. Dit komt mede doordat de adsorptie capaciteit in evenwicht is met de influentconcentratie en niet met de effluentconcentratie. Experimenten met een kleine kolom zijn uitgevoerd om de adsorptie van LAS op GAC-1240 te onderzoeken. De kolom wordt ontworpen voor lange gebruikstijden en door de instabiliteit van LDH op de lange termijn wordt LDH niet meegenomen in het onderzoek. De invloed van stroomsnelheid, bed hoogte, initiële LAS concentratie, externe massaoverdracht en

stroomrichting op de doorbraakcurve werd onderzocht. Daarnaast is een wiskundig model gemaakt dat de experimentele resultaten goed beschrijft. De belangrijkste verschillen tussen het model en de experimentele resultaten werd veroorzaakt doordat de GAC-1240 een deeltjesgrootte verdeling heeft (315 tot 500 μm) in plaats van de uniforme deeltjesgrootte die het model aanneemt. Het model is gebruikt om een kolom voor de RWR te ontwerpen waarin 25 liter spoelwater per dag kan worden behandeld. Hieruit zijn twee ontwerpen geselecteerd: een kolom (Diameter=0.06 m; Hoogte=0.18 m) met een stroomsnelheid van 50 ml/min en met een stroomsnelheid van 100 ml/min. De adsorbent kosten van de kolom zijn $12-15 per jaar.

Er zijn drie RWR prototypen ontwikkeld voor het schoonmaken van het spoelwater. Twee prototypen bestaan uit een kolom met GAC-1240: een prototype bestaand uit twee emmers en een hevel prototype. Het derde prototype is een poreus zakje dat het water tijdens het spoelen schoonmaakt. Doordat deze methode een korte gebruikstijd heeft, zijn GAC-1240 en LDH onderzocht op hun toepasbaarheid. De benodigde hoeveelheid GAC-1240 en LDH om één liter spoelwater schoon te maken was dusdanig hoog dat de kosten en de hoeveelheid afval te hoog zijn. Daarom is het poreuze zakje afgewezen. De twee prototypen met de kolom zijn getest in het laboratorium met model spoelwater. Model spoelwater bestaat uit een hoge concentratie stof en kleideeltjes. Deze deeltjes bezinken niet en verstoppen de filters en de kolom. Een additionele stap is nodig om deze vaste deeltjes te verwijderen. De combinatie coagulatie en adsorptie is erg effectief in het verwijderen van LAS, STP, parfums en de vaste deeltjes. De twee prototypen voldoen aan alle gestelde criteria en worden verder getest met consumententesten in India.

In Phulera, Rajasthan, India zijn de prototypen voor discussie voorgelegd aan twee groepen met ieder acht consumenten, vervolgens hebben vier individuele consumenten de prototypen succesvol getest. Volgens de consumenten is de stroomsnelheid een belangrijk punt ter verbetering. Dit zou kunnen worden verbeterd door het vergroten van de kolom of door de LAS adsorptie snelheid te verhogen, bijvoorbeeld door het verkleinen van de adsorbent deeltjesgrootte. De consumenten zijn geïnteresseerd in het aanschaffen en gebruiken van de prototypen. De prototypen zijn gemakkelijk in gebruik, klein en maken het spoelwater zo schoon dat het goed is her te gebruiken voor andere huishoudelijke doeleinden.

1. General introduction

1.1. Background

"*Girls cannot go to school because they need to fetch water for their family*" Crown Prince of the Netherlands, Willem-Alexander van Oranje-Nassau [1]. "*For the past few weeks residents of posh Juhu area in Mumbai have been receiving such filthy yellow water in their taps that they have been forced to stock up on 20 litre bottles of mineral water every single day*." Hrithik Roshan is an award winning Bollywood actor and lives in one of the buildings receiving the filthy water [2]. "*I'm sorry, but we have to cancel the videoconference, the whole area will be evacuated because of possible violence*" Vijay Ramakrishnan calling from Hindustan Unilever in Bangalore, Karnataka, India. The possible violence is caused by the verdict of a tribunal which is set up in 1990 to decide on a century-old dispute between Tamil Nadu and Karnataka about sharing water from the Cauvery River. Both states rely on the river for their water supply [3]. The verdict: Tamil Nadu state will get 11.9 billion cubic metres of water a year and Karnataka will get only 7.6 billion cubic metres of water. Karnataka will appeal against the verdict [4].

These are just some examples found in magazines, newspapers or experienced myself from the water related problems in India. Our Dutch "Water Prince" explains: 1.2 billion people do not have sustainable access to safe drinking water and 2.6 billion people do not have access to safe sanitation. Daily 7,500 people die from water-related diseases, from which 70% are children under the age of five [1]. The UN is aware of the problem and formulated targets for improvements by 2015: the millennium development goals [5]. The seventh goal is to ensure environmental sustainability: reduce by half the proportion of people without sustainable access to safe drinking water and basic sanitation.

Although water related problems also affects famous Bollywood stars, like Hrithik Roshan [2], it is mainly a concern of the poorest of society. The UN estimates that the urban population of the less developed world is expected to nearly double in size between 2000 and 2030 from a little under 2 billion to 4 billion people. Typical incomes in the less developed world, representing a large part of the world population, are in the dollars-a-day range. Therefore, it is essential to develop low cost technologies for sustainable decentral water usage on a household scale.

The aim of this project is to develop a low cost technology for the decentral recycling of water in laundry washing. The basic idea is to clean-up the polluted rinse water to allow multiple use cycles. This means that the main components to be removed concern the added detergent ingredients and "dirt" constituents that are removed from the fabrics during rinsing. The water will be re-used for household or irrigation purposes. The idea of the project originated in India which makes it a market-pull project. Although it is devoted to India, the technology can be applied to every country facing water scarcity.

1.1.1. What is water scarcity?

"What is water scarcity?" seems to be a question with a straight forward answer. It is having too little water available and/or of poor quality. From my trips to India and talking to the local people it became clear to me that water scarcity involves much more than this. Water scarcity also means walking for many kilometres to the nearest water source and waiting for hours in long queues to obtain water. It means no time for education for children because they need to fetch water for their family. It means being confined to the tap because of the unpredictable water supply. In this case water scarcity takes a part of your freedom. In short, water scarcity is not only scarcity in terms of its volume and available quality; it also involves inconveniences associated with respect to time, money and effort to make it available [6].

1.1.2. Water usage in India

In urban areas in India water is supplied to the tap at home or in big tanks at the street corners. In small villages in rural areas water is usually obtained from large tanks at the street corners or from surface water. Water from taps or tanks is mainly municipal water and the quality is usually good for most purposes but is not always fit for drinking. In times of scarcity, water is supplied by water tankers. Many local water tankers deliver water at houses. It is often unclear where the tankers collected the water and the quality is doubtful. The tanker water is often very hard. Using hard water in laundry reduces the lifetime of fabric and using hard water for personal wash gives an unclean feeling. The price of the tanker water is controlled by the local supplier and can be ten times higher compared to municipal water [1].

Household water is mainly used for cooking, bathing and laundry. Doing laundry consumes about half of the daily amount of water. From this water, one third is used for the cleaning (washing) and two third is used for rinsing. This rinsing water is relatively clean, a large volume (around 25 dm^3 per day [7]) and therefore an interesting source for water re-use.

1.1.3. Doing laundry

Wearing clean clothes every day is a privilege that is highly appreciated. Therefore, doing laundry is an important part of a household and differs all over the world. It depends on culture, but also on the amount of water available. In India 99% of the people, mainly women, do their laundry by hand (figure 1). Washing machines are known in India (5% of the households own a washing machine [7]) but are hardly used in times of water scarcity because they consume much more water compared to hand wash [8].

Figure 1: Doing laundry in India

Hand wash usually takes place every day, depending on the size of the family. At first the clothes are soaked in a bucket of water with detergent powder. The clothes are soaked for 5 to 30 minutes depending on their dirtiness. After soaking, each cloth is scrubbed on a flat stone. A brush and detergent bar are used to scrub the stains. After being intensely scrubbed, the clothes are rinsed. Two to five buckets are filled with water and the clothes are rinsed from the first to the last bucket. It depends on the amount of water available how often the clothes are rinsed. Finally, the clothes are wrung and hanged to dry in the sun.

1.1.4. Laundry rinsing water

In a warm country like India clothes become very dirty, because of sweat, dust etc. Therefore, the water used for washing is very dirty and not suitable for re-use (figure 2A). The rinsing water is much cleaner compared to the washing water and therefore much more suitable for re-use (figure 2B and 2C). The main constituents of rinsing water are ingredients from the detergents used and dirt constituents released from clothes.

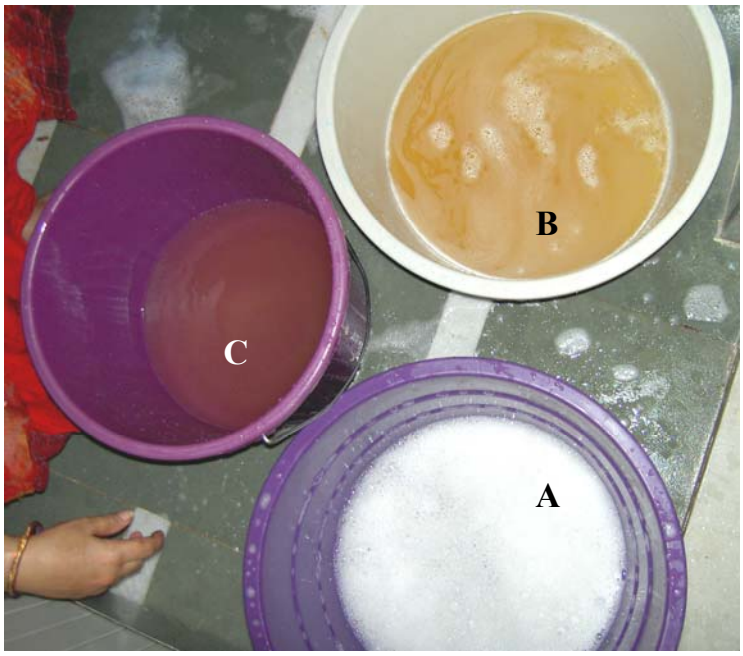

Figure 2: Laundry washing water (A), first rinse (B) and second rinse (C).

The main component of a detergent is the surfactant (table 1). Surfactants have the unique ability to remove both particulate soils and oily soils. Linear alkyl benzene sulfonate (LAS) is the main used anionic surfactant in detergents. In hard water surfactants precipitate with magnesium and calcium ions and lose their functionality. This can be prevented by complexation, precipitation or ion exchange of magnesium and calcium ions by builders. Examples of builders are phosphates (like sodium triphosphate, STP), sodium silicates and aluminosilicates (zeolites). Builders also provide alkalinity, a buffer to stabilize the pH and prevent redeposition of the removed dirt. Other additives are chemical bleaches, enzymes, fluorescing agents, perfumes, fillers (aluminium silicate), foam regulators etc. [9].

Table 1: Composition of different detergents in mass% [8]. ABS is alkyl benzene sulfonate (branched), LAS is linear alkyl benzene sulfonate and STP is sodium triphosphate (builder).

Constituents	Typical laundry bar	Hand wash powder	Machine powder	Simple liquid detergent
ABS/LAS	15-30	15-30	10-20	6-9
Non-ionics		0-3	0-5	2-4
STP	2-10	3-20	15-30	20-30
Sodium carbonate	2-10	5-10	5-15	
Aluminosilicate	0-5			
Sodium silicate	2-5	5-10	5-15	1-3
Calcite	0-20			
Aluminium sulphate	0-5			
Kaolin	0-15			
Sodium sulphate	5-20	20-50	5-15	

Dirt constituents in laundry rinsing water are mainly particulate soil and oily soil. The particulate soil, which consists of clays and other minerals, are released from clothes and end up in the laundry rinsing water. Another source of particulate soil is the laundry bar, which contains up to 20% of calcite and up to 15% of kaolin (see table 1). Oily soil in rinsing water is released from clothes and consists of grease, sebum and oils for example from cooking. Particulate and oily soils are usually removed from clothes by wetting and dispersing processes. In detergents anionic surfactants (LAS) and sodium triphosphate (STP) are responsible for these processes [9]. The rinsing water also contains some dyes. Fabrics are usually coloured with vegetable dyes that leach in the water during washing and rinsing.

1.1.5. Re-use of laundry rinsing water

Laundry washing water is usually discharged on land, in the sewer or in surface water, because it is too dirty to be used for other purposes. The cleanest part of the rinsing water (the last rinse) is often used for cleaning the floor or flushing the toilet. Irrigation with untreated laundry water is mistakenly considered safe. Wiel-Shafran et. al. (2006) [10] investigated surfactant accumulation in soil due to grey water irrigation. Grey water is waste water from laundry, kitchen and personal wash. Surfactants present in grey water adsorb onto soils and can create water-repellent soils, thereby affecting soil flow patterns and productivity. When surfactants are discharged in rivers, they can cause foaming and short term as well as long-term changes in ecosystem [11]. Therefore, it is important to remove surfactants from rinsing water. When rinsing water is cleaned it can be used for many other purposes, for example doing laundry, irrigation or cleaning.

1.2. Surfactants and surfactant removal

1.2.1. Surfactants in general

Surfactant is an acronym for surface active agent. Surfactants are characterized by the tendency to accumulate at surfaces or interfaces [12]. The reason for this behaviour can be explained by the structure of a surfactant. A surfactant is amphiphilic, they have a ‘water loving’ (hydrophilic) head and a ‘water hating’ (hydrophobic) tail (figure 3A).

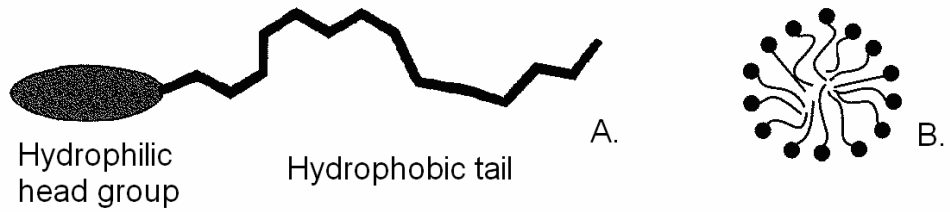

Figure 3: Schematic illustration of a surfactant molecule (A) and micelle (B) [9].

When the concentration of the surfactant molecules exceed a certain concentration, micelles will be formed (figure 3B). This concentration is known as the critical micelle concentration (CMC). The formation of micelles will decrease the contact of hydrophobic tails with water by packing the hydrophobic tails together and situate the

hydrophilic heads outwards. If surfactant molecules are dissolved in an oily solvent, the surfactant molecules create reverse micelles; the hydrophobic tails are situated outwards and the hydrophilic heads are situated inwards [9].

Surfactants can be grouped in four classes depending on the charge of the head group: anionics, non-ionics, cationics and zwitterionics. Anionic surfactants are most widely used and have a negative charge when dissolved in water. They are particularly effective in oily soil removal and soil suspension. Non-ionic surfactants do not have a charge when dissolved in water. Natural and synthetic ethoxylated fatty alcohols are usually used as non-ionic surfactants. Non-ionic surfactants are generally mixed with anionic surfactants in detergents. Cationic surfactants carry a positive charge in water. They are used in fabric softeners and create antistatic benefits. Cationics are also used in combination with non-ionics. Zwitterionics contain both a negative and a positive charge over a certain pH range. Despite their good detergency properties, these surfactants are rarely used in laundry detergents, primarily due to their high cost [9].

A rough estimation of the worldwide surfactant production is 10 million tons per year of which anionic surfactants are about 60% [9]. Anionic surfactants are popular detergent ingredients due to their low production costs because of their simple synthesis [9]. Figure 4 shows the chemical structure of the main anionic surfactants used in detergent formulations: linear alkyl benzene sulfonates (A) and α-olefinsulfonates (B).

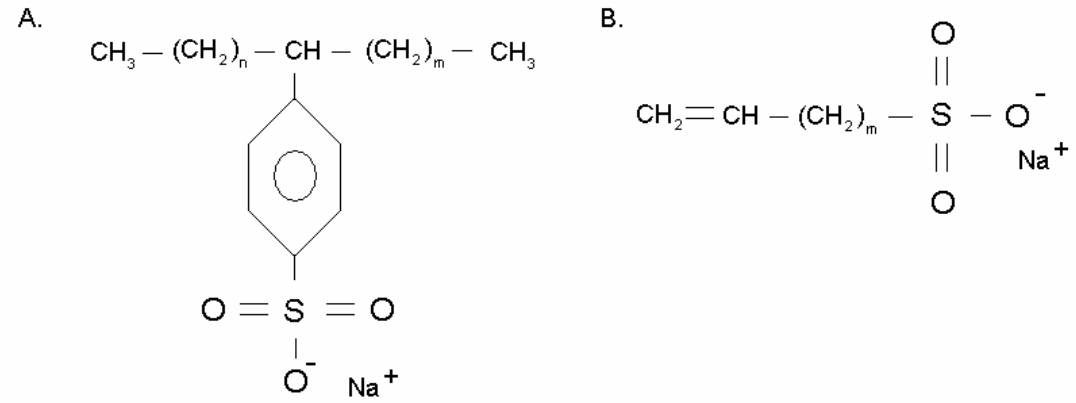

Figure 4: Linear alkyl benzene sulfonate (LAS) *n,m*: integers (*m*+*n*=7-10) (A) and α-olefinsulfonate (AOS) *m*: integers (*m*=12-14) (B).

1.2.2. Surfactant removal

The conventional methods for surfactant removal from water may involve processes such as biodegradation, membrane filtration, filtration, chemical oxidation, coagulation, photo catalytic degradation, crystallisation/precipitation, adsorption etc. [11, 13]. In this paragraph the removal of surfactants is studied, furthermore the removal of other components present in laundry rinsing water is also taken into consideration.

Biodegradation
In the environment surfactants are degraded by micro-organisms. During biodegradation, micro-organisms convert surfactants into carbon dioxide, water and oxides of other elements. Biodegradation is an important process in sewage treatment plants to remove surfactants from raw sewages. In sewage treatment plants LAS is biodegraded in 1-2 days. Branched alkyl benzene sulfonates (ABS, table 1) require months for biodegradation and when environmental aspects became an issue in the 1960s and 1970s, these surfactants were replaced by their counterparts with linear alkyl chains [9].

Ying (2006) [14] investigated the fate, behaviour and effects of surfactants and their degradation products in the environment. Aerobic degradation of LAS in river water is well documented with half times less than 3 days. LAS is biodegraded for more than 99% by natural micro-organisms in river water even at 7^{o}C. When LAS is applied on land, the half time of degradation in soil is between 9 and 33 days. LAS can influence the soil properties and therefore, direct irrigation with laundry water is discouraged [10].

The biodegradation time required for LAS in water by micro-organisms is a few days. The initial idea is to clean-up the rinsing water and re-use it directly or the next day. Furthermore, an additional technique would be necessary to remove the micro-organisms. Therefore, biodegradation is not applicable as small scale technology for the recycling of laundry rinsing water.

Membrane filtration
Membranes are increasingly used for the recovery of water from waste water [15]. Membranes offer the advantages of reducing the amount of chemicals needed and they can be applied in small scale units. The main problems in practical applications of membrane filtration are the reduction of permeate flux with time, caused by the accumulation of feed components in the pores and on the membrane surface (fouling). Membranes needs proper feed pre-treatment and a well-developed cleaning protocol because fouling can directly influence the membrane lifecycle costs [16]. Sostar-Turk et. al. (2005) [17] worked on the re-use of laundry wastewater with ultrafiltration (UF) and reverse osmosis (RO) membranes for non-potable water. They found that the presence of some oxidants like chlorine ions (from bleaches) can chemically damage polymer membranes. They propose to remove chloride with adsorption onto activated carbon or use costly ceramic membranes. Furthermore, they found that the UF membrane was not sufficient to remove the anionic surfactants, a second step, RO is needed. The economical analyses showed that the membrane filtration is still more expensive compared to methods like coagulation and adsorption. Therefore, membrane filtration will not be used as technology for the recycling of laundry rinsing water in this study.

Filtration
Filtration is not suitable to remove dissolved organic components from water, but can be very effective in removing particulate soil from water. Ahmad and El-Dessouky

(2008) [18] designed a low cost treatment system for laundry waste water consisting of sedimentation and filtration. The results showed that the process reduced the pH, turbidity, total hardness and total suspended solids (TSS) to acceptable limits and the total dissolved solids (TDS) to some extent. On the other hand, it had negligible effect on chemical oxygen demand (COD) and biological oxygen demand (BOD). These are measures for the amount of organic components present. Filtration can be used as pre-treatment to remove particulate soil, but is not suitable to remove components like dyes and surfactants.

Oxidation

Lin et. al. (1999) [19] investigated the Fenton oxidation process to degrade surfactants. Hydrogen peroxide (H_2O_2) and ferrous sulphate ($FeSO_4$) are added to water and form a strong oxidizing agent. The oxidation removed 95% of the surfactants; this is the optimum at pH 3. The pH in laundry rinsing water is around 9, so the pH should be decreased for an optimal oxidation performance. Furthermore, coagulation was used to remove the small flocks generated during the Fenton oxidation. Adding many chemicals for oxidation, pH decrease and coagulation is not preferred because the process should be absolutely safe for the consumers and dosing of chemicals is often a challenge. Therefore, oxidation does not seem promising to apply in a low cost, small scale technology for the recycling of laundry rinsing water.

Coagulation

Coagulation and flocculation are often used in industrial processes and have high efficiencies for removal of pollutants. Aboulhassan et. al. (2006) [13] investigated surfactant removal from industrial waste water with coagulation and flocculation. At the right pH level coagulation and flocculation with $FeCl_3$ can remove 99% of the surfactants. The removal of surfactants is a combination of coagulation/flocculation and adsorption onto the formed flocks. Sostar-Turk et. al. (2005) [17] investigated the coagulation of laundry waste water with $Al_2(SO_4)_3 \cdot H_2O$. They found that coagulation only was insufficient to remove dyes from water. An additional method is necessary to remove dyes as well. Therefore, coagulation can be useful but should be combined with another technique to remove all the selected components from laundry rinsing water.

Photo catalytic degradation

Zhang et. al. (2003) [20] described the photo catalytic degradation of anionic surfactants. TiO_2 is added to the surfactant solution and exposed to highly concentrated solar radiation. The technique does not seem easily applicable in low cost technology for the recycling of laundry rinsing water.

Crystallization/precipitation

Brasser (1998) [21] investigated the recycling of surfactants from laundry washing plants. Ionic surfactants are able to crystallize when the solutions are cooled below a specific temperature, known as the Krafft point. Crystals of pure surfactant can be separated by centrifugation, settling and filtration. According to Brasser (1998) [21] this process is feasible on a large scale. However, cooling small amounts of laundry

rinsing water is not a sustainable, low cost solution. Furthermore, crystallization might be difficult with many contaminants present in the rinsing water. Precipitation of anionic surfactants is widely described. Anionic surfactants can precipitate with calcium and magnesium ions. Precipitation in combination with filtration can be used to remove the anionic surfactants but fails to remove other components, like dyes from laundry rinsing water [9].

Adsorption

Adsorption technology has been applied to remove organic contaminants for many years with very good results [22]. Adsorption technology can be applied in small devices and can operate without electricity. Adsorbents can be made from waste materials and therefore can be low cost. For these reasons, adsorption technology has the potential to become a suitable technology for re-use of laundry rinsing water.

Surfactant adsorption depends on the surfactant structure and the properties of the adsorbent. If a surfactant adsorbs at a hydrophobic surface (figure 5A) interaction will take place between the surfactant tail and the surface (hydrophobic interaction). At higher surfactant concentrations the surfactant head groups will face the solution and depending on the surfactant hydrophobicity micelles are formed. At a hydrophilic surface with opposite charges the polar head is in contact with the surface and the hydrophobic tail is directed towards the solution (figure 5B). At higher concentrations, two different structures at the surface are possible. If there is a strong attraction between the surfactant head group and the surface, a monolayer is formed; the surfactant head groups are in contact with the surface and the tails are in contact with the solution. This adsorption structure will create a hydrophobic surface, which in turn will adsorb other surfactants; a surfactant bilayer is formed. If the attraction between the surfactant head group and the surface is less strong, the interactions between the hydrophobic tails is stronger and micelles are formed at the surface [9].

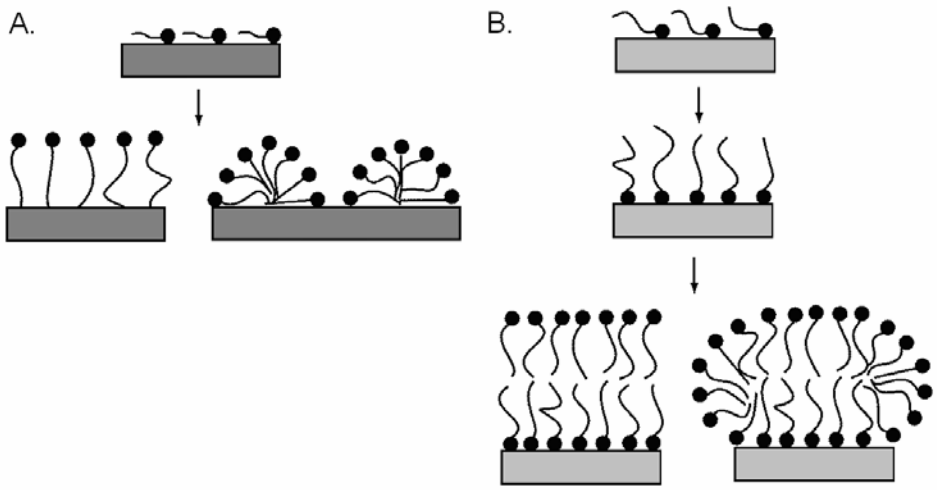

Figure 5:Adsorption of surfactants on hydrophobic surface (A) on a hydrophilic surface (B) [9].

1.3. Adsorption devices

Many small scale water technologies are developed to treat water and obtain safe drinking water. They are developed to remove micro-organisms or heavy metals (for example arsenic) from drinking water. These technologies often use adsorption for the removal of contaminants or the by-products from disinfection (figure 6). Warwick (2002) [23] described two two-bucket systems (figure 6A). In the first system the water is filtered in the top bucket with a ceramic filter and in the lower bucket the water is chlorinated. A second system contains filtration and chlorination in the top bucket and adsorption of the by-products by activated carbon in the lower bucket. In 2007 Abul Hassam won the Grainger Challenge Prize for Sustainability (1 million dollars) with the SONO filter that removes arsenic from drinking water [24]. The SONO filter consists of two buckets placed above each other, see figure 6B [25]. The top bucket contains river sand and a composite ion matrix, the lower bucket contains sand and activated carbon. The composite ion matrix adsorbs inorganic arsenic components and the activated carbon adsorbs organic arsenic components. An up-flow water filter was developed by UNICEF [26]. The system consists of two tanks, see figure 6C. In the upper tank the untreated water is stored and the lower tank contains gravel, sand, crushed charcoal and fine sand. The water in the upper tank is introduced in the bottom of the lower tank and the water flows up through the layers in the lower tank. Hindustan Unilever developed the Pure-it which combines filtration, disinfection and adsorption (figure 6D) [27]. The system is gravity driven and uses siphons to treat the water step by step. Given the success of other adsorption based small scale devices, the application of adsorption in a column operation has the potential to become a suitable technology for re-use of laundry rinsing water.

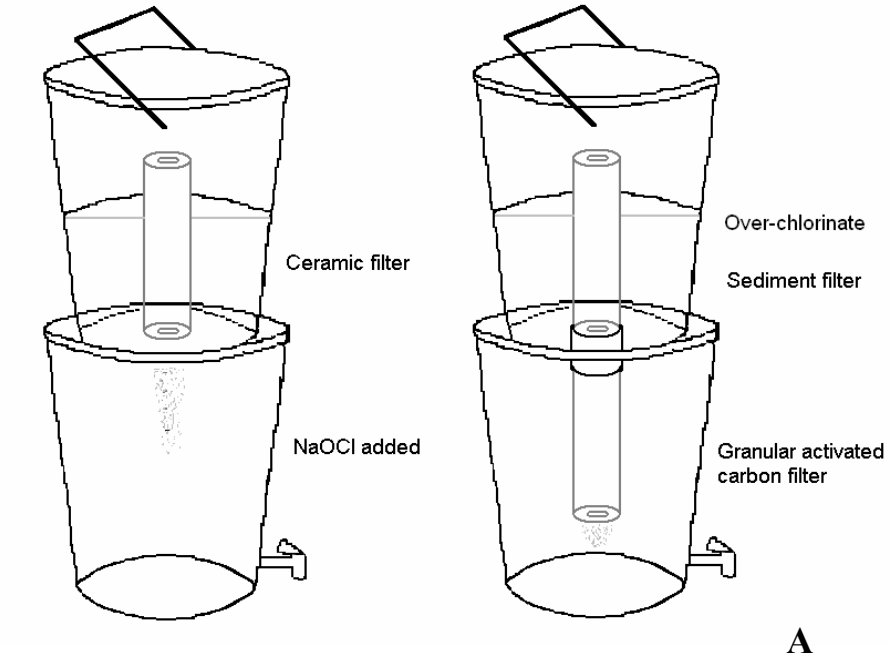

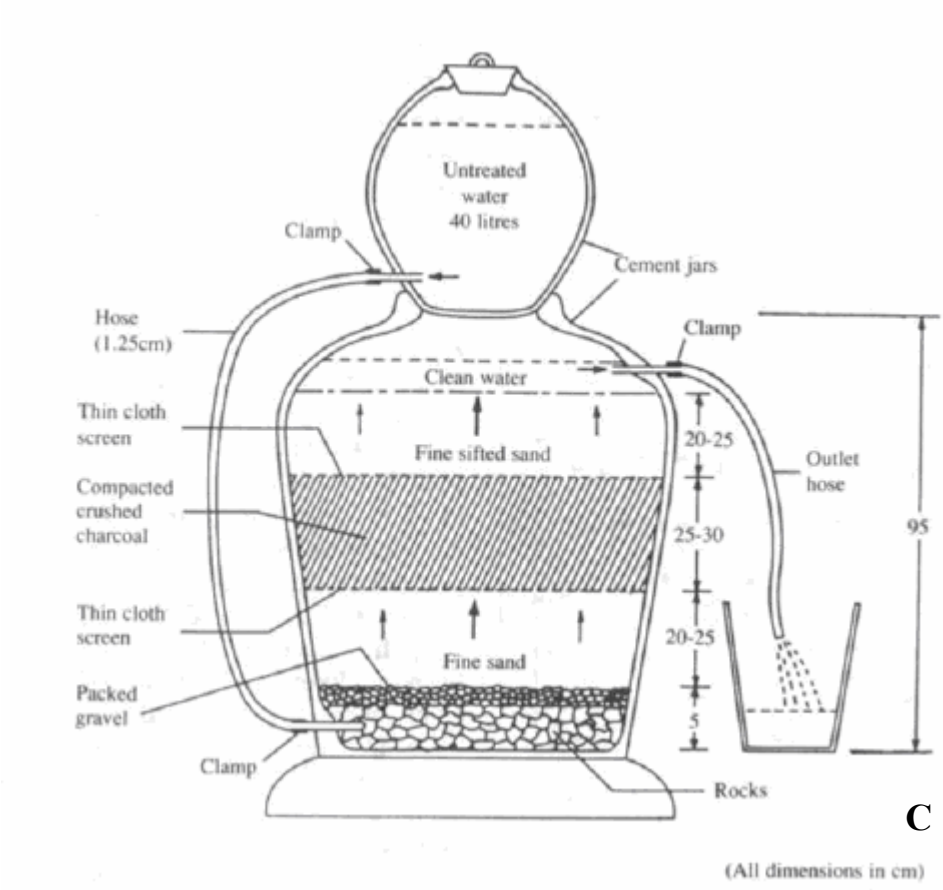

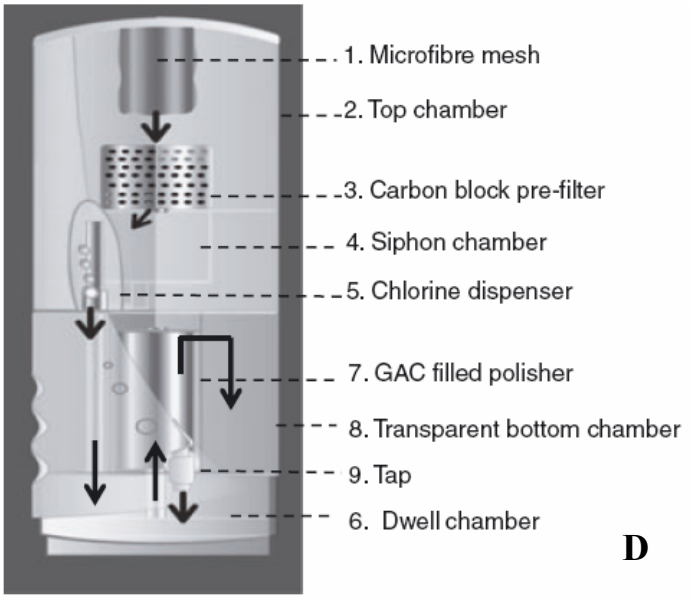

Figure 6: Small scale water filters: Two two-bucket systems [23](A), SONO water filter [25](B), Unicef up-flow water filter [26](C) and Unilever Pure-it [27](D).

1.4. Objective and outline

The objective of this project is to design a rinsing water recycler (RWR) for low cost decentral recycling of laundry rinsing water. To design a RWR with an optimal performance, the following criteria need to be fulfilled:

- removal of the main components in model rinsing water; the treated water should be suitable for doing laundry, cleaning and irrigation
- household scale; the RWR should be able to treat laundry rinsing water produced by one average household (around 25 litres per day) [7]
- low cost; the investment and operating costs for the RWR should be low compared to the local water price ($0.75-1.00 per cubic meter water) [28]
- no power requirements; in developing countries power is not always available and therefore the RWR should not depend on electricity or other power sources
- the RWR should be easy to use, easy to maintain, portable and safe
- low amount of waste; the amount of waste should be minimized
- attractive to culture and the RWR should not interfere with the consumer habits
- no recycling of the adsorbent; on a household level it seems difficult to collect the spend adsorbent and recycle it. Therefore, the adsorbent should be compatible with the environment and safely dischargeable.

Table 2 shows the components and their concentration in washing water and rinsing water. Also the maximum concentration of the components aimed for in the recycle water is included the table. The concentration of anionic surfactants in rinsing water is around 0.1 g/dm^3. To re-use the water it should be decreased to 0.01 g/dm^3. At this concentration the water will not have the ability to foam and it is safe for irrigation [29]. The particulate soil and oily soil should also be removed and may not be visible in the recycle water. The pH level is high in rinsing water and should be decreased to 7-8. The salt level (NaCl) is reasonable and can remain in the recycle water. There are many different dyes available in India and it is impossible to investigate each dye available, but the recycle water should at least be colourless.

Table 2: Concentration of different components in washing and rinsing water. The last column shows the maximum allowable concentrations of the components in the recycle water.

Components	Washing water	Rinsing water	Recycle water
Surfactants [g/dm^3]	0.3	0.1	0.01
Particulate soil [g/dm^3]	0.53	0.53	clear
Oily soil [g/dm^3]		0.06	clear
pH [-]	10.5	9.4	7-8
Salt level (NaCl) [g/dm^3]	0.1	0.1	0.1
Dyes/colour [-]	variable	variable	colourless

To reach the objective, the following chapters are included in this thesis:

- In **chapter two** a systematic selection of adsorbents for the removal of anionic surfactants is described. Different commercial adsorbents with different adsorption mechanisms were selected. The adsorption capacity/cost ratio was

determined and the adsorbents with the highest ratio were chosen for further investigation.

- In **chapter three** the adsorption of anionic surfactants on calcined layered double hydroxides (LDH) is described. LDH appeared to be a very promising material for the adsorption of anionic surfactants. The influence of the preparation of LDH on the LAS adsorption capacity and LDH stability was studied.
- **Chapter four** presents the adsorption kinetics of LAS onto activated carbon and LDH measured with the zero length column (ZLC) method. The influence of pre-treatment, flow rate, particle size and initial LAS concentration was investigated. A mathematical model was used to determine the rate controlling step and obtain the accompanying coefficient.
- The influence of other contaminants present in rinsing water on the adsorption of LAS is investigated in **chapter five**. The LAS adsorption capacity and adsorption kinetics were determined with equilibrium experiments and with the ZLC method, respectively.
- In **chapter six** the adsorption of LAS onto activated carbon in a small column operation is described. The influence of flow rate, bed height, initial LAS concentration, external mass transfer and flow direction was investigated. The experimental results were simulated with a mathematical model and the model was used to scale up the process to determine the dimensions of the column needed in the RWR prototypes.
- In **chapter seven** the RWR prototypes were constructed according to the stated criteria. The prototypes were tested with model laundry rinsing water and the design was improved until all the criteria were met. The final RWR prototypes were tested with consumers in India. The consumers were asked for their feedback and suggestions for improvement.
- **Chapter eight** presents the conclusions of this work and an outlook is presented for further development of the RWR.

1.5. References

1. Joosten, C., *"Bij ons gaan de jasjes uit, de mouwen omhoog"*, in *Elsevier*. December 2007. p. 115-118.
2. Phadke, V., *And you thought only you get dirty, smelly water!*, in *Metronow*. 2 February 2008.
3. http://www.american.edu/ted/ice/CAUVERY.HTM, 25 June 2008.
4. http://news.bbc.co.uk/1/hi/world/south_asia/6333907.stm, *BBC news*. 6 February 2007.
5. UnitedNations, *Water for People Water for Live. World Water Development Report. UNESCO WWAP*. 2003, United Nations.
6. Unilever, *Personal communication*. January/February 2008: Unilever Research India, 165/166, Backbay Reclamation, Mumbai - 400020, India.
7. Unilever, *Personal communication*. December 2004: Hindustan Unilever Research India, 64 Main Road, Whitefield P.O. Bangalore 560066, India.

8. Ho Tan Tai, L., *Formulating detergents and personal care products*. 1st ed. 2000, New York, USA: AOCS Press.
9. Holmberg, K., et al., *Surfactants and polymers in aqueous solution*. 2nd ed. 2003, West Sussex, UK: Wiley.
10. Wiel-Shafran, A., et al., *Potential changes in soil properties following irrigation with surfactant-rich grey water.* Ecological Engineering, 2006. **26**(4): p. 348-354.
11. Adak, A., M. Bandyopadhyay, and A. Pal, *Removal of anionic surfactant from wastewater by alumina: a case study.* Colloids and Surfaces A: Physicochemical and Engineering Aspects, 2005. **254**(1-3): p. 165-171.
12. Torn, L.H., *Polymers and Surfactants in Solution and at Interfaces*. 2000, Thesis Wageningen University: Wageningen, The Netherlands.
13. Ahboulhassan, M.A., et al., *Removal of surfactant from industrial wastewaters by coagulation flocculation process.* International journal of environmental Science and Technology, 2006. **3**(4): p. 327-332.
14. Ying, G.G., *Fate, behaviour and effects of surfactants and their degradation products in the environment.* Environment International, 2006. **32**: p. 417-431.
15. Kowalska, I., *Surfactant removal from water solutions by means of ultrafiltration and ion-exchange.* Desalination, 2008. **221**(1-3): p. 351-357.
16. Mulder, M., *Basic principles of membrane technology*. 2nd ed. 1996, Dordrecht, The Netherlands: Kluwer Acedemic Publishers.
17. Sostar-Turk, S., I. Petrinic, and M. Simonic, *Laundry wastewater treatment using coagulation and membrane filtration.* Resources, Conservation and Recycling, 2005. **44**(2): p. 185.
18. Ahmad, J. and H. El-Dessouky, *Design of a modified low cost treatment system for the recycling and reuse of laundry waste water.* Resources, Conservation and Recycling, 2008. **52**(7): p. 973-978.
19. Lin, S.H., C.M. Lin, and H.G. Leu, *Operating characteristics and kinetic studies of surfactant wastewater treatment by Fenton oxidation.* Water Research, 1999. **33**(7): p. 1735-1741.
20. Zhang, T., et al., *Photocatalytic decomposition of the sodium dodecylbenzene sulfonate surfactant in aqueous titania suspensions exposed to highly concentrated solar radiation and effects of additives.* Applied Catalysis B: Environmental, 2003. **42**(1): p. 13-24.
21. Brasser, P., *Recycling of surfactants from wastewater of laundry washing plants*. 1998, Thesis Technical University Delft: Delft, The Netherlands.
22. Sontheimer, H., J.C. Crittenden, and R.S. Summers, *Activated carbon for water treatment*. 2nd ed. 1988, Karlsruhe, Germany: DVGW-Forschungsstelle.
23. Warwick, T.P., *Does point of use for the developing world really work?* Water Conditioning & Purification, 2002: p. 66-69.
24. http://pubs.acs.org/subscribe/journals/esthag-w/2007/mar/tech/rc_hussam.html, July 2008.
25. Schroeder, D.M., *Field experience with SONO filters.* https://www.dwc-water.com/fileadmin/images/PDF_files/SIM_Reports.pdf, 2007.
26. Singh, V.P. and M. Chaudhuri, *A performance evaluation and modification of the UNICEF upward flow water filter.* Waterlines, 1993. **12**(2): p. 29-31.

27. Clasen, T., S. Nadakatti, and S. Menon, *Microbiological performance of a water treatment unit designed for household use in developing countries.* Tropical Medicine and International Health, 2006. **11**(9): p. 1399.
28. Phulera, *Personal communication: Local water prices in Phulera, Rajasthan, India.* January/February 2008.
29. http://www.lasinfo.org/w_las_nut.html, July 2008.

2. Selection and evaluation of adsorbent for the removal of anionic surfactants form laundry rinsing water

Abstract

Low-cost adsorbents were tested to remove anionic surfactants from laundry rinsing water to allow re-use of water. Adsorbents were selected corresponding to the different surfactant adsorption mechanisms. Equilibrium adsorption studies of linear alkyl benzene sulfonate (LAS) show that ionic interaction results in a high maximum adsorption capacity on positively charged adsorbents of 0.6 to 1.7 g_{LAS}/g. Non-ionic interactions, such as hydrophobic interactions of LAS with non-ionic resins or activated carbons, result in a lower adsorption capacity of 0.02 to 0.6 g_{LAS}/g. Negatively charged materials, such as cation exchange resins or bentonite clay, have negligible adsorption capacities for LAS. Similar results are obtained for alpha olefin sulfonate (AOS). Cost comparison of different adsorbents shows that an inorganic anion exchange material (layered double hydroxide) and activated carbons are the most cost effective materials in terms of the amount of surfactant adsorbed per dollar worth of adsorbent.

2.1. Introduction

The UN estimates that between 2000 and 2030 the urban population of developing countries will nearly double in size from 2 billion to about 4 billion people. This population growth will dramatically intensify the economic and physical water scarcity already existing in developing countries [1]. One way of dealing with this increasing water scarcity is the development of technologies for wastewater clean-up and re-use. However, in large parts of the developing world, incomes are only around one US dollar a day. Therefore, water re-use technologies can only be successfully implemented if they are low-cost. A promising source of water for re-use is rinsing water from laundry washing. In countries such as India, many families do their laundry by hand. Laundry accounts for half of the daily domestic water consumption. Cleaning up the main wash liquor would pose a major challenge. However, the major part of laundry water is rinsing water, which is relatively clean in comparison. Rinsing water is highly suitable for clean-up and re-use.

The current work is part of a project that aims to develop low-cost technologies for the local decentralised recycling of laundry rinsing water. The basic idea is to clean up the polluted rinse water to allow multiple use cycles. When the main contaminants from the rinsing water have been removed, it can be re-used for household or irrigation purposes. Main contaminants are the added detergent ingredients and "dirt" released from the fabrics during rinsing. The focus of the current chapter is on removing anionic surfactants, as the main active component of detergents used in low income markets. Typically, hand wash detergent powders contain 15 to 30% anionic surfactants [2]. A rough estimate of worldwide surfactant production is 10 million tonnes per year of which anionic surfactants account for about 60%. Anionic surfactants are popular detergent ingredients, because of their straightforward synthesis and consequently low production costs [3].

The conventional methods for surfactant removal from water involve processes such as chemical and electrochemical oxidation, membrane technology, chemical precipitation, photo-catalytic degradation, adsorption and various biological methods [3, 4]. Many of these processes are not cost effective and/or not suitable for application on household scale. Adsorption technology can be low-cost and can be applied in small devices. It is offers therefore potential for use on household scale, also in low-income households. The re-use of the spent adsorbent is not considered in this project. We propose to use an environmentally harmless low cost absorbent that can be discarded or burnt as low volume domestic waste.

Adsorbents are "low-cost" when they require little processing and are abundant, either in nature, or as a by-product or waste material from another industry [5-7]. Anionic surfactant adsorption from water has been studied extensively. Many adsorbent materials have been investigated, for example alumina [4], zeolites [8, 9], sediment [10], bentonite [11], sand [12], sludge [13], silica gel [14], resins [15], activated carbons [16-20] and waste tyre rubber [16]. However, few studies [14, 20] compare a range of materials. This chapter describes the results of adsorption equilibrium studies on a range of materials with different adsorption mechanisms. This resulted in a better

understanding of the adsorption mechanisms of anionic surfactants and enabled identification of the most suitable materials.

The objective of this study is to find the most suitable adsorbents for anionic surfactants by studying adsorbents with different surfactant adsorption mechanisms. Equilibrium adsorption experiments were carried out with two anionic surfactants, which are most frequently used in low cost detergents, i.e. linear alkyl benzene, sulfonate (LAS) and α-olefinsulfonate (AOS). The properties of the adsorbents were characterised in terms of pore volume, surface area and pore size distribution and these properties were correlated to the surfactant adsorption capacity. The chapter concludes with a comparison between the amount of LAS adsorbed and the cost of the material for the selected adsorbents.

2.2. Adsorbent Selection

The basic idea is to pack the adsorbent in a small device for domestic use in a hand wash environment. The adsorbent should therefore satisfy certain performance criteria and should be low in cost. The criterion for an adsorbent selection is a high adsorption capacity at surfactant concentrations of 0.1 to 0.3 g/dm^3 water, typically found in rinsing water [21]. The main mechanisms of surfactant adsorption are [22]:

- ion exchange
- ion pairing
- hydrophobic interactions
- aromatic interactions
- adsorption by dispersion (Van der Waals) forces

Among these mechanisms, Van der Waals forces are the weakest interactions and are therefore not further considered. A number of commercial adsorbents with the remaining interaction forces were selected and are listed in table 1.

Table 1: Characterization of the adsorbents. BET surface area, pore volume and average pore size are measured using the Micromeritics Tristar 3000. The total pore volume is measured at a relative pressure of 0.99. BET and pore size data marked with * are obtained from suppliers and ** indicates: unable to measure, because Amberlite IRA-410 is a gel. Resins are obtained from Fluka. I.E. cap. is ion exchange capacity.

Resins	Functional group	Matrix	BET Surface area [m^2/g]	Pore volume [cm^3/g] at p/p_0=0.99	Average Pore size [nm]	Cost [$/kg]	I.E. cap. [meq/g] dry [meq/ml] wet
Amberlite XAD-4	none	polystyrene	719 800*	1.04	5.8 5.0*	30	-
Amberlite XAD-16	none	polystyrene	814 >800*	1.45	7.1 10.0*	23	-
Amberlyst A21	tertiary amine	polystyrene	33 25*	0.17	20.1	15	4.8 1.3
Amberlite IRA-900	trimethyl amine	styrene-divinyl benzene (DVB)	20	0.18	37.2	16	4.2 1.0
Amberlite IRA-410	dimethyl ethanol amine	styrene-DVB	**	**	**	12	3.4 1.4
Amberlite-200	sulfonic acid	styrene-DVB	41	0.29	28.7	11	4.3 1.75
Activated carbons	Raw material	Activation method	BET Surface area [m^2/g]	Pore volume [cm^3/g] at p/p_0=0.99	Average pore size [nm]	Cost [$/kg]	Supplier
PK1-3	peat	steam	827 875*	0.55	2.7	3.0	Norit
SAE2	peat/wood	steam	928 875*	0.67	2.9	2.0	Norit
SAE Super	peat/wood	steam	1363 1300*	0.88	2.6	2.1	Norit
C Gran	wood	phosphoric acid	1423 1400*	1.06	3.0	3.7	Norit
Haycarb GAC	coconut	steam	1270	0.58	1.8	1.5	Haycarb
Bagasse fly ash	bagasse	hydrogen peroxide	106	0.06	2.4		[23]
Inorganic materials	Cation/anion exchanger	Activation method	BET Surface area [m^2/g]	Pore volume [cm^3/g] at p/p_0=0.99	Average pore size [nm]	Cost [$/kg]	Supplier
Bentonite	cation	-	81	0.09	4.7		Unilever
Bentonite	cation	H_2SO_4	294	0.50	6.9		This work
LDH	anion	450 ^oC for 4.5 hours	200	0.79	15.9	6.0	This work
Syntal HSA 696	anion	450 ^oC for 4.5 hours	222	0.52	9.3	6.0	Süd Chemie

To understand the influence of surface charge, cation and anion exchange materials were tested. We selected resin Amberlite-200, because of its high cation exchange adsorption capacity. Two anion exchange resins are selected, Amberlite IRA-900 and IRA-410, because the dimethylethanolamine functionally of IRA-410 has a slightly lower basicity than the trimethylamine functionality of IRA-900. Furthermore, the IRA-900 has a macro reticular structure whereas IRA-410 has a gel structure. These resins are strong ion exchangers. Also a weak anion exchanger was selected in order to understand the interaction of LAS with the tertiary ammonium groups of the resin Amberlyst A21. A common natural cation exchanger is bentonite [24]. According to Ozcan and Ozcan (2004) [25] the specific surface area and surface acidity can be easily and significantly increased by acid activation and therefore both, natural bentonite and acid activated bentonite were investigated. Another inorganic anion exchanger is layered double hydroxide (LDH). LDH can be easily synthesised at relatively low-cost [26]. The most common LDH is hydrotalcite with the chemical formula: $[Mg_6^{2+}\ Al_2^{3+}(OH)_{16}]\ (CO_3^{2-})_3 \cdot 4H_2O$. LDHs consist of two brucite like layers that become positively charged when a magnesium cation is replaced by an aluminium cation. In order to balance the residual charge, anions that can be exchanged by other anions are intercalated between the layers [26]. Two types of LDHs were tested: LDH synthesised on laboratory scale (LDH) and a commercially available LDH (Syntal).

Hydrophobic interactions are tested with XAD resins and activated carbons. They can take place when the LAS alkyl chain interacts with a hydrophobic surface. Additional interactions can take place between the LAS aromatic group and aromatic groups of the XAD matrix or activated carbon. Two different XAD resins are tested: XAD-4 and XAD-16. XAD-16 has larger pores, a larger pore volume and a higher surface area. Three commercially available activated carbons are selected: Norit PK1-3, Norit SAE2 and Norit SAE Super. PK 1-3 is made from peat and the SAEs are made from peat or wood. These carbons were all steam-activated. Also activated carbon produced locally from waste materials were studied as they can be assumed to be very low-cost materials. An activated carbon produced from bagasse fly ash was provided by Gupta [23]. An activated carbon obtained locally is granular activated carbon (GAC) provided by Haycarb, Sri Lanka. This carbon has a large surface area, mainly composed of micro pores. Finally, to study the influence of pore size and activation method, Norit C Gran a phosphoric acid activated carbon with meso pores was selected.

2.3. Materials and methods

2.3.1. Materials

Anionic surfactants, linear alkyl benzene sulfonate (LAS) and alpha olefin sulfonate (AOS), were obtained from Unilever R&D, Vlaardingen, The Netherlands. Purity is around 92 wt% for both surfactants. The chain length of LAS is C10 to C13 (equally distributed; average molecular weight of LAS-acid is 312 g/mol) and the AOS chain length is C14 and C16 (equally distributed; average molecular weight of AOS-acid is 286 g/mol). AOS is a mixture of ± 65% alkene sulfonate and 35% 3-hydroxyalkane

sulfonate (or 4-hydroxyalkane sulfonate). The critical micelle concentrations (CMC) are respectively 2 mM [27] and 8 mM [28] for LAS and AOS.

All adsorbents listed in table 1 were commercially obtained, except for the LDH, which is synthesised on laboratory scale. Magnesium nitrate ($Mg(NO_3)_2 \cdot 6H_2O$), aluminium nitrate ($Al(NO_3)_2 \cdot 9H_2O$), sodium carbonate (Na_2CO_3) and sodium hydroxide (NaOH) are analytically pure reagents and obtained from Boom (Meppel, The Netherlands), Merck (Darmstadt, Germany) and Sigma-Aldrich (Steinheim, Germany).

2.3.2. Methods

LDH was produced as described by Reichle (1986) [29]. A solution of 43 gram $Mg(NO_3)_2 \cdot 6H_2O$ and 32 gram $Al(NO_3)_3 \cdot 9H_2O$ in 100 ml Milli-Q water was added to a second solution of 18.6 gram NaOH and 11 gram Na_2CO_3 in 100 ml Milli-Q water. Both solutions were pumped at a rate of 10 ml/min in a beaker and mixed with a magnetic stirrer. During dosing the precipitation starts immediately. At the end of the dosing the precipitate formed was allowed to age overnight at 60^oC under continues stirring. The aged precipitate was filtered with a Buchner funnel and washed 10 times with each time 100 ml of fresh Milli-Q water in a centrifuge. The final product was dried overnight at 105^oC and calcined at 450^oC for 4.5 hours.

The specific surface area, pore size and pore volume distribution were measured using nitrogen adsorption at -196^oC (liquid nitrogen temperature) with the Micromeritics Tristar 3000. The samples were pre-treated overnight to remove water and other contaminants from the pores. During the pre-treatment, a nitrogen flow was applied and the samples were heated. Resins were heated to 70^oC for 16 hours, activated carbons were heated to 250^oC for 6 hours and Syntal and LDH were heated to 105^oC for 16 hours. The measured physical properties are listed in table 1.

The adsorption experiments were conducted at different initial surfactant concentrations ranging from 0.1 to 3 g/dm^3 water. Surfactants were dissolved in milli-Q water. 0.1 gram of adsorbent and 80 ml of surfactant solution were mixed in a screw capped flask and placed in a shaking bath (Julabo SW22) at 25^oC. Initially experiments were carried out to determine the minimum time required to attain equilibrium for each adsorbent. From these experiments, it appeared that between 0.1 and 30 hours equilibrium was reached for all adsorbents. To be absolutely certain that equilibrium was reached 48 hours equilibrium time was used in all further experiments. The water phase was sampled with a syringe equipped with a filter to remove suspended solids (Spartan 30/0.45RC (0.45μm)) and the surfactant concentration was measured by spectrophotometry at 223 nm (Shimadzu UV-1650PC) (accuracy correlation curve: 2%). AOS was determined by TOC (Shimadzu TOC-VPH) (accuracy correlation curve: 2%).

2.4. Results and discussion

2.4.1. Data correlation

The obtained data are correlated with the well-known Langmuir model (equation 1):

$$q = \frac{q_m bC}{1 + bC} \qquad (1)$$

where q is the adsorbent capacity at equilibrium concentration C, q_m is the maximum adsorption capacity, and b is a measure of the adsorbate affinity for the surface and accessibility of the surface.

Estimated model parameters for both LAS and AOS adsorption are listed in table 2. Also the adsorption capacity at a surfactant concentration of 0.1 g/dm^3 water is shown, since this concentration of LAS is expected to be at least present in rinsing water [21]. This concentration is well below the CMC value of LAS (2mM ≈ 0.6 g_{LAS}/dm^3) and therefore it is assumed monomer adsorption will take place. At concentrations above 0.6 g_{LAS}/dm^3 micelles will exist next to the LAS monomer. It is expected that at equilibrium concentrations above the CMC the adsorption capacity will approach a constant value because the free monomer concentration becomes approximately constant. This can be assumed because the equilibrium between the micelles and monomers is very rapid. The experimental data together with the correlated isotherms are shown in figures 1, 2, 4 and 5.

Table 2: Parameters obtained from correlation with Langmuir isotherm model for LAS and AOS adsorption.

LAS Adsorption	q_m [g_{LAS}/g]	b [dm^3/g]	R^2 [-]	q at C=0.1 g/dm^3 [g_{LAS}/g]
Resins				
Amberlite XAD-4	0.59	6	0.977	0.22
Amberlite XAD-16	0.94	2.3	0.991	0.18
Amberlyst A21	0.42	18	0.973	0.27
Amberlite IRA-900	1.21	55	0.911	1.02
Amberlite IRA-410	0.67	1156	0.834	0.66
Activated carbon				
Norit PK1-3	0.15	42	0.995	0.12
Norit SAE2	0.3	336	0.864	0.29
Norit SAE Super	0.32	71	0.929	0.28
Norit C Gran	0.53	2.7	0.908	0.11
Haycarb GAC	0.15	1043	0.936	0.15
Bagasse fly ash	0.027	11	0.963	0.01
Clays				
LDH	1.81	13	0.978	1.02
Syntal HSA 696	1.74	34	0.938	1.34
AOS Adsorption	q_m [g_{AOS}/g]	b [dm^3/g]	R^2 [-]	q at C=0.1 g/dm^3 [g_{AOS}/g]
Resins				
Amberlite XAD-16	0.69	2.1	0.992	0.12
Amberlite IRA-900	1.09	55	0.919	0.92
Activated carbon				
Norit SAE Super	0.40	29	0.927	0.30
Haycarb GAC	0.13	28	0.975	0.10
Clays				
LDH	0.98	24	0.997	0.69
Syntal HSA 696	1.24	93	0.847	1.12

For most adsorbents, the Langmuir model gives an acceptable description of the experimental data, as can be seen from the correlation coefficients (R^2). Although we know that when surfactant adsorption occurs on oppositely charged surfaces it is common to plot the isotherm data on a log-log scale so that a typical four-region isotherm can be observed [9, 30]. At the measured concentrations, the second, third and fourth region can be distinguished. We did not measure at concentrations where the first region can be seen, because the concentrations are too low to be interesting for this application. The Langmuir model was selected because of its simplicity, easy incorporation in future design models and previously demonstrated ability to describe surfactant adsorption [9, 14, 15, 18]. The correlation results listed in table 2 are described in more detail during the discussion of the adsorbents in the paragraphs below.

2.4.2. Equilibrium experiments using LAS

The adsorption isotherms of LAS on the different types of resins are shown in figure 1. Three groups of isotherms can be distinguished. Firstly, the cation exchanger Amberlite-200 shows a negligible adsorption capacity. It is clear that negatively charged functional groups have no interaction or might even repel the anionic surfactant molecules. Secondly, XAD-4 and XAD-16 are characterized by non-ionic interactions, like hydrophobic and aromatic interactions. The alkyl chain and the benzene group of LAS can interact with aromatic sites on the carbon chains in the XAD polystyrene matrix. This results in higher adsorption capacities compared to Amberlite-200. The maximum adsorption capacity of XAD-16 is higher than for XAD-4. Because XAD-16 has a larger internal surface area, a larger internal volume and a larger pore size compared to XAD-4. Amberlyst A21 is also an anion exchange resin, but at neutral pH adsorption is characterized by non-ionic interactions. At neutral pH, the tertiary amine groups of this weak anion exchanger are uncharged. The experiments took place at neutral pH and consequently adsorption capacities are similar to those of the XAD resins. These non-ionic interactions result in maximum capacities between 0.4 and 0.9 g_{LAS}/g. The interactions are not strong and therefore, the slopes of the isotherms are shallow and the affinity coefficient *b* in table 2 is low. The adsorption capacity for all three resins is rather low around 0.2-0.3 g_{LAS}/g at equilibrium concentration $0.1 g_{LAS}/dm^3$.

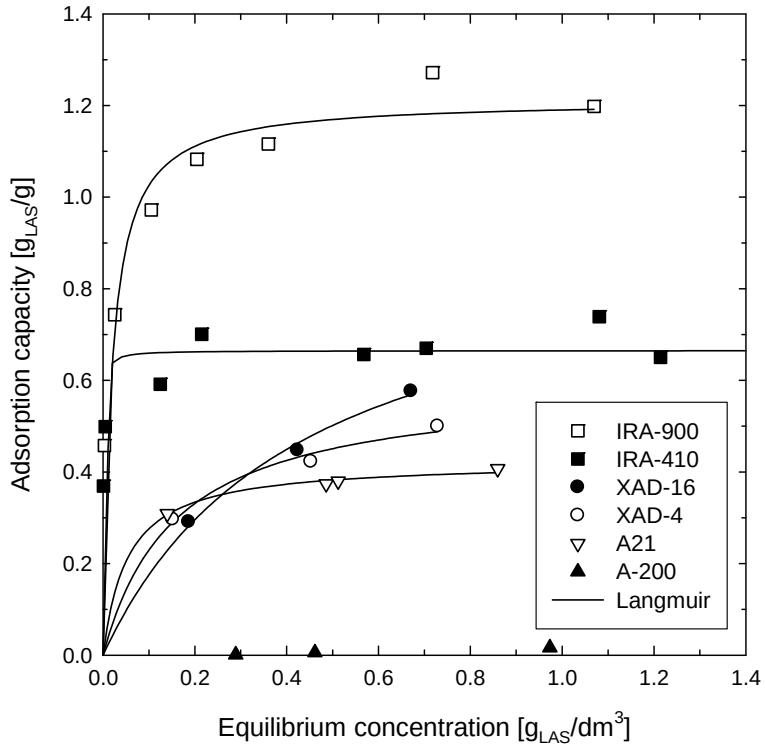

Figure 1: Adsorption isotherms for LAS and different types of resins. The obtained Langmuir parameters are shown in table 2.

Thirdly, figure 1 shows that the anion exchangers IRA-900 and IRA-410 have the highest adsorption capacities of 1.0 g_{LAS}/g and 0.66 g_{LAS}/g, respectively, at equilibrium concentration 0.1 g_{LAS}/dm^3. The anionic surfactant head will probably adsorb onto the

cationic charged surface. This strong interaction results in a steep slope (high values of *b*) of the isotherm and the maximum adsorption capacity is obtained at the CMC. The maximum adsorption capacity of IRA-900 is 3.7 $mmol_{LAS}/g$ dry resin, which is close to the specified ion exchange capacity of 4.2 meq/g dry resin. This indicates that most functional groups are occupied by the anionic surfactant. The maximum adsorption capacity of IRA-410 is 2.1 $mmol_{LAS}/g$ dry resin, which differs more from the specified ion exchange capacity of 3.4 meq/g dry resin. The observed difference in adsorption capacity for IRA-410 can be explained by the lower basicity of the dimethylethanolamine functionality compared to trimethylamine functionality of the IRA-900. Additionally, the difference can be due to differences in the matrix structure. The IRA-410 resin has a gel structure. The diffusion of LAS molecules through a gel structure is more difficult than diffusion through the macro reticular structure of the IRA-900 resin.

Three groups of adsorption isotherms can be distinguished in figure 1, highlighting the importance of surface charge. The negatively charged (Amberlite 200) shows hardly any adsorption capacity. The uncharged resins (XADs and A21) show a much lower maximum adsorption capacity compared to the positively charged resins. The positively charged resins (IRA-900 and IRA-410) show high capacities even at low concentrations (0.1-0.3 g_{LAS}/dm^3).

Figure 2 shows the adsorption capacity of LAS for different types of activated carbons at equilibrium concentrations. The most important adsorption interactions between LAS and activated carbon are hydrophobic/aromatic interactions and, depending on the pH and charge of the surface, ion paring interactions. The maximum adsorption capacity of the activated carbons ranges from 0.02 to 0.5 g_{LAS}/g carbon (table 2).

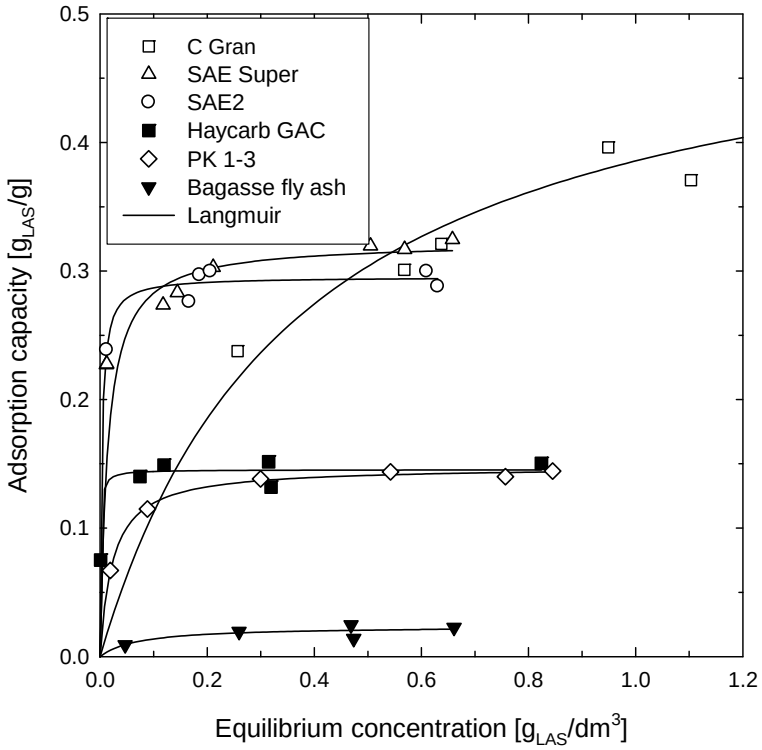

Figure 2: Adsorption isotherm of LAS and activated carbons. The obtained Langmuir parameters are shown in table 2.

Norit SAE 2 and SAE Super both show a maximum adsorption capacity (q_m) around 0.3 g_{LAS}/g. Norit PK 1-3 has a lower maximum adsorption capacity of approximately 0.15 g_{LAS}/g. An explanation might be found in surface area and pore size distribution. Figure 3 shows the amount of surface area of activated carbons in three pore diameter ranges. When the capacities in figure 2 and surface areas in figure 3 are compared, a qualitative relation is found between the maximum LAS adsorption capacity and the amount of surface area, but only when the pore diameter is larger than 2 nm. Above this pore size the maximum adsorption capacity increases when the amount of surface area increases. Apparently, LAS molecules cannot easily enter pores with a diameter smaller than 2 nm, since the diameter of a LAS molecule is around 1.3 nm (calculated from the molecular geometry).

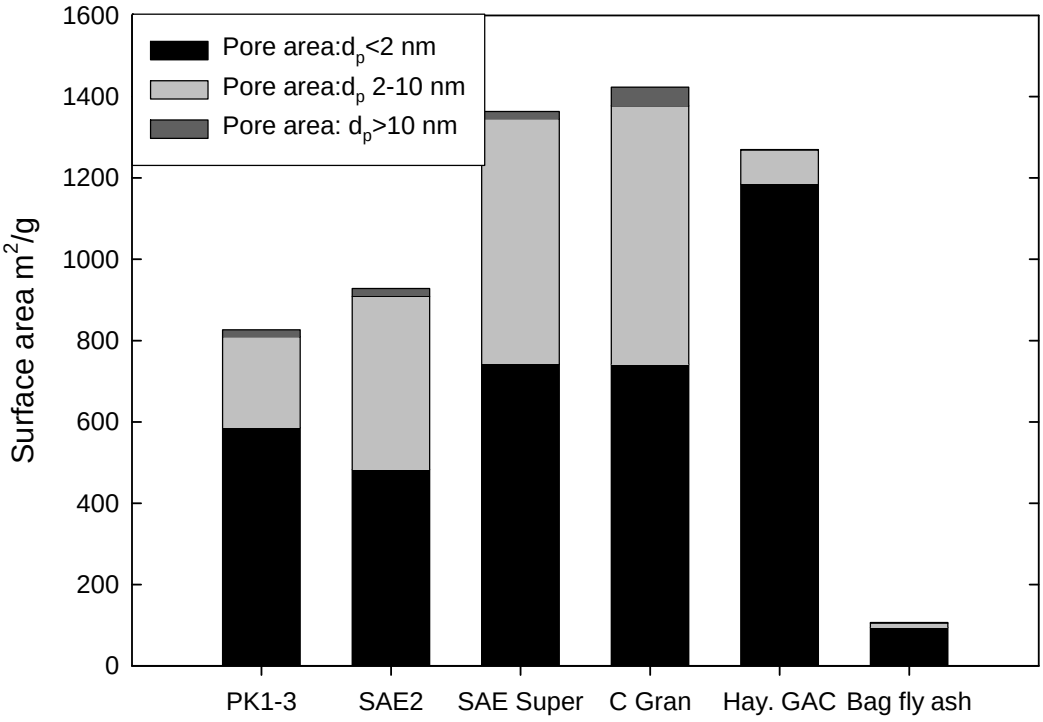

Figure 3: Surface area distribution of activated carbons in the pore diameter ranges: <2 nm, 2-10 nm and >10 nm.

As can be seen in figure 2, the pores size in Norit C Gran contains are largely in the meso and macro range. This results in the highest adsorption capacity (q_m) as can be seen in table 2 (approximately 0.5 g_{LAS}/g). The shape of the isotherm deviates from the other isotherms. The affinity coefficient of LAS on Norit C Gran (b in table 2) is lower compared to the other activated carbons. This is most likely the result of the different activation method for Norit C Gran, which was activated with phosphoric acid instead of steam. Activation with phosphoric acid results in more oxygen groups at the surface and will give a weakly negatively charged, acidic surface [31]. Wu and Pendleton (2001) [17] stated that an inverse linear relationship exists between the amount of anionic surfactant adsorbed and the oxygen content of the adsorbent surface.

Bagasse fly ash has the lowest adsorption capacity of around 0.02 g_{LAS}/g as shown in figure 2. The main component (around 60%) of bagasse fly ash is silica (SiO_2) [23]. Both the negative charged silica [5] and the low surface area in the meso and macro pore range (figure 3) result in the low adsorption capacity.

A deviation from the proposed qualitative relation is Haycarb GAC. Despite the fact that more than 90% of the surface can be found in micro pores, the adsorption capacity is unexpectedly high. The exact pore size of the micro pores could not be measured with the Micromeritics Tristar 3000 surface area and porosimetry analyzer. A major part of the micro pores might be close to 2 nm. LAS molecules could still fit in these micro pores, which could explain the unexpected higher capacity.

The following overall picture emerges. Equilibrium adsorption of LAS on activated carbon shows that pores in meso and macro pore range are favourable. Micro pores do

not contribute much to the LAS adsorption, because a LAS molecule is too large to access the surface area that is provided by the micro pores.

Figure 4 shows the adsorption capacity of LAS for two types of inorganic ion exchangers, bentonite and LDH, with respect to equilibrium concentration. The cation exchanger, bentonite has been acid activated to increase the specific surface area and surface acidity [25]. As can be seen in table 1, the surface area of bentonite is increased by activation from 81 to 294 m^2/g. The total pore volume increased from 0.095 to 0.505 cm^3/g. For both bentonite, acid activated and untreated, the amount of LAS adsorbed is negligible (figure 4). Even though, the acid activated bentonite has an increased internal surface area and pore volume, the acidic (negatively charged) surface does not interact with the LAS molecules.

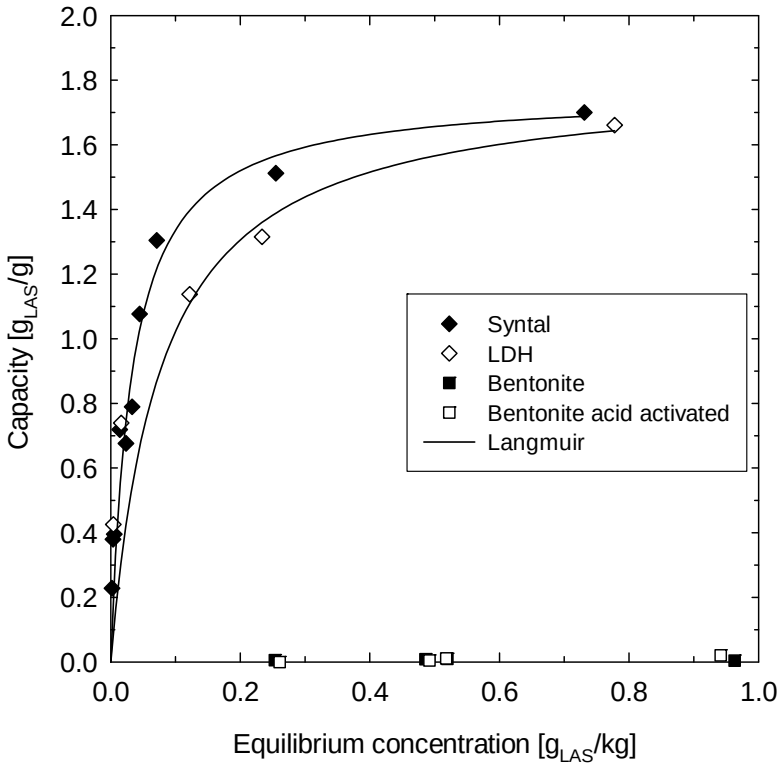

Figure 4: Adsorption isotherm of LAS and LDH, Syntal (commercially available LDH), bentonite and acid activated bentonite. The obtained Langmuir parameters are shown in table 2.

As can be seen in figure 4 the maximum LAS adsorption capacities of both LDH and Syntal are very high. The adsorption isotherm is comparable to that of the anion exchange resins (figure 1), because similar interactions take place. LDHs consist of two brucite like layers that become positively charged when a magnesium cation is replaced by an aluminium cation. In order to balance the residual charge, anions are intercalated between the layers and can be exchanged by other anions [26]. The ionic interaction between the positive charge on the surface and the negatively charged surfactant results in a steep isotherm and therefore a high affinity coefficient *b* is obtained (table 2). At equilibrium concentration 0.1 g_{LAS}/dm^3 the adsorption capacity is 1.0 and 1.3 g_{LAS}/g for LDH and Syntal respectively. LDHs combine the preferred

properties identified from the previously described experiments, being that they contain mainly meso and macro pores with a positively charged surface (table 1).

2.4.3. Equilibrium experiments using AOS

Equilibrium experiments using another anionic surfactant AOS (alpha olefinsulfonate), were carried out to verify if similar results would be obtained with LAS. AOS is less frequently used in detergents than LAS. AOS is often used in combination with LAS [3]. Figure 5 shows the results for AOS adsorbed per gram of adsorbent at AOS equilibrium concentration. The molecular weight of both anionic surfactants is similar (AOS 286 g/mol and LAS 312 g/mol) therefore, the adsorption capacities of AOS can be directly compared with those of LAS.

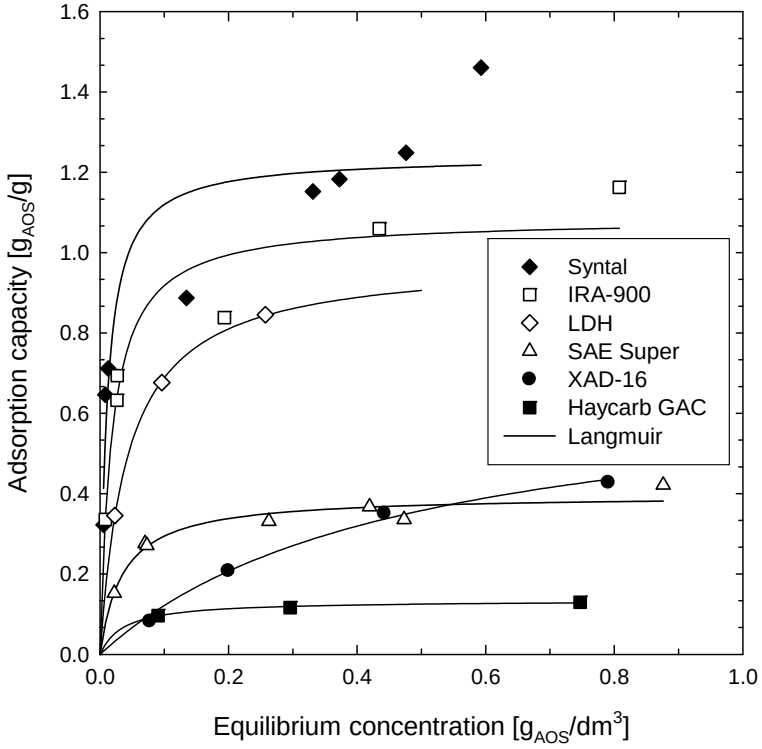

Figure 5: Adsorption isotherm of AOS and different adsorbents. The obtained Langmuir parameters are shown in table 2.

The experimental adsorption isotherms for AOS adsorption are similar to those for LAS adsorption. In figure 5 two groups of isotherms can be distinguished. The first group is characterized by hydrophobic interactions of AOS with the surface (XAD-16, SAE Super and Haycarb GAC). Aromatic interactions will not take place, because AOS does not contain aromatic groups. Therefore, the maximum adsorption capacity for AOS on XAD-16 is lower than that of LAS (table 2). SAE Super shows a higher maximum adsorption capacity for AOS. AOS is more hydrophobic, because of its longer hydrocarbon chain and the absence of a benzene ring. The hydrophobic interactions with the hydrophobic carbon surface are stronger for AOS compared to LAS.

The second group is characterized by ionic interactions (IRA-900, LDH and Syntal). The interaction between the negative AOS and the positive surface is similar to the LAS interactions and therefore similar capacities are obtained.

2.4.4. Costs

The main goal of this project is the removal of anionic surfactants from rinsing water in water-stressed low-income markets. It is therefore of key importance that the adsorbent is cheap. Therefore, the amount of surfactant adsorbed per dollar of adsorbent is a key parameter. This parameter is derived from the measured isotherms at a fixed equilibrium concentration of 0.1 g_{LAS}/dm^3 water, being the lowest expected concentration of LAS in rinsing water (table 2). The costs of existing absorbent materials were obtained from their suppliers. The cost of LDH made on laboratory scale is taken equal to Syntal which is commercially available (table 1). With these data, the amount of LAS adsorbed per US dollar at a LAS concentration of 0.1 g_{LAS}/dm^3 water is calculated and presented in figure 6.

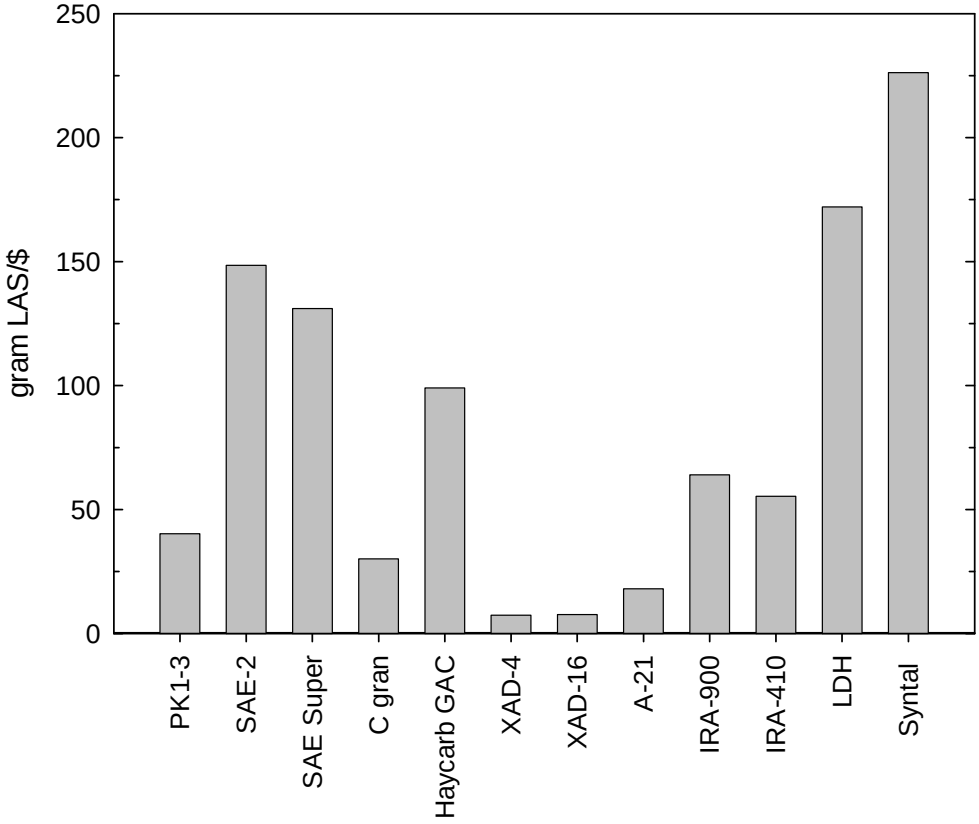

Figure 6: The amount of LAS adsorbed per US dollar of material for different materials at a LAS concentration of 0.1 g_{LAS}/dm^3 water.

The best performing adsorbents are Syntal and LDH, because of their very high adsorption capacity at 0.1 g_{LAS}/dm^3. The SAE2 and SAE Super activated carbons are also promising materials to investigate, because of their low price. As would be expected, the resins are too expensive to use for this purpose.

2.5. Conclusions

A selected group of potential adsorbents for the adsorption of anionic surfactants were studied. This selection was made to include a range of different surfactant adsorption mechanisms. The following conclusions can be derived from the experimental data:

1. It is clear that the surface charge of adsorbents is the most important parameter. Positive charges can be provided as functional groups (anion exchange resins) or can be built into the structure itself (LDH).
2. Secondly, the pore size is important. Meso (2-50 nm) or macro pores (>50nm) are preferable, because surfactants are large molecules and have difficulties in accessing the surface area provided by the micro pores (<2nm). From the equilibrium experiments with activated carbons, a qualitative relation is found between the capacity and the surface area in the meso pore size range.
3. The Langmuir model describes the results from equilibrium experiments well.
4. LDH and Syntal combine the favourable properties: positive surface charge and large pores. This results in a high LAS adsorption capacity (1-1.6 g_{LAS}/g) for anionic surfactants at typical rinsing water concentrations (0.1-0.3 g_{LAS}/dm^3). The adsorption of other anionic surfactants, such as AOS, is almost as good as for LAS.
5. Comparing the adsorbents based on LAS adsorption capacity and cost shows layered double hydroxide (Syntal and LDH prepared in the laboratory) are suitable, mainly as a result of the very high adsorption capacity while activated carbons (Norit SAE2 and SAE Super) can be of interest due to their relatively low costs.

2.6. References

1. UnitedNations, *Water for People Water for Live. World Water Development Report. UNESCO WWAP*. 2003, United Nations.
2. Ho Tan Tai, L., *Formulating detergents and personal care products*. 1st ed. 2000, New York, USA: AOCS Press.
3. Holmberg, K., et al., *Surfactants and polymers in aqueous solution*. 2nd ed. 2003, West Sussex, UK: Wiley.
4. Adak, A., M. Bandyopadhyay, and A. Pal, *Removal of anionic surfactant from wastewater by alumina: a case study.* Colloids and Surfaces A: Physicochemical and Engineering Aspects, 2005. **254**(1-3): p. 165-171.
5. Gupta, V.K. and I. Ali, *Adsorbents for water treatment: development of low-cost alternatives to carbon.* Encyclopedia of Surface and Colloid Science, 2003.
6. Pollard, S.J.T., et al., *Low-cost adsorbents for waste and waste water treatment: a review.* The Science of the Total Environment, 1992. **116**: p. 31-52.
7. Crini, G., *Non-conventional low-cost adsorbents for dye removal: A review.* Bioresource Technology, 2006. **97**(9): p. 1061-1085.
8. Savitsky, A.C., B.H. Wiers, and R.H. Wendt, *Adsorption of organic compounds from dilute aqueous solutions onto the external surface of type A zeolite.* Environmental Science and Technology, 1981. **15**(10): p. 1191-1196.
9. Yang, W.B., et al., *Adsorption of branched alkylbenzene sulfonate onto styrene and acrylic ester resins.* Chemosphere, 2006. **64**(6): p. 984-990.

10. Westall, J.C., et al., *Sorption of linear alkylbenzenesulfonates on sediment materials.* Environmental Science & Technology, 1999. **33**(18): p. 3110-3118.
11. Gunister, E., et al., *Effect of sodium dodecyl sulfate on flow and electrokinetic properties of Na-activated bentonite dispersions.* Bulletin Of Materials Science, 2004. **27**(3): p. 317-322.
12. Khan, M.N. and U. Zareen, *Sand sorption process for the removal of sodium dodecyl sulfate (anionic surfactant) from water.* Journal of Hazardous Materials, 2006. **133** (1-3): p. 269-275.
13. Garcia, M.T., et al., *Structure-activity relationships for association of linear alkylbenzene sulfonates with activated sludge.* Chemosphere, 2002. **49**(3): p. 279-286.
14. Purakayastha, P.D., A. Pal, and M. Bandyopadhyay, *Adsorbent selection for anionic surfactant removal from water.* Indian Journal of Chemical Technology, 2005. **12**(3): p. 281-284.
15. Garcia-Delgado, R.A., L.M. Cotoruelo-Minguez, and J.J. Rodriguez, *Equilibrium study of single-solute adsorption of anionic surfactants with polymeric XAD resins.* Separation science and technology, 1992. **27**(7): p. 975-987.
16. Purakayastha, P.D., A. Pal, and M. Bandyopadhyay, *Sorption kinetics of anionic surfactant on to waste tire rubber granules.* Separation and Purification Technology, 2005. **46**(3): p. 129-135.
17. Wu, S.H. and P. Pendleton, *Adsorption of anionic surfactant by activated carbon: Effect of surface chemistry, ionic strength, and hydrophobicity.* Journal Of Colloid And Interface Science, 2001. **243**(2): p. 306-315.
18. Gonzalez-Garcia, C.M., et al., *Removal of an ionic surfactant from waste water by carbon black adsorption.* Separation science and technology, 2002. **37**(12): p. 2823-2837.
19. Gonzalez-Garcia, C.M., et al., *Ionic surfactant adsorption onto activated carbons.* Journal of Colloid and Interface Science, 2004. **278**(2): p. 257-264.
20. Gupta, S., et al., *Performance of waste activated carbon as a low-cost adsorbent for the removal of anionic surfactant from aquatic environment.* Journal of Environmental Science and Health - Part A Toxic/Hazardous Substances and Environmental Engineering, 2003. **38**(2): p. 381-397.
21. Unilever, *Personal communication*. December 2004: Hindustan Unilever Research India, 64 Main Road, Whitefield P.O. Bangalore 560066, India.
22. Paria, S. and K.C. Khilar, *A review on experimental studies of surfactant adsorption at the hydrophilic solid-water interface.* Advances in Colloid and Interface Science, 2004. **110**(3): p. 75-95.
23. Gupta, V.K. and I. Ali, *Utilisation of bagasse fly ash (a sugar industry waste) for the removal of copper and zinc from wastewater.* Separation and Purification Technology, 2000. **18**(2): p. 131-140.
24. Espantaleón, A.G., et al., *Use of activated clays in the removal of dyes and surfactants from tannery waste waters.* Applied Clay Science, 2003. **24**(1-2): p. 105-110.

25. Ozcan, A.S. and A. Ozcan, *Adsorption of acid dyes from aqueous solutions onto acid-activated bentonite.* Journal of Colloid and Interface Science, 2004. **276**(1): p. 39-46.
26. Pavan, P.C., G.d.A. Gomes, and J.B. Valim, *Adsorption of sodium dodecyl sulfate on layered double hydroxides.* Microporous and Mesoporous Materials, 1998. **21**(4-6): p. 659-665.
27. Basar, C.A., et al., *Removal of surfactants by powdered activated carbon and microfiltration.* Water Research, 2004. **38**(8): p. 2117-2124.
28. Abed, M.A., A. Saxena, and H.B. Bohidar, *Micellization of alpha-olefin sulfonate in aqueous solutions studied by turbidity, dynamic light scattering and viscosity measurements.* Colloids and Surfaces A: Physicochemical and Engineering Aspects, 2004. **233**(1-3): p. 181-187.
29. Reichle, W.T., *Synthesis of anionic clay minerals (mixed metal hydroxides, hydrotalcite).* Solid State Ionics, 1986. **22**(1): p. 135-141.
30. Somasundaran, P. and S. Krishnakumar, *Adsorption of surfactants and polymers at the solid-liquid interface.* Colloids and Surfaces A: Physicochemical and Engineering Aspects, 1997. **123-124**: p. 491-513.
31. Baker, F.S., R.A. Daley, and R.H. Bradley, *Surface chemistry of wood-based phosphoric acid-activated carbons and its effects on adsorptivity.* Journal of Chemical Technology and Biotechnology, 2005. **80**: p. 878-883.

3. Optimization of LDH stability and adsorption capacity for anionic surfactant

Abstract

Low cost adsorption technology offers high potential to clean up laundry rinsing water. From an earlier selection of adsorbents [1], layered double hydroxide (LDH) proved to be an interesting material for the removal of anionic surfactant, linear alkyl benzene sulfonate (LAS) which is the main contaminant in laundry rinsing water. The main research question was to identify the effect of process parameters of the LDH synthesis on the stability of the LDH structure and the adsorption capacity of LAS. LDH was synthesized with the co-precipitation method of Reichle (1986) [2]; a solution of $M^{2+}(NO_3)_2$ and $M^{3+}(NO_3)_3$ and a second solution of NaOH and Na_2CO_3 were pumped in a beaker and mixed. The precipitate that was formed was allowed to age and was subsequently washed, dried and calcined. The process parameters that were investigated are the concentration of the initial solutions, M^{2+}/M^{3+} ratio and type of cations. The crystallinity can be improved by decreasing the concentration of the initial solutions; this also decreases the leaching of M^{3+} from the brucite-like structure into the water. The highest adsorption capacity is obtained for Mg^{2+}/Al^{3+} with a ratio 1 and 2 because of the higher charge density compared to ratio 3. Storing the LDH samples in water resulted in a reduction of adsorption capacity and a decrease in surface area and pore volume. Therefore, LDH is not applicable in a small device for long term use in aqueous surroundings. The adsorption capacity can be maintained during storage in a dry N_2 atmosphere.

3.1. Introduction

Recycling of water is crucial in times of water scarcity. In developing countries typically half of the daily amount of water is used for doing laundry. Laundry rinsing water is relatively clean and therefore highly suitable for water re-use. To re-use the rinsing water, the main contaminants need to be removed such as the added detergent ingredients and "dirt" constituents released from the fabrics during rinsing. In this chapter we focus on removing the main component of detergents, namely the surfactants.

The conventional methods for surfactant removal from water involve processes such as chemical and electrochemical oxidation, membrane technology, chemical precipitation, photo-catalytic degradation, adsorption and various biological methods [3, 4]. Many of these processes are not cost effective and/or not suitable for application on a household scale. However, adsorption technology can be applied in small devices, is applicable on household scale and therefore has the potential to become a suitable low cost technology.

From a previous investigation [1] layered double hydroxide (LDH) proved to be a suitable material for the adsorption of anionic surfactants. The adsorption capacity was found to be very high: 1.3 g_{LAS}/g_{LDH} at typical surfactant concentrations found in rinsing water (0.1 g_{LAS}/dm^3 water [5]). LAS is linear alkyl benzene sulfonate, which is predominantly used in detergents. The high adsorption capacity compared to the relatively low cost make LDH an interesting material for further research.

Layered double hydroxides derive their name from their structure. They consist of two brucite like layers; sheets of octahedrons of magnesium hydroxide. If a magnesium cation is replaced by an aluminium cation, the layer will be charged positive. In order to balance the residual charge, anions are intercalated between the layers. The general formula of a LDH is: $[M^{2+}_{1-x}\ M^{3+}_{x}\ (OH)_2]^{x+}\ X^{m-}_{x/m} * nH_2O$, where M^{2+} represents the bivalent cation, M^{3+} the trivalent cation, X^{m-} the intercalated anion with m- charge and n is the number of water molecules. An LDH that can be found in nature is hydrotalcite ($[Mg_6\ Al_2\ (OH)_{16}]\ (CO_3^{2-}) * 4H_2O$) although it is rare. Fortunately, LDH is commercially available at large quantities and low cost [6].

There are several methods to produce LDHs. Reichle (1986) [2] reported co-precipitation as an easy and efficient method to prepare large amounts of LDH. Figure 1 shows the co-precipitation process schematically with the main process parameters and process steps. The M^{2+}/M^{3+} ratio influences the amount of positive charges. A low M^{2+}/M^{3+} ratio indicates a high M^{3+} content and a high charge density. Ratios between 2 and 4 resulted in LDH only; other ratios resulted partly in a LDH and other metal oxides. Cations M^{2+} and M^{3+} having an ionic radius not too different from that of Mg^{2+} can form an LDH [2]. The concentration of initial solutions will influence the size and crystallinity of the nanoparticles. Low saturation conditions usually increase crystallinity compared to higher saturation conditions. In the latter situation the nucleation rate is higher than the rate of crystal growth and this result in a large number of small crystallites [7].

Each production step influences the properties of the final product. Aging will increase the crystallinity [7]. Reichle (1986) [2] and Ulibarri et. al. (1995) [8] reported a high surface area and more crystalline materials at aging temperatures of 60 to 80 °C. Washing is essential to remove unreacted reagents. During calcination the water molecules between the layers will be removed and the CO_3^{2-} is converted to CO_2. The CO_2 eludes and leaves a porous structure behind [8]. Furthermore, the hydroxyl groups of the brucite structure will be converted to oxide groups resulting in a mixed metal oxide. An important property of the calcined LDH is the memory effect; in aquatic environments it can easily return to its original layered structure [8-10].

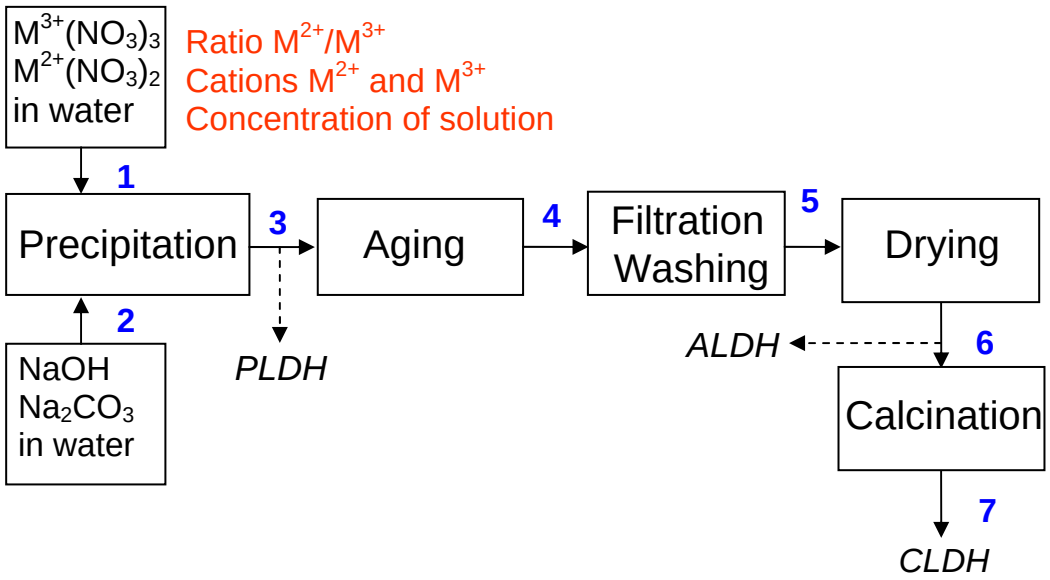

Figure 1: Schematic representation of the co-precipitation method of LDH and the main process parameters investigated. Samples are taken at point 3, precipitated LDH (PLDH), point 6 aged LDH (ALDH) and point 7, calcined LDH (CLDH).

Because of their structure LDHs can exchange intercalated anions and can be applied in broad areas as adsorbents, catalysts, anion exchangers, acid residue scavengers, and antacids in the medical field [2]. Adsorption of different adsorbates is often studied and reported; examples are arsenates [11], chromates [12, 13], acidic pesticides [9], phenols [8], anionic dyes [10] and phosphorus contaminates [14]. Pavan et. al. (1999, 2000, 1998) [15-17], Kopka et. al. (1988) [18], Anbarasan et. al. (2005) [19] and Reis et. al. (2004) [20] investigated the adsorption of anionic surfactants on LDH. The adsorption of anionic surfactants takes place on the external surface area as well as intercalated in the LDH, which is also described in Pavan et. al. (2000) [15], Kopka et. al. (1988) [18], Anbarasan et. al. (2005) [19]. However, no studies were reported on the effect of synthesis parameters of LDH on the adsorption capacity for anionic surfactants and the stability of such materials.

In the application under investigation, we aim to apply LDH in small household scale devices. Assuming that this device will be used for several months, the LDH stability is important during that period. The adsorption capacity should remain both during storage and use, where the latter means in aquatic surroundings. The objective of this study is to identify the effect of process parameters for LDH synthesis and storage on

the LDH structure, stability and adsorption capacity for LAS. To investigate the best storage method to maintain the stability, the LDH samples are stored in different atmospheres, such as dry N_2 (exclusion of CO_2), dry air, open air, a vial and in water. The process parameters that are varied are the M^{2+}/M^{3+} ratio, type of cations and concentration of initial solutions. Furthermore, the influence of aging and calcination is studied. The LDH was characterized (surface area and pore volume) and its LAS adsorption capacity was measured after each step.

3.2. Materials and Methods

3.2.1. Materials

Magnesium nitrate ($Mg(NO_3)_2*6H_2O$), aluminium nitrate ($Al(NO_3)_2*9H_2O$), zinc nitrate ($Zn(NO_3)_2*6H_2O$), iron nitrate ($Fe(NO_3)_2*9H_2O$), sodium carbonate (Na_2CO_3) and sodium hydroxide (NaOH) are analytically pure reagents and obtained from Boom (Meppel, The Netherlands), Merck (Darmstadt, Germany) and Sigma-Aldrich (Steinheim, Germany). Anionic surfactant, linear alkyl benzene sulfonate (LAS), was obtained from Unilever R&D, Vlaardingen, The Netherlands. Purity is around 92 wt%. The chain length of LAS is C10 to C13 (equal distributed, average molecular weight of LAS-acid is 312 g/mol).

3.2.2. Preparation of LDH

The concentration of the initial solutions, M^{2+}/M^{3+} ratios and aging are expected to influence the crystallinity. The concentration of the aluminium nitrate solution was taken at the saturation point (HC: high concentration) and at 50% of the saturation point (LC: low concentration). For a given ratio the concentration of the magnesium nitrate solution is fixed. Ratios investigated are 1.5, 2 and 3 (mol ratio). Ratio 4 is not used, because a high charge density is preferred to obtain a high adsorption capacity. Ratio 1.5 is investigated to understand the influence of charge density and the possible production of other metal oxides. The influence of aging and calcination is studied by taking samples at different points in the production process, which is shown in Figure 1; point 3, precipitated LDH (PLDH), point 6, aged LDH (ALDH) and point 7, calcined LDH (CLDH). The sample taken at point 3 is immediately washed and dried to investigate the effect of aging. Four cations were investigated: magnesium (Mg^{2+}), aluminium (Al^{3+}), zinc (Zn^{2+}) and iron (Fe^{3+}). Combinations with other metal ions were not investigated because either the production process becomes too complicated, or no LDH is formed or leaching of one of the cations would result in hazardous contamination of the cleaned water. The carbonate anion is used to produce an open structure after calcination. Mg and Al are used to find the optimal production method with the highest adsorption capacity for anionic surfactants. Subsequently, the optimal production method was used for the other combinations: MgFe and ZnAl-LDHs. Since LDH stability is essential for long time use it was investigated for different circumstances during an extended period of time.

To produce high concentration (HC) LDH a solution of 86 gram $Mg(NO_3)_2*6H_2O$ and 64 gram $Al(NO_3)_3*9H_2O$ in 100 ml Milli-Q water was added to a second solution of

18.6 gram NaOH and 11 gram Na_2CO_3 in 100 ml Milli-Q water. To produce low concentration (LC) LDH a solution of 43 gram $Mg(NO_3)_2*6H_2O$ and 32 gram $Al(NO_3)_3*9H_2O$ in 100 ml Milli-Q water was added to a second solution of 18.6 gram NaOH and 11 gram Na_2CO_3 in 100 ml Milli-Q water.

Both solutions were pumped at a rate of 10 ml/min in a beaker and mixed with a magnetic stirrer. During dosing the precipitation starts immediately. At the end of the dosing the precipitate formed was allowed to age overnight at 60°C under continues stirring. The aged precipitate was filtered with a Buchner funnel and washed 10 times with each time 100 ml of fresh Milli-Q water in a centrifuge. The final product was dried overnight at 105°C and calcined at 450°C for 4.5 hours [2].

3.2.3. Storage

The materials were stored in five different atmospheres: in a desiccator with silica and flushed with N_2 (dry N_2: no water vapour and CO_2 present), in a desiccator with silica not flushed with N_2 (dry air: no water vapour, but CO_2 present), in a closed vial, in open air and stored in water.

3.2.4. Characterization

The samples were characterized by powder X-ray diffraction (XRD), thermo gravimetric analysis (TGA) and scanning electron microscope (SEM). X-ray diffraction patterns of the powdered samples were obtained using a PANalytical APD with CuKα radiatior (50kV and 35mA) at a scanning rate of 1.5°/min. Thermo gravimetric analysis were carried out using a Setaram Setsys 16. The temperature programmed rate was 1 °C/min, and the weight change was measured from 20 to 800 °C. The nitrogen gas flow was 49 ml/min. The morphology was observed using a Jeol Scanning Electron Microscope JSM-6480LV.

The specific surface area, pore size and pore volume distribution were measured using nitrogen adsorption at -196°C (liquid nitrogen temperature) with the Micromeritics Tristar 3000. The samples are pre-treated overnight to remove water and other contaminants from the pores. During the pre-treatment, a nitrogen flow is applied and the samples are heated to 105°C. The amount of cations in the samples was measured by ICP (Perkin Elmer 5300 DV).

3.2.5. Adsorption experiments

The adsorption experiments were conducted at different initial surfactant concentrations ranging from 0.5 to 1 g_{LAS}/dm^3 water. Surfactants are dissolved in milli-Q water. An amount of 0.1 gram LDH and 80 ml surfactant solution were mixed in a screw capped flask and placed in a shaking bath (Julabo SW22) at 25°C. With a preliminary experiment the equilibrium time was determined to be 48 hours; equilibrium was reached well within this time. The initial solution is pH neutral. After equilibration the pH is measured again. The water phase was sampled with a syringe

equipped with a filter to remove suspended solids (Spartan 30/0.45RC (0.45μm)) and the surfactant concentration was measured. The concentration of LAS was determined by spectrophotometry at 223 nm (Shimadzu UV-1650PC) (accuracy correlation curve: 2%).

3.3. Results and discussion

3.3.1. Characterization

Table 1 summarizes the measured characteristics of the produced LDH samples. In most cases the expected M^{2+}/M^{3+} ratio is confirmed by the measured ratio. The Mg^{2+}/Al^{3+} ratio 1.5 is actually 1 and Zn^{2+}/Al^{3+} ratio 2 is measured 5.5. From this point onwards these measured ratios will be used. The amount of M^{3+} per gram of CLDH is calculated. At M^{2+}/M^{3+} ratio 2, there is approximately 5 mmol M^{3+}/g CLDH present. The BET surface area of PLDH is increased after aging (ALDH) and increased further after calcination (CLDH). The surface area of MgAl-CLDH is in the range 160-200 m^2/g. This is higher than the surface area of 120 m^2/g described by Reichle (1986) [2]. The difference can be explained by calcination; the samples of Reichle are not calcined. During calcination the CO_3^{2-} molecules are converted to CO_2. CO_2 eludes and leaves a porous structure behind and thus a higher surface area. Increasing the M^{2+}/M^{3+} ratio to 3 decreases the surface area and pore volume substantially. LDH with the other cations also gave a substantial decrease of surface area and pore volume.

Table 1: Characteristics of the produced LDHs. PLDH is precipitated LDH, ALDH is aged LDH, CLDH is calcined LDH (figure 1).

Sample	Cations M^{2+} and M^{3+}	Ratio M^{2+}/M^{3+} [-]	Measured ratio [-]	Amount of mmol M^{3+}/g	BET Surface area [m^2/g]	Pore volume [cm^3/g] at p/p_0=0.99	d (003) [nm]	a [nm]	c [nm]
CLDH	Mg^{2+} Al^{3+}	2	2.1	4.8	169	0.47			
CLDH	Mg^{2+} Al^{3+*}	2	1.9	5.0	164	0.37			
CLDH	Mg^{2+} Al^{3+}	1.5	1.0	7.4	193	0.57			
CLDH	Mg^{2+} Al^{3+}	2	1.7	4.8	183	0.58			
CLDH	Mg^{2+} Al^{3+}	3	2.9	3.7	65	0.29			
PLDH	Mg^{2+} Al^{3+}				0.02	0	0.741	0.304	2.22
ALDH	Mg^{2+} Al^{3+}				69	0.23	0.735	0.303	2.21
CLDH	Mg^{2+} Al^{3+}	2	2.1	3.6	188	0.62			
PLDH	Mg^{2+} Fe^{3+}				1.6	0	0.736	0.310	2.21
ALDH	Mg^{2+} Fe^{3+}				72	0.21	0.740	0.310	2.22
CLDH	Mg^{2+} Fe^{3+}	2	1.9	5.3	87	0.34			
CLDH	Zn^{2+} Al^{3+}	2	5.5	1.9	31	0.15			

* This LDH is produced with high concentration (HC) initial solutions; all other LDHs are produced with low concentration (LC) initial solution.

The XRD measurements of the powdered MgAl and MgFe-LDHs with M^{2+}/M^{3+} ratio 2 are shown in figure 2 and 3. The three samples shown in these figures are samples taken during synthesis as indicated in figure 1: at point 3 after precipitation and before aging (PLDH), at point 6 after aging (ALDH) and at point 7, after calcination (CLDH).

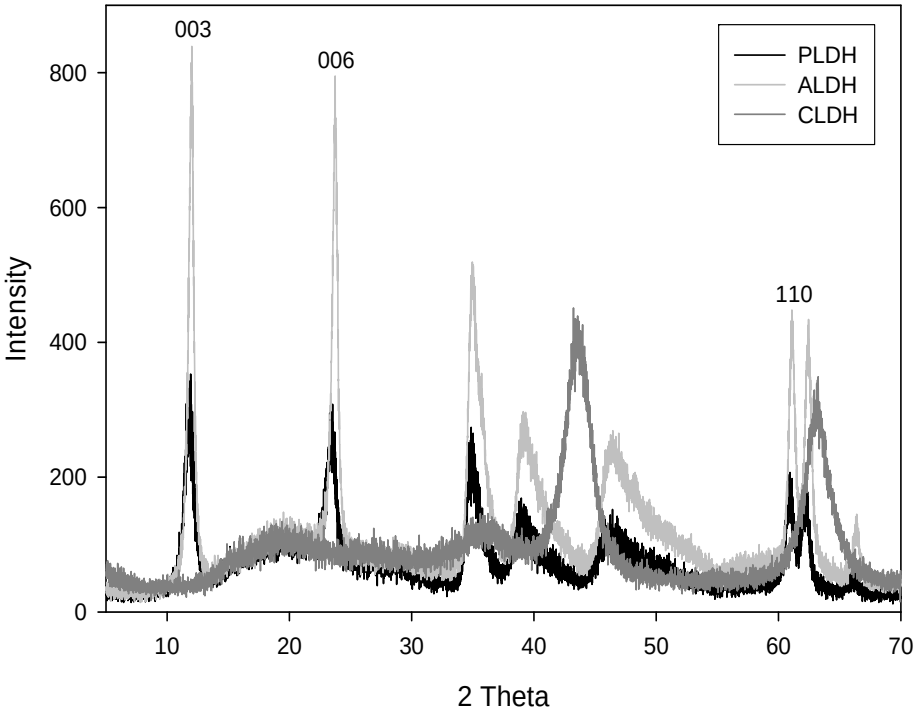

Figure 2: XRD patterns of MgAl-LDH: samples taken before aging (PLDH), after aging (ALDH) and after calcination (CLDH) (M^{2+}/M^{3+} ratio 2; LC initial solutions).

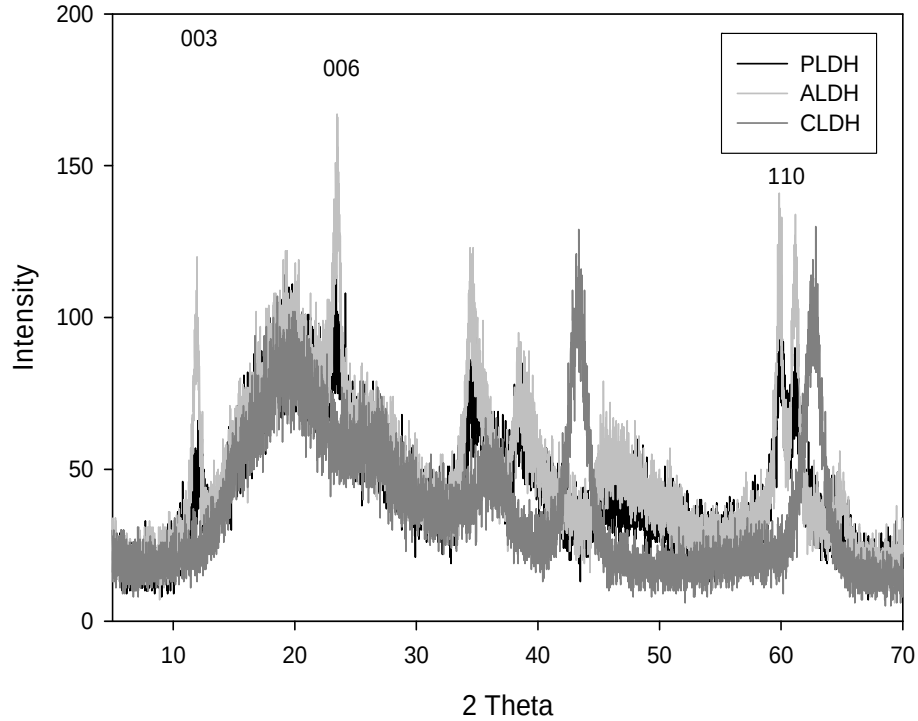

Figure 3: XRD patterns of MgFe-LDH: samples taken before aging (PLDH), after aging (ALDH) and after calcination (CLDH) (M^{2+}/M^{3+} ratio 2; LC initial solutions).

The XRD patterns for PLDH and ALDH samples show well defined (00*l*) reflections at lower 2θ values and clear (110) reflections at higher 2θ values, indicating a typical LDH pattern for both MgAl and MgFe. The reflections are indexed to a hexagonal

lattice with rhombohedral 3R symmetry [21]. The lattice parameters are calculated accordingly and presented in table 1. The sharp peak at $d = 0.74$ nm ($2\theta = 12°$) is ascribed to the diffraction by planes (003) and is referred to as the basal spacing. From the width of the brucite-like layers (0.48 nm), the interlayer space is calculated and is 0.26 nm. This indicates a carbonate anion located between the layers. Lattice parameter *a* corresponds to the average closest metal-metal distance within a layer and is calculated as twice the position of the *d*(110) ($2\theta = 60°$) [22]. The parameter *c* is a function of the average charge of the metal cations, the nature of interlayer anion and the water content. The values for *d*(003), *a* and *c* shown in table 1 are in agreement with those reported in the literature for LDHs [21, 22].

The intensity of the reflection is much higher and accordingly the line width is smaller for MgAl (figure 2) compared to MgFe-LDH (figure 3). This corresponds to a higher crystallinity of MgAl-LDH [23]. This can also be concluded for the aged samples (ALDH) compared to the not aged samples (PLDH). During aging the crystallinity increases, as expected.

For the calcined samples (CLDH) the absence of the (003) reflection peak indicate the destruction of the layered structure by calcination. The samples show a similar pattern to the one of magnesium oxide, as expected and described in literature [2, 7, 24].

Figure 4 shows the TGA for MgAl-ALDH with a M^{2+}/M^{3+} ratio of 2. A three-stage degradation mechanism can be identified in this figure. The first weight loss up to 190 °C is due to the removal of physisorbed and interlayer water molecules. The second stage up to 380 °C is due to the conversion of hydroxyl groups of the brucite-like layers into oxide groups. The third stage up to 620 °C is due to the decomposition of the interlayer carbonate anion [19]. The formed carbon dioxide will elude from the LDH and a porous structure will stay behind [8]. This is a typical TGA for LDH [25].

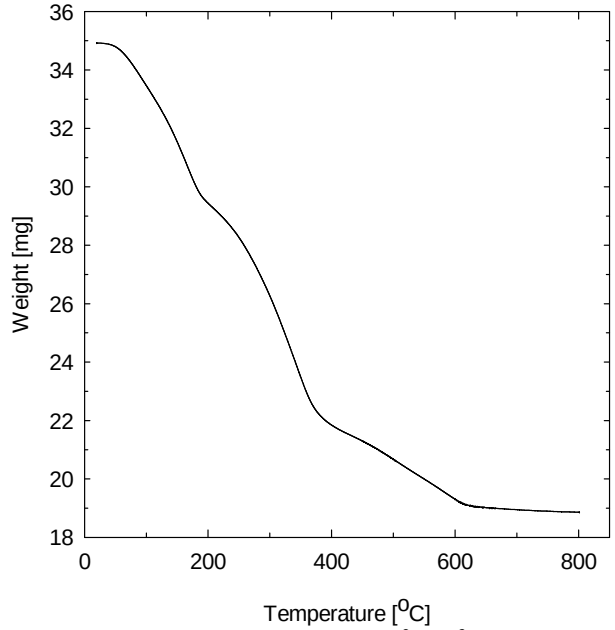

Figure 4: TGA analysis of MgAl-ALDH (M^{2+}/M^{3+} ratio 2; LC initial solutions).

A SEM picture of MgAl ALDH with a M^{2+}/M^{3+} ratio of 2 is shown in figure 5. The picture shows an aggregate that consists of crystallites with a size of tens of nanometres [26]. In between the nanoparticles (crystallites) a porous network exists. The size of the pores in this network is in same order of magnitude, namely between 10 and 80 nm (not shown, measured with the Micromeritics Tristar 3000).

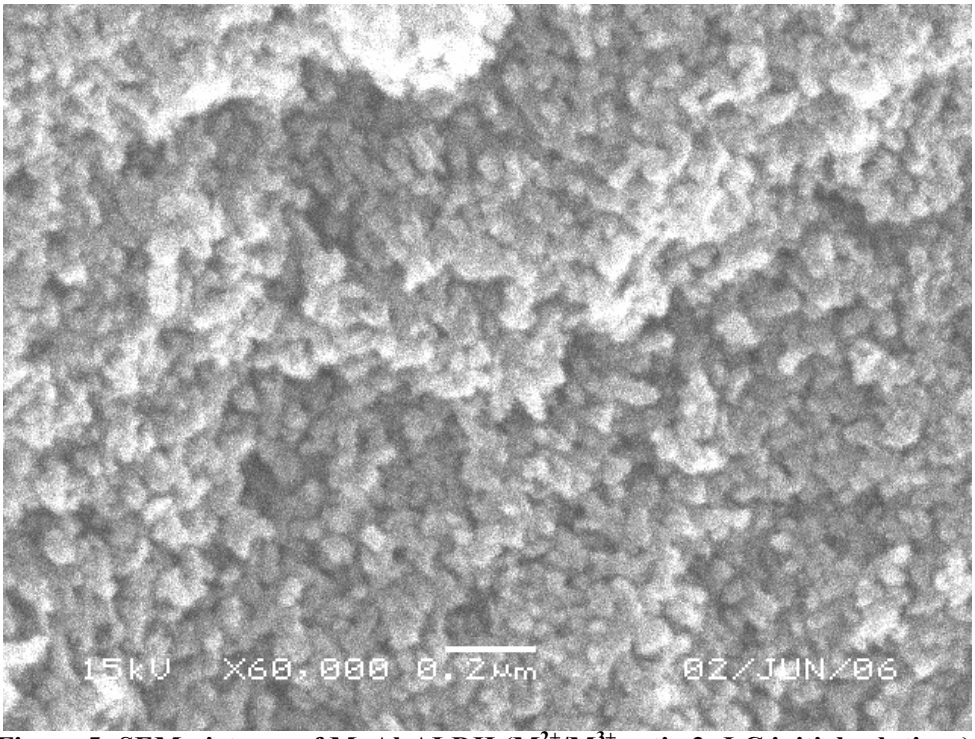

Figure 5: SEM pictures of MgAl-ALDH (M^{2+}/M^{3+} ratio 2; LC initial solutions).

3.3.2. Adsorption experiments

Increasing the crystallinity could increase the stability [26]. The crystallinity can be increased by decreasing the concentration of the initial solutions; therefore the initial concentration of the magnesium nitrate and aluminium nitrate solution is varied. The high concentration (HC) solution was taken at the saturation point of aluminium nitrate and the low concentration (LC) was at 50% of that saturation point. The amount of magnesium nitrate was fixed because of the fixed M^{2+}/M^{3+} ratio. The difference in adsorption capacity between the fresh CLDHs prepared with high concentration (HC) and low concentration (LC) appeared not significant (not shown). The HC and LC-CLDH samples are both stored at different conditions; dry N_2, dry air, in a vial, in open air and in water. During storage, samples were taken in time and the adsorption capacity, specific surface area and pore volume were measured. The specific surface areas and pore volumes are shown in table 2. The adsorption capacities for LC-CLDH stored in dry N_2 and in water are shown in figure 6.

Table 2: BET surface area and pore volume of fresh CLDH samples and after storage. Y = years, m = months.

Cations M^{2+} and M^{3+}	Ratio M^{2+}/M^{3+} [-]	Concentration of initial solutions	Storage method	Time of Storage	BET Surface area [m^2/g]	Pore volume [cm^3/g] at p/p_0=0.99
Mg^{2+} Al^{3+}	2	LC	-	0	169	0.47
Mg^{2+} Al^{3+}	2	LC	dry N_2	4m	149	0.50
Mg^{2+} Al^{3+}	2	LC	dry air	4m	154	0.48
Mg^{2+} Al^{3+}	2	LC	vial	4m	116	0.43
Mg^{2+} Al^{3+}	2	LC	air	4m	77	0.39
Mg^{2+} Al^{3+}	2	LC	water	4m	58	0.29
Mg^{2+} Al^{3+}	2	HC	-	0	164	0.37
Mg^{2+} Al^{3+}	2	HC	dry N_2	4m	104	0.25
Mg^{2+} Al^{3+}	2	HC	dry air	4m	85	0.25
Mg^{2+} Al^{3+}	2	HC	vial	4m	132	0.33
Mg^{2+} Al^{3+}	2	HC	air	4m	42	0.17
Mg^{2+} Al^{3+}	2	HC	water	4m	66	0.26
Mg^{2+} Al^{3+}	1	LC	-	0	193	0.57
Mg^{2+} Al^{3+}	1	LC	vial	1.5y	95	0.30
Mg^{2+} Al^{3+}	1	LC	water	*2.3m	100	0.43
Mg^{2+} Al^{3+}	2	LC	-	0	183	0.58
Mg^{2+} Al^{3+}	2	LC	vial	1.5y	33	0.13
Mg^{2+} Al^{3+}	2	LC	water	*2.3m	97	0.35
Mg^{2+} Al^{3+}	3	LC	-	0	65	0.29
Mg^{2+} Al^{3+}	3	LC	vial	1.5y	13	0.07
Mg^{2+} Al^{3+}	3	LC	water	*2.3m	12	0.03
Mg^{2+} Al^{3+}	2	LC	-	0	188	0.62
Mg^{2+} Al^{3+}	2	LC	water	2.5m	60	0.24
Zn^{2+} Al^{3+}	5.5	LC	-	0	31	0.15
Zn^{2+} Al^{3+}	5.5	LC	vial	1y	41	0.15
Zn^{2+} Al^{3+}	5.5	LC	water	*2.3m	37	0.14
Mg^{2+} Fe^{3+}	2	LC	-	0	87	0.34
Mg^{2+} Fe^{3+}	2	LC	water	2.5m	26	0.06

*After storage in a vial (time: see line above), subsequently stored in water.

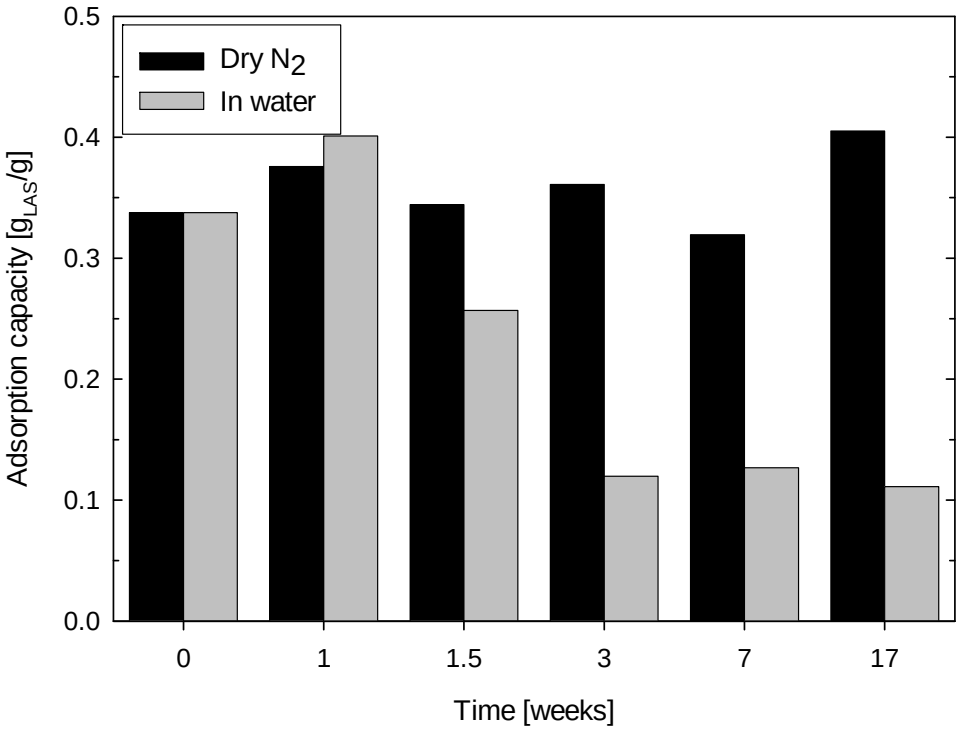

Figure 6: LAS adsorption capacity in time of MgAl-CLDH stored in dry N_2 and in water (M^{2+}/M^{3+} ratio 2; LC initial solutions). Experiments are carried out with 80 ml initial solution (0.5 g_{LAS}/dm^3 water) and 0.1 gram of CLDH.

The surface area and pore volume of LC-CLDH stored in dry N_2 decreased slightly (table 2). The largest decrease in surface area and pore volume was found after storage in water. The presence of water vapour (closed vial and open air) also induces a decrease in surface area and pore volume. The presence of CO_2 (in dry air) does not have any effect. The decrease in adsorption capacity was related to the storage method in the same way as the surface area and pore volume. Storage in dry N_2 had no effect on adsorption capacity (figure 6). The fluctuation of the adsorption capacity is within the error limits. Whereas storage in water decreased adsorption capacity to about 30% of its initial adsorption capacity. In all the adsorption experiments the pH increased, due to the exchange of OH^- ions for LAS molecules. The pH increases with increasing adsorption capacity.

CLDH is hydrophilic and will adsorb water from the air. When CLDH is stored in water, the interconnection between the crystallites is more easily destroyed. After drying, the crystallites form denser aggregates. This decreases the surface area and pore volume and accordingly the adsorption capacity. Furthermore, Al^{3+} is leaching from the brucite-like structure into the water. The amount of Al^{3+} leached to the storage water for HC-CLDH is higher (0.18 mmol/gLDH) compared to LC-CLDH (0.02 mmol/gLDH). This is explained by a higher crystallinity for LC-CLDH. Therefore, CLDHs in this study are further produced with low concentration initial solutions.

Figure 7 represents the LAS adsorption capacity for MgAl-CLDH prepared with ratios 1, 2 and 3. The LAS adsorption capacity obtained for MgAl ratio 1 and 2 are higher

compared to ratio 3. The lower ratio indicates more Al^{3+} cations and by that a higher charge density which should lead to a higher LAS adsorption capacity. MgAl ratio 1 did not result in a higher adsorption capacity compared to ratio 2; this can be caused by the production of other metal oxides next to LDH [2]. Based on the measured adsorption capacity for fresh CLDH, the ratio 2 seems to be optimal and was selected for further experiments. This optimum ratio is comparable to Zhao and Nagy (2004) [27] for the adsorption of sodium dodecyl sulphate onto MgAl-CLDH.

After synthesis the materials have been stored in a vial for 1.5 year. Subsequently the materials were stored in water for two months. After both storage conditions the LAS adsorption capacity, specific surface area and pore volume were measured. The results are presented in figure 7 and table 2.

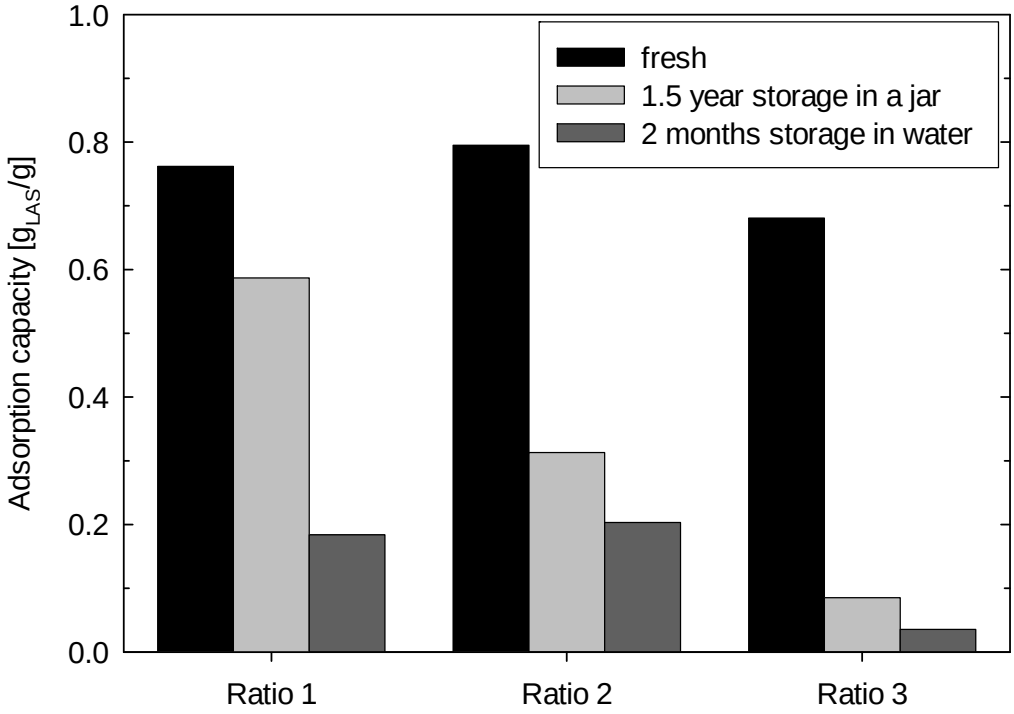

Figure 7: LAS adsorption capacity of CLDH with different Mg/Al ratios (LC initial solutions); fresh, after 1.5 year storage in a jar and after 2 months of storage in water. Experiments are carried out with 80 ml initial LAS solution (1 g_{LAS}/dm^3 water) and 0.1 gram of CLDH.

After 1.5 year of storage, the adsorption capacity reduced dramatically for ratios 2 and 3 but only a small reduction was observed for ratio 1. Subsequently, storing the samples in water for 2 months induced a further reduction of the adsorption capacity of all three CLDH samples (figure 7). The specific surface area and pore volume show a decrease after storing in a vial for 1.5 year (table 2). This can be explained by the rearrangement of the nano sized crystallites of the LDH aggregates. The crystallites form aggregates through interconnection at the edges of different crystallites and the glue effect of amorphous LDH materials [26]. In time the crystallites can slip past each other and form a denser structure, which explains the decrease in surface area, pore volume and thereby the reduction in adsorption capacity. A further reduction of

adsorption capacity after storing in water can be caused by leaching of Al^{3+} from the brucite-like structure.

The last process parameter that was investigated is the type of cations. Four cations were used to produce CLDH: Mg^{2+}, Zn^{2+} and Al^{3+}, Fe^{3+}. Three sets of cations with ratio 2 were used to prepare CLDH starting from an initial solution with a low concentration: MgAl, MgFe and ZnAl-CLDH. The LAS adsorption capacity, specific surface area and pore volume were measured after synthesis and after storage. The results are presented in figure 8 and table 2. MgAl and MgFe-CLDH were stored in water for two months and ZnAl-CLDH was stored in a vial for one year and subsequently stored in water for two months.

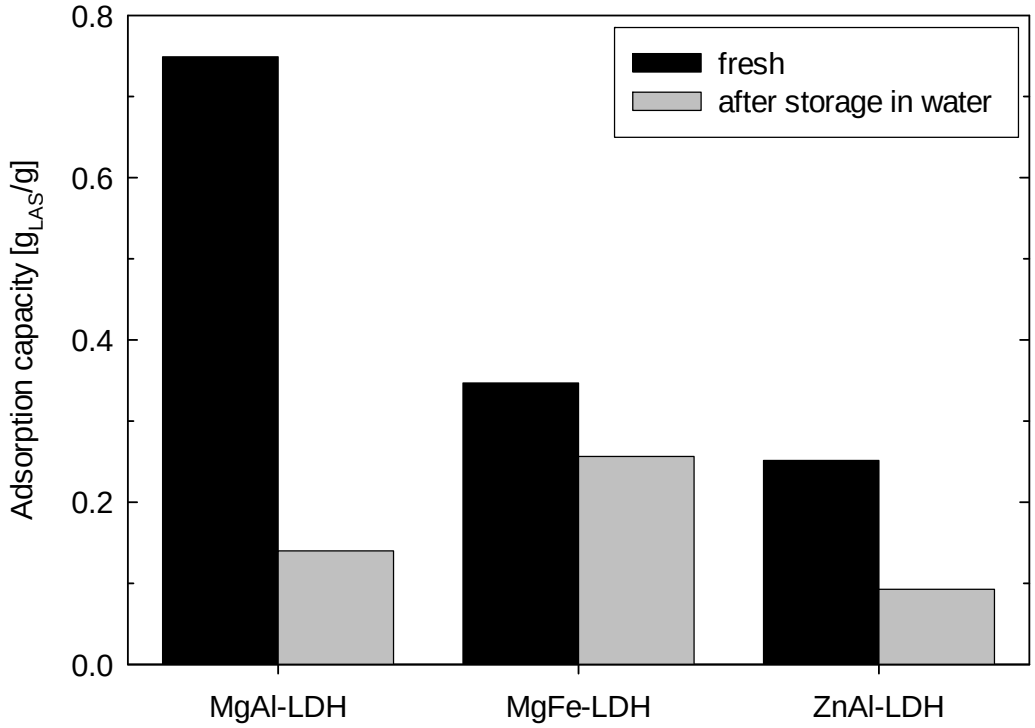

Figure 8: LAS adsorption capacity of MgAl, MgFe and ZnAl-CLDH (Mg^{2+}/Al^{3+} or Fe^{3+} ratio 2; Zn^{2+}/Al^{3+} ratio 5.5; LC initial solutions). Results are given for samples just after preparation (fresh) and after 2 months of storage in water. ZnAl-CLDH was stored beforehand in a vial for 1 year. Experiments are carried out with 80 ml initial solution (1 g_{LAS}/dm^3 water) and 0.1 gram of CLDH.

The adsorption capacity directly after preparation is much higher for MgAl-CLDH compared to MgFe and ZnAl-CLDH (figure 8). This is in agreement with the higher specific surface area and pore volume of MgAl-CLDH as shown in table 2. The XRD measurements of MgAl-LDH and MgFe-LDH already showed a large difference in intensity, which indicates a difference in crystallinity (figure 2 and 3). During MgFe-LDH synthesis only a small amount of MgFe-LDH is formed next to iron oxides (Fe_2O_3) and magnesium oxides (MgO), which explains the lower adsorption capacity. The lower adsorption capacity for ZnAl-CLDH is explained by the lower charge density, because of the lower M^{2+}/M^{3+} ratio (5.5 instead of 2).

The adsorption capacity of the CLDHs after storage in water is reduced mainly for MgAl and ZnAl. The measured adsorption capacity for MgFe-CLDH is mainly the adsorption capacity of Fe_2O_3 and MgO and they seem to be more stable in aqueous surroundings. Therefore, these oxides could be of interest as alternative water stable low cost detergent adsorbents.

3.4. Conclusions

In this work the process parameters of the co-precipitation method to produce LDH and their effect on the LDH structure, stability and adsorption capacity for LAS are investigated. The BET surface area of precipitated LDH (PLDH) is increased after aging (ALDH) and increased further after calcination (CLDH). During calcination the CO_3^{2-} molecules are converted to CO_2, which leaves a porous structure behind. XRD measurements show an increase in crystallinity after aging and a destruction of the layered structure after calcination. The highest adsorption capacity is obtained for CLDH with a M^{2+}/M^{3+} ratio of 1 and 2 because of the higher charge density compared to ratio 3. Storing the CLDH samples in water resulted in a reduction of adsorption capacity and a decrease in surface area and pore volume. This is caused by the rearrangement of the nano size crystallites of which a LDH aggregate exist. The crystallites slip past each other and form a denser structure. The crystallinity can be improved by using low concentration initial solutions; this decreases the leaching of M^{3+} from the brucite-like structure into the water. The ideal storage method is in a dry N_2 atmosphere. The highest LAS adsorption capacity was obtained for MgAl-CLHD, where the production process was not optimal for ZnAl and MgFe-CLDH. The application of CLDH in a small device to re-use laundry rinsing water is not promising for long term use. CLDH is instable and the adsorption capacity of anionic surfactants reduces dramatically in aqueous surroundings.

3.5. References

1. Schouten, N., et al., *Selection and evaluation of adsorbents for the removal of anionic surfactants from laundry rinsing water.* Water Research, 2007. **41**(18): p. 4233-4241 (Chapter 2).
2. Reichle, W.T., *Synthesis of anionic clay minerals (mixed metal hydroxides, hydrotalcite).* Solid State Ionics, 1986. **22**(1): p. 135-141.
3. Holmberg, K., et al., *Surfactants and polymers in aqueous solution*. 2nd ed. 2003, West Sussex, UK: Wiley.
4. Adak, A., M. Bandyopadhyay, and A. Pal, *Removal of anionic surfactant from wastewater by alumina: a case study.* Colloids and Surfaces A: Physicochemical and Engineering Aspects, 2005. **254**(1-3): p. 165-171.
5. Unilever, *Personal communication*. December 2004: Hindustan Unilever Research India, 64 Main Road, Whitefield P.O. Bangalore 560066, India.
6. SudChemie, *Personal communication*. July 2005: Ostenrieder Str. 15, 85368 Moosburg, Germanu.
7. Cavani, F., F. Trifiro, and A. Vaccari, *Hydrotalcite-type anionic clays. Preparation, properties and applications.* Catalysis Today, 1991. **11**(2): p. 173.

8. Ulibarri, M.A., et al., *Hydrotalcite-like compounds as potential sorbents of phenols from water.* Applied Clay Science, 1995. **10**(1-2): p. 131.
9. Pavlovic, I., et al., *Adsorption of acidic pesticides 2,4-D, Clopyralid and Picloram on calcined hydrotalcite.* Applied Clay Science, 2005. **30**(2): p. 125-133.
10. Zhu, M.-X., et al., *Sorption of an anionic dye by uncalcined and calcined layered double hydroxides: a case study.* Journal of Hazardous Materials, 2005. **120**(1-3): p. 163-171.
11. Lazaridis, N.K., A. Hourzemanoglou, and K.A. Matis, *Flotation of metal-loaded clay anion exchangers. Part II: the case of arsenates.* Chemosphere, 2002. **47**(3): p. 319.
12. Lazaridis, N.K., K.A. Matis, and M. Webb, *Flotation of metal-loaded clay anion exchangers. Part I: the case of chromates.* Chemosphere, 2001. **42**(4): p. 373.
13. Lazaridis, N.K. and D.D. Asouhidou, *Kinetics of sorptive removal of chromium(VI) from aqueous solutions by calcined Mg-Al-CO_3 hydrotalcite.* Water Research, 2003. **37**(12): p. 2875.
14. Shin, H.S., et al., *Phosphorus removal by hydrotalcite-like compounds (HTLcs).* Water Science And Technology, 1996. **34**(1-2): p. 161-168.
15. Pavan, P.C., E.L. Crepaldi, and J.B. Valim, *Sorption of anionic surfactants on layered double hydroxides.* Journal Of Colloid And Interface Science, 2000. **229**(2): p. 346-352.
16. Pavan, P.C., et al., *Adsorption of sodium dodecylsulfate on a hydrotalcite-like compound. Effect of temperature, pH and ionic strength.* Colloids And Surfaces A-Physicochemical And Engineering Aspects, 1999. **154**(3): p. 399-410.
17. Pavan, P.C., G.d.A. Gomes, and J.B. Valim, *Adsorption of sodium dodecyl sulfate on layered double hydroxides.* Microporous and Mesoporous Materials, 1998. **21**(4-6): p. 659-665.
18. Kopka, H., K. Beneke, and G. Lagaly, *Anionic surfactants between double metal hydroxide layers.* Journal of Colloid and Interface Science, 1988. **123**(2): p. 427.
19. Anbarasan, R., W.D. Lee, and S.S. Im, *Adsorption and intercalation of anionic surfactants onto layered double hydroxides - XRD study.* Bulletin of Materials Science, 2005. **28**(2): p. 145.
20. Reis, M.d., et al., *Effects of pH, temperature, and ionic strength on adsorption of sodium dodecylbenzenesulfonate into Mg-Al-CO3 layered double hydroxides.* Journal of Physics and Chemistry of Solids, 2004. **65**(2-3): p. 487.
21. Zou, K., H. Zhang, and X. Duan, *Studies on the formation of 5-aminosalicylate intercalated Zn-Al layered double hydroxides as a function of Zn/Al molar ratios and synthesis routes.* Chemical Engineering Science, 2006. **62**(7): p. 2022-2031.
22. Trujillano, R., et al., *Preparation, physicochemical characterisation and magnetic properties of Cu-Al layered double hydroxides with CO32- and anionic surfactants with different alkyl chains in the interlayer.* Physica B: Condensed Matter, 2006. **373**(2): p. 267-273.

23. Kloprogge, J.T., L. Hickey, and R.L. Frost, *The effects of synthesis pH and hydrothermal treatment on the formation of zinc aluminum hydrotalcites.* Journal of Solid State Chemistry, 2004. **177**(11): p. 4047-4057.
24. Tao, Q., et al., *Synthesis and characterization of layered double hydroxides with a high aspect ratio.* Journal of Solid State Chemistry, 2006. **179**(3): p. 708-715.
25. Frost, R.L., W.N. Martens, and K.L. Erickson, *Thermal decomposition of the hydrotalcite: Thermogravimetric analysis and hot stage Raman spectroscopic study.* Journal of Thermal Analysis and Calorimetry, 2005. **82**(3): p. 603.
26. Xu, Z.P., et al., *Stable suspension of layered double hydroxide nanoparticles in aqueous solution.* Journal of the American Chemical Society, 2006. **128**(1): p. 36-37.
27. Zhao, H. and K.L. Nagy, *Dodecyl sulfate-hydrotalcite nanocomposites for trapping chlorinated organic pollutants in water.* Journal of Colloid and Interface Science, 2004. **274**(2): p. 613-624.

4. Kinetic analysis of anionic surfactant (LAS) adsorption from aqueous solution onto activated carbon and layered double hydroxide with the zero length column method

Abstract

Low cost adsorption technology offers high potential to clean up laundry rinsing water. From an earlier selection of adsorbents [1], layered double hydroxide (LDH) and granular activated carbon (GAC) proved to be interesting materials for the removal of anionic surfactant, linear alkyl benzene sulfonate (LAS), which is the main contaminant in rinsing water. The main research question is to identify adsorption kinetics of LAS onto GAC-1240 and LDH. The influence of pre-treatment of the adsorbent, flow rate, particle size and initial LAS concentration on the adsorption rate is investigated in a zero length column (ZLC) set-up. The rate determining step is obtained by fitting an adsorption model and an ion exchange model describing intra particle diffusion to the experimental data. GAC-1240 is well described with the adsorption model following Fick's second law. The effective diffusion coefficient of GAC-1240 is $1.3 \cdot 10^{-10} \pm 0.2 \cdot 10^{-10}$ m^2/s and is not influenced by particle sizes or initial LAS concentrations. The ion exchange of LAS onto LDH is not well described by the ion exchange model. The rate determining step is obtained by comparing several models to different experimental data. A double layer model resulted in a good description of the experimental data. At the outer surface of LDH a stagnant film resistance originating from an electric double layer is assumed. The double layer mass transfer coefficient is $7 \cdot 10^{-5} \pm 2 \cdot 10^{-5}$ m/s.

4.1. Introduction

Shortage of water is a growing global problem. One way of dealing with this problem is the development of technologies for wastewater clean-up and re-use. Laundry accounts typically for more than half of the daily domestic water consumption in countries like India. The major part of laundry water is rinsing water, which is relatively clean and therefore highly suitable for clean-up and re-use.

The current work is part of a project that aims to develop low cost technologies for the local decentralised recycling of laundry rinsing water. The basic idea is to clean the polluted rinse water to allow multiple use cycles. When the main contaminants have been removed from the rinsing water, it can be re-used for household or irrigation purposes. Main contaminants are the added detergent ingredients and "dirt" released from the fabrics during rinsing. The focus of the current paper is on removing anionic surfactants, as the main active component of detergents used in low income markets. Typically, hand wash detergent powders contain 15 to 30% anionic surfactants. Linear alkyl benzene sulfonate (LAS) is the most commonly used anionic surfactant in detergent powders [2]. A rough estimate of the worldwide surfactant production is 10 million tonnes per year of which anionic surfactants account for about 60% [3]. The conventional methods for surfactant removal from water involve processes such as chemical and electrochemical oxidation, membrane technology, chemical precipitation, photo-catalytic degradation, adsorption and various biological methods [3, 4]. Many of these processes are not cost effective and/or not suitable for application on a household scale.

Adsorption technology offers high potential to clean the laundry rinsing water. Adsorption can be low cost and can be applied in small devices and is therefore suitable for use on low-income household scale. Our previous research on adsorbent selection showed that activated carbon and layered double hydroxide (LDH) proved to be interesting adsorbents for LAS removal. Adsorption of LAS onto activated carbons is dominated by hydrophobic interactions while adsorption onto LDH is dominated by ionic interactions. Both materials demonstrated a high adsorption capacity per dollar of material [1]. Activated carbons are often used in water purification [5]. They offer the advantage of removing a wide range of organic compounds. Layered double hydroxides derive their name from their structure. They consist of two brucite like layers; sheets of octahedrons of magnesium hydroxide. If magnesium cations are partly replaced by aluminium cations, the layer will be positively charged. In order to balance the residual charge, anions are intercalated between the layers. The intercalated anion is exchanged by LAS anions [6].

To develop a low cost adsorption device for recycling of laundry rinsing water, it is needed to gain insight in the adsorption kinetics of LAS. For this reason the adsorption kinetics of LAS onto activated carbon and LDH is studied in this work with the zero length column (ZLC) method. The influence of pre-treatment of the adsorbent, flow rate, particle size and initial LAS concentration on the LAS adsorption rate were investigated. The ZLC method has been established by Eic and Ruthven (1988) [7] for gas-zeolite systems and later Ruthven and Stapleton (1993) [8] expanded the method

to liquid systems. The method applies a differential bed where axial dispersion can be neglected. The effective diffusion coefficient can be calculated by fitting the experimental data to a model. Recently, Djekic (2008) [9] developed a simplified model that describes the differential mass balance in a macro porous particle. This model is referred to as the adsorption model and is used to describe the adsorption of LAS onto activated carbon. The adsorption kinetics onto LDH are often described with simple models, such as the first order model, second order model and Elovich model [10-17]. Valverde et. al. [18] describes a model for ion exchange in a macro porous particle. This model is based on the differential mass balance for ion exchange and is used to analyse the adsorption kinetics of LAS onto LDH. The model parameters have been obtained by fitting the adsorption model and ion exchange model to the experimental data.

4.2. Theory

4.2.1. Adsorption model (activated carbon)

The kinetic model that describes the adsorption in a zero length column is based on the mass balance for the adsorbate. The following assumptions are made [9, 19]:

- no external mass transfer; the flow rate is sufficiently high to neglect the film layer resistance around the particle
- the rate of adsorption is controlled by intra particle diffusion only
- no concentration gradient over the adsorbent bed; the length of the bed is sufficiently small
- the adsorbent consists of spherical particles with uniformly distributed pores
- equilibrium between the solid and liquid phase is described by the Langmuir isotherm model
- intra particle diffusion can be described by Fick's second law

The differential mass balance of an adsorbate in a macro porous spherical particle is given by Ruthven (1984) [20]:

$$\left(1-\varepsilon_p\right)\rho_s\frac{\partial q}{\partial t}+\varepsilon_p\frac{\partial C}{\partial t}=D_{eff}\left(\frac{\partial^2 C}{\partial r^2}+\frac{2}{r}\frac{\partial C}{\partial r}\right) \qquad (1)$$

where ε_p is the particle porosity, ρ_s is the solid density of the particle, q is the LAS adsorption capacity of the particle, t is time, C is the LAS concentration in the solution, D_{eff} is the effective diffusion coefficient and r is the radial position within the particle.

Equilibrium between LAS on the solid phase and in the liquid phase is described with the Langmuir isotherm model [1]:

$$\frac{q}{q_m}=\frac{bC}{1+bC} \qquad (2)$$

where q_m is the maximum capacity of particle and b is the affinity coefficient. Equation (1) can be rewritten by inserting equation (2), the Langmuir isotherm model:

$$\frac{\partial C}{\partial t} = \left[\frac{(1-\varepsilon_p)\rho_s b q_m}{(1+bC)^2} + \varepsilon_p \right]^{-1} D_{eff} \left(\frac{\partial^2 C}{\partial r^2} + \frac{2}{r}\frac{\partial C}{\partial r} \right) \quad (3)$$

The initial conditions are:
For t=0 and r=R: $C=C_0$ and (4)
for t=0 and r<R: C=0 (5)
where R is the radius of the particle and C_0 is the initial LAS concentration.

The boundary conditions are:
For t>0 and r=R: $C=C_{bulk}$ (6)
for t>0 and r=0: $\left(\frac{\partial C}{\partial r}\right) = 0$, due to symmetry (7)
where C_{bulk} is the bulk concentration. The bulk concentration is also the concentration at the particle interface (R) since external mass transfer can be neglected. The bulk concentration is given by the mass balance:

$$\frac{dC_{bulk}}{dt} = -\frac{m}{V}\frac{d\bar{q}}{dt} \quad (8)$$

where V is the volume of the LAS solution, m the mass of the adsorbent and $\bar{q}$ is the average capacity of the adsorbent which is calculated by:

$$\bar{q} = \frac{3}{R^3}\int_0^R r^2 q dr \quad (9)$$

4.2.2. Ion exchange model (LDH)

A mathematical model for ion exchange is proposed by Valverde et. al. [18]. The model describes a flux of ions A entering the particle and a flux of ions B leaving the particle. The flux of LAS into the particle is assumed to be positive. Both pore diffusion and surface diffusion are taken into account. The differential mass balance of an adsorbate A in a macro porous spherical particle changes to:

$$(1-\varepsilon_p)\rho_s \frac{\partial q_A}{\partial t} + \varepsilon_p \frac{\partial C_A}{\partial t} = \frac{\varepsilon_p}{r^2}\frac{\partial}{\partial r}\left(-r^2 N_{pA}\right) + \frac{(1-\varepsilon_p)\rho_s}{r^2}\frac{\partial}{\partial r}\left(-r^2 N_{sA}\right) \quad (10)$$

$$N_{pA} = \frac{-D_{pA}D_{pB}C_0}{C_A(D_{pA}-D_{pB}) + D_{pB}C_0}\frac{\partial C_A}{\partial r} \quad (11)$$

$$N_{sA} = \frac{-D_{sA}D_{sB}q_m}{q_A(D_{sA}-D_{sB}) + D_{sB}q_s}\frac{\partial q_A}{\partial r} \quad (12)$$

where N_{pA} is the flux of LAS in the pores, D_{pA} is the diffusion coefficient of LAS in the pores and D_{pB} is the diffusion coefficient of OH^- in the pores. N_{sA} is the flux of LAS at the solid phase, D_{sA} is the diffusion coefficient of LAS at the solid phase and D_{sB} is the diffusion coefficient of OH^- at the solid phase.

Equilibrium between LAS on the solid phase and in the liquid phase is also described with the Langmuir isotherm model. Equation (13), showing the first derivative of q in time, is added separately to the model:

$$\frac{\partial q}{\partial t} = \frac{b\frac{\partial C}{\partial t}}{(1+bC)^2} \qquad (13)$$

The initial conditions are:
For t=0 and r=R: $C_A=C_0$ and $C_B=0$ (pH=7) (14)
for t=0 and r<R: $C_A=0$ (15)

The boundary conditions are:
For t>0 and r=R: $C_A=C_{bulk}$ (16)
for t>0 and r=0: $\left(\frac{\partial C_A}{\partial r}\right)=0$, due to symmetry (17)

The ion exchange model is further similar to the adsorption model.

4.2.3. Parameter estimation

The kinetic model equations (3), (8) and (9) with initial conditions (4) and (5) and boundary conditions (6) and (7) are implemented in g-PROMS 3.0.3 (Process Systems Enterprise). The value of D_{eff} is obtained by fitting the model to experimental data using the parameter estimation function.

The ion exchange model equations (10), (11), (12), (13), (8) and (9) with initial conditions (14) and (15) and boundary conditions (16) and (17) are also implemented in g-PROMS. The estimation is started without equation (12). The diffusion coefficient (D_{pB}) is taken from Valverde et al. [18] and the D_{pA} is obtained by estimating by hand. This is repeated by estimating D_{pB} and keeping D_{pA} at the value obtained from the last estimation. Subsequently, equation (12) is added. The values of D_{sA} and D_{sB} are also taken from Valverde et. al [18] and the estimation approach is equal to the estimation of D_{pA} and D_{pB}.

4.3. Materials and Methods

4.3.1. Materials

The anionic surfactant, linear alkyl benzene sulfonate (LAS) was obtained from Unilever R&D, Vlaardingen, The Netherlands. Purity is around 92 wt% and the chain length is C_{10} to C_{13} (equally distributed; average molecular weight of LAS-acid is 312 g/mol). The critical micelle concentration (CMC) is 2 mM [21]. From earlier investigation [1] activated carbon and LDH proved to be interesting adsorbents. The adsorbents used in this investigation were powdered materials. The application of a powdered adsorbent in a column will induce a large pressure drop. Therefore, granular adsorbents with the same material properties as the adsorbents in the earlier investigation were obtained. Granular activated carbon, GAC-1240 was supplied by

Norit, Amersfoort, The Netherlands and extrudates of LDH were supplied by Akzo Nobel, Arnhem, The Netherlands.

4.3.2. Characterization

The activated carbon granules and LDH extrudates were grinded and sieved in four fractions; 100-315 μm, 315-500 μm, 500-800 μm and 800-1000 μm. The specific surface area, pore size and pore volume distribution of these fractions were measured using nitrogen adsorption at -196^{o}C (liquid nitrogen temperature) with the Micromeritics Tristar 3000. The samples are pre-treated overnight to remove water and other contaminants from the pores. During the pre-treatment, a nitrogen flow is applied and the samples are heated to 105^{o}C for several hours. The solid density of LDH is measured with a pycnometer (Micromeritics, AccuPyc 1330).

4.3.3. Adsorption equilibrium experiments

The adsorption equilibrium experiments were conducted at different initial LAS concentrations ranging from 0.05 to 3 g/dm^3 milli-Q water. 0.065 grams of GAC-1240 and 0.091 grams of LDH and 80 ml of LAS solution were mixed in a screw capped flask and placed in a shaking bath (Julabo SW22) at 25^{o}C. With a preliminary experiment the equilibrium time was determined to be 48 hours; equilibrium was reached well within this time. The water phase was sampled with a syringe equipped with a filter (Spartan 30/0.45RC (0.45μm)) to remove suspended solids. The LAS concentration was measured by spectrophotometry at 223 nm with an accuracy of 2% (Shimadzu UV-1650PC).

4.3.4. ZLC set-up

The zero length column (ZLC) set-up that was used to determine the adsorption kinetics of LAS on GAC-1240 and LDH is illustrated in figure 1. The set-up consists of a pump (Knauer Preparative HPLC Pump 1800), a UV detector (Knauer Smartline 2500) and a column (Omnifit chromatography column with a 6.6 mm internal diameter and two adjustable end-pieces).

The set-up can be operated in a non-recycle and recycle mode. In the non-recycle mode the inlet tube and outlet tube are placed in two separate beakers. This mode is used for calibration and cleaning purposes. In the recycle mode the inlet tube and outlet tube are placed in the same beaker. The beaker is equipped with a stirrer to assure good mixing. This mode is used for the kinetic experiments.

The adsorbent will be used in a device to clean up laundry rinsing water. The operation time of this device should be limited to a relatively short period of time in order to be user friendly. Therefore, a high ratio of adsorbent mass to LAS solution volume is used in the ZLC experiments. The experiments were conducted according to the following procedure. The adsorbents were pre-treated to remove air from the pores; milli-Q water was added to the adsorbent and vacuum was applied. The time of

treatment depends on the material. Since GAC-1240 is hydrophobic the treatment time was 16, 24 and 31 hours, LDH is hydrophilic and the required treatment time was only 30 and 60 minutes. The column was packed with the adsorbent. The bed height was 4 mm (0.065 grams of GAC-1240 and 0.091 grams of LDH). The column was equilibrated with nitrogen-sparged milli-Q water. After equilibration water was replaced with 50 ml LAS solution and the LAS concentration was monitored with the UV detector at 223 nm. All the experiments were conducted at room temperature (around 20^{o}C).

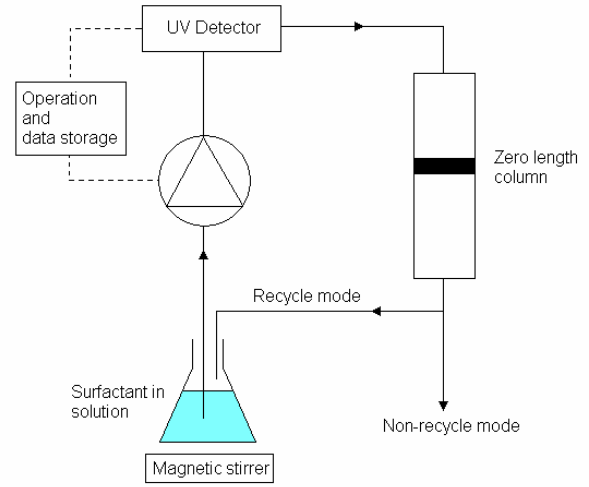

Figure 1: Schematic representation of the zero length column set-up.

4.3.5. Calibration of the ZLC set-up

The water in the set-up will dilute the initial solution and therefore needs to be known. The volume of the set-up is calculated by measuring the difference in concentration between the recycle mode and non-recycle mode. The column is filled with spherical glass beads (particle size 1 mm) to a bed height of 4 mm. The volume of the ZLC set-up can be calculated with equation (18):

$$C_{NRM} V = C_{RM} (V + V_{ZLC}) \qquad (18)$$

where C_{NRM} is the LAS concentration in the non-recycle mode, V is the volume of the LAS solution, C_{RM} is the LAS concentration in the recycle mode and V_{ZLC} is the volume of the ZLC set-up. Figure 2 shows the LAS concentration in the non-recycle mode and recycle mode. The calculated volume of the ZLC set-up was found to be 11.15 ml. The concentration of the recycle mode was taken as initial concentration C_0 in the experiments.

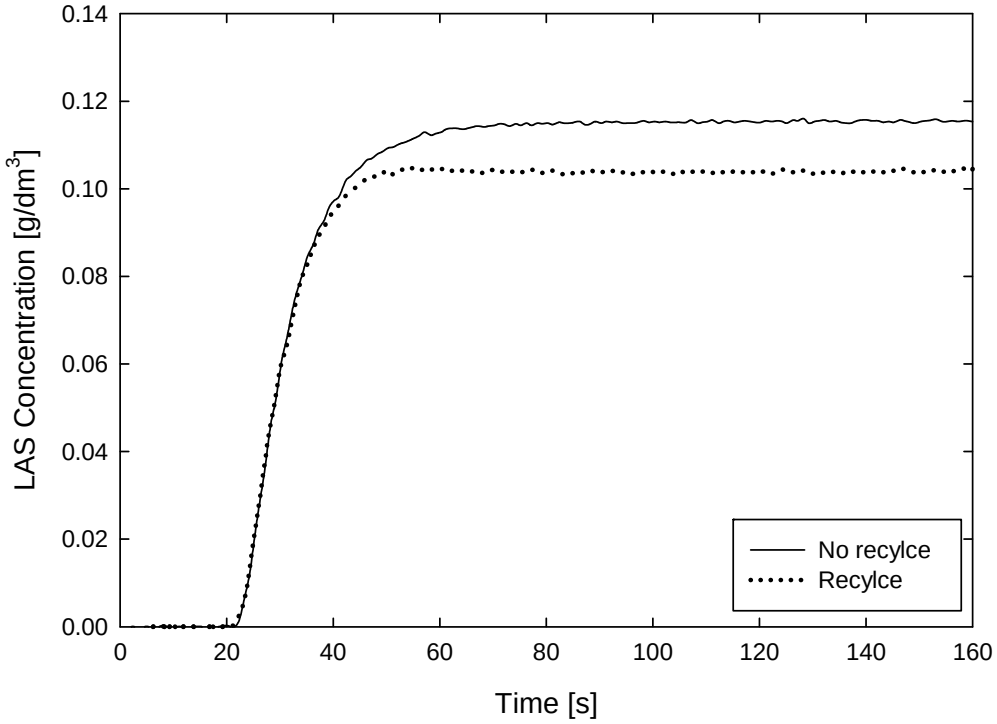

Figure 2: LAS concentration in recycle and non-recycle mode. Flow rate is 20 ml/min.

4.4. Results and discussion

4.4.1. Characterization

Table 1 shows the properties of the adsorbents and the adsorbent fractions. The solid density of GAC-1240 is assumed to be equal to that of graphite [22]. The solid density of LDH is measured with a pycnometer. The porosity is calculated from the solid density and total pore volume. The specific surface area, pore volume and average pore size remain almost the same among the different particle size fractions of the adsorbents (table 1).

Table 1: Properties of adsorbents and adsorbent fractions.

Material	Raw material	Activation method	Particle porosity ε_p [-]	Solid density ρ_s [g/cm^3]
GAC-1240	coal	steam	0.57	2.34
LDH dry	-	-	0.51	3.13
Particle size [µm]	Specific surface area (BET) [m^2/g]	Pore volume [cm^3/g] at p/p_0=0.99	Average pore size [nm]	
GAC-1240				
100-315	1071	0.60	4.2	
315-500	1159	0.65	4.1	
500-800	1131	0.64	4.2	
800-1000	1071	0.61	4.3	
LDH				
100-315	132	0.34	8.8	
315-500	136	0.35	8.7	
500-800	131	0.33	8.6	
800-1000	121	0.34	9.5	

4.4.2. Adsorption equilibrium experiments

The LAS adsorption isotherms of GAC-1240 and LDH are shown in figure 3. A clear difference can be distinguished between the adsorption isotherm of activated carbon (GAC-1240) and LDH. As described in Schouten, et. al. [1] the adsorption isotherm depends on the interaction of LAS with the surface of the adsorbent and the pore size of the adsorbent. The ionic interactions between LAS and LDH are stronger than the hydrophobic/aromatic interactions between LAS and activated carbon. Furthermore, LDH consists of larger pores compared to GAC-1240 (table 1). The micro pores of GAC-1240 are not accessible for the LAS molecules. This results in a higher adsorption capacity of LDH compared to GAC-1240.

The data are fitted to the well-known Langmuir model, which was selected because of its simplicity and previously demonstrated ability to describe surfactant adsorption [1]. The Langmuir isotherm model gives a good description of both adsorption isotherms. The Langmuir parameters are obtained by fitting the experimental data with the Langmuir isotherm model and are shown in table 2. The initial slope of the LDH isotherm is steeper compared to GAC-1240, which is caused by the stronger interactions. For GAC-1240 the maximum adsorption capacity q_m is reached at lower equilibrium concentrations, therefore the affinity coefficient b is higher compared to LDH. The maximum adsorption capacity of LDH is three times higher than GAC-1240, which was already explained above.

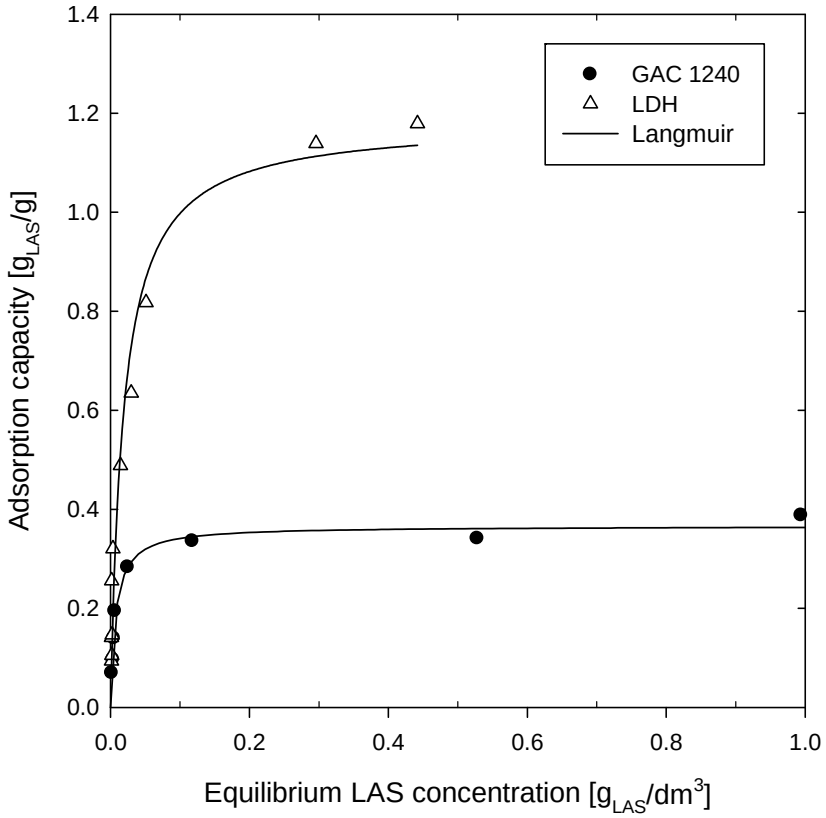

Figure 3: Adsorption isotherms of LAS for GAC-1240 and LDH. The symbols are experimental data and the lines are the fitted Langmuir isotherm model. The obtained Langmuir parameters are shown in table 2.

Table 2: Langmuir isotherm parameters fitted from the experimental data in figure 3.

Material	b [dm^3/g]	q_m [g_{LAS}/g]
GAC-1240	137 ± 18	0.37 ± 0.01
LDH	53 ± 11	1.18 ± 0.07

4.4.3. Pre-treatment/reproducibility

Figure 4 shows the influence of pre-treatment time of GAC-1240 (A) and LDH (B) on the LAS adsorption rate. Pre-treatment is performed to remove air from the pores and fill the pores with water. Milli-Q water was added to the GAC-1240 samples and exposed to vacuum applied for 16, 24 and 31 hours. LDH is hydrophilic and therefore these samples needed to be exposed to vacuum for only 30 and 60 minutes. Different times were applied to obtain the necessary pre-treatment time. There is no very clear relation between the LAS adsorption rate and the pre-treatment times for GAC-1240 samples (figure 4A). To be sure that the pre-treatment time does not influence the subsequent experiments, each GAC-1240 sample was pre-treated for 16 hours. LDH shows a difference between the pre-treated and not pre-treated samples (figure 4B). In water LDH tends to swell due to the hydration of the layers [23]. This results in larger pores and an increase in internal volume and therefore a higher adsorption rate. There is no difference between 30 and 60 minutes pre-treatment time, therefore LDH is pre-

treated for 30 minutes in the subsequent experiments. The reproducibility of three experiments appeared within 3% for both materials.

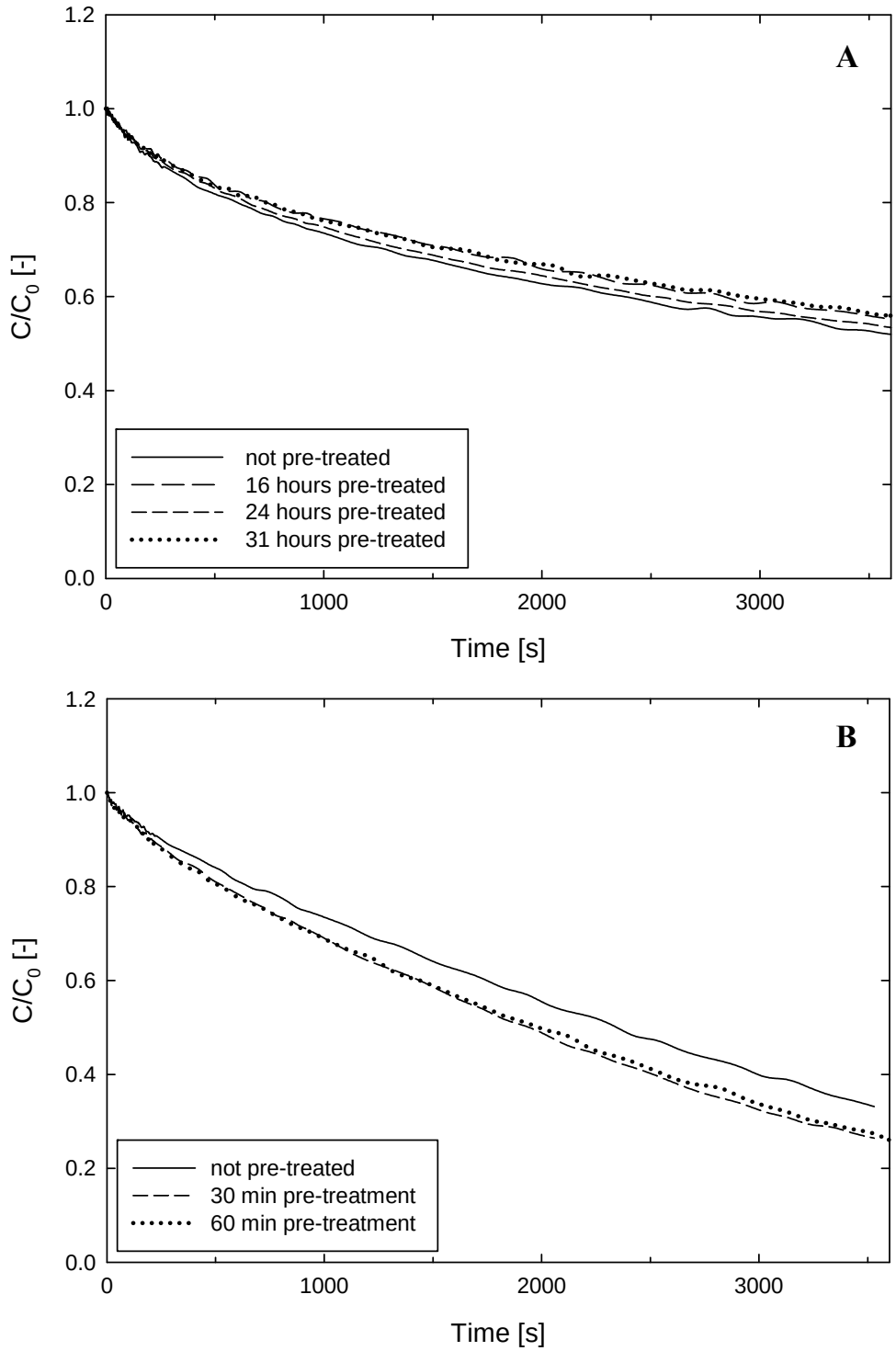

Figure 4: Relative LAS concentration in time for GAC-1240 (A) and LDH (B) with different pre-treatment times. The initial LAS concentration is 0.09 g/dm^3, the adsorbent particle size is 500-800 µm and the flow rate is 60 ml/min for GAC-1240 and 20 ml/min for LDH.

4.4.4. Influence of flow rate

The influence of flow rate on the LAS adsorption rate for GAC-1240 and LDH is shown in figure 5A and B, respectively. The adsorption rate is a combination of external and internal mass transfer. To eliminate the contribution of external mass transfer the flow rate is increased. For GAC-1240 (figure 5A), there is no significant change in the relative LAS concentration in time at flow rates higher than 40 ml/min for the smallest particles (100-315 μm). For LDH (figure 5B) this is valid above 60 ml/min. A flow rate of 60 ml/min is applied for the subsequent experiments for both materials and the resulting data is used to estimate the effective diffusion coefficient.

By comparing figure 5A with 5B it is clearly seen that the LAS adsorption rate onto LDH is faster compared to GAC-1240. It must be taken into account that the amount of LDH is higher compared to GAC-1240 (0.065 grams of GAC-1240 and 0.091 grams of LDH). At time equals t=1000 seconds the relative LAS concentration of GAC-1240 is around 0.4 and LDH is below 0.2. This difference is larger than the difference in mass. This indicates that the diffusion of LAS into LDH is faster compared to GAC-1240 and the LDH diffusion coefficients are expected to be higher compared to the GAC diffusion coefficients.

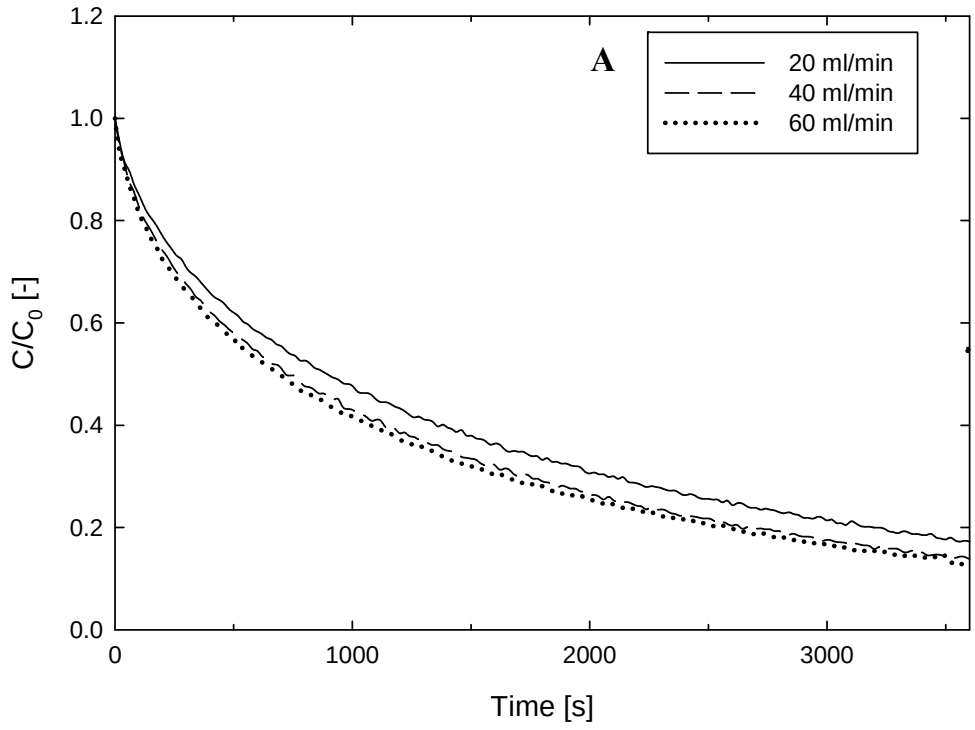

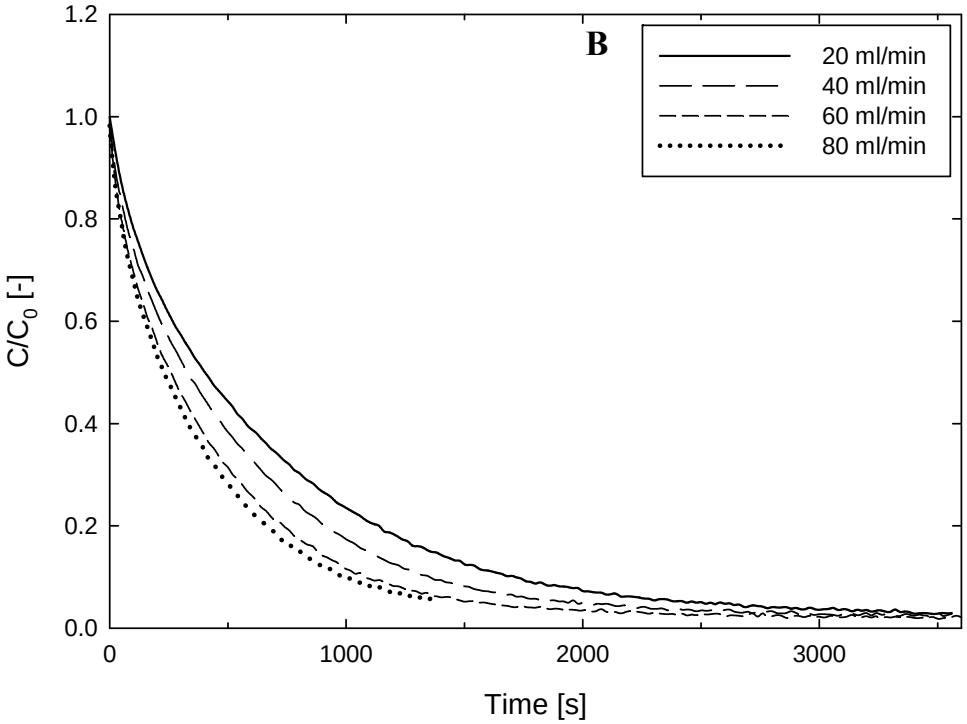

Figure 5: Relative LAS concentration in time for GAC-1240 (A) and LDH (B) with different flow rates. The initial LAS concentration is 0.09 g/dm^3 and adsorbent particle size is 100-315 µm.

4.4.5. Influence of particle size

The influence of particle size on the LAS adsorption rate is shown in figure 6 for GAC-1240. As expected, the LAS adsorption rate increases significantly with decreasing particle size. Figure 6 illustrates that the adsorption model (equations 3 to 9) provides a good description of the LAS adsorption process onto GAC-1240.The experimental results can be fitted with the same effective diffusion coefficient for each particle size (table 3). The obtained average effective diffusion coefficient of LAS in GAC-1240 is $1.3 \cdot 10^{-10} \pm 0.2 \cdot 10^{-10}$ m^2/s. The molecular diffusion coefficient of LAS in water is about $4 \cdot 10^{-10}$ m^2/s [24]. Both diffusion coefficients are related according to equation (19).

$$D_{eff} = \frac{\varepsilon_p}{\tau} D_m \qquad (19)$$

where τ is the tortuosity and D_m the molecular diffusion coefficient in water. For a porosity ε_p of 0.51, this results in a tortuosity of about 2, which is a realistic value [5].

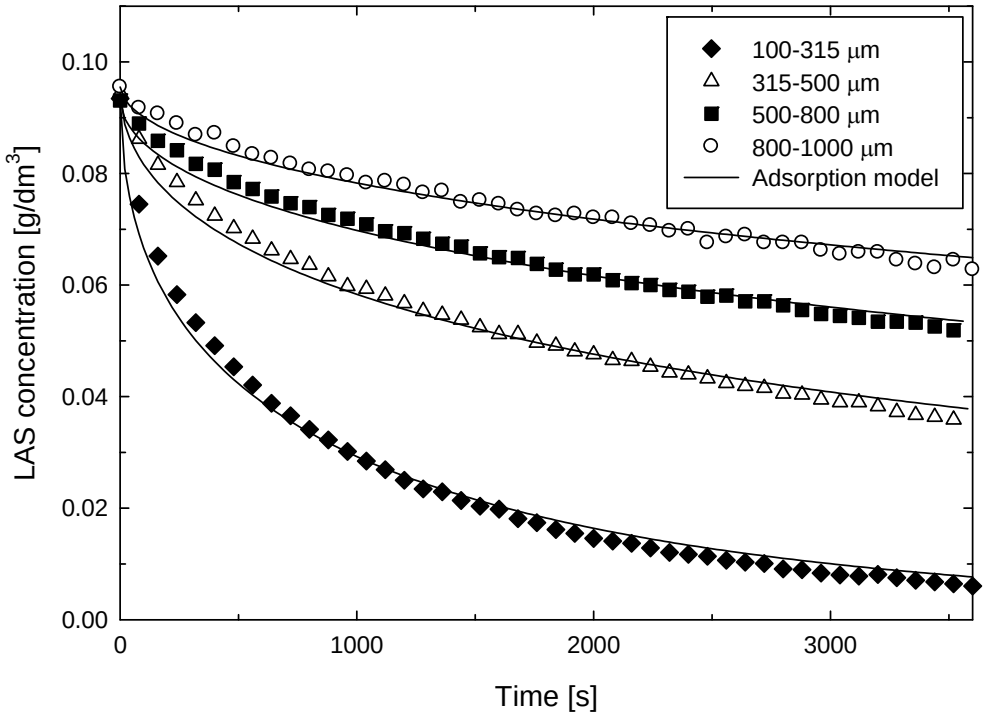

Figure 6: LAS concentration in time for GAC-1240 with different particle sizes. The initial LAS concentration is 0.09 g/dm^3 and the flow rate is 60 ml/min. The solid lines represent the results of the adsorption model.

Table 3: Effective diffusion coefficient obtained from fitting experimental data with the adsorption model for GAC-1240.

Particle size [μm]	100-315	315-500	500-800	800-1000
D_{eff} [m^2/s]	$1.4 \cdot 10^{-10}$	$1.4 \cdot 10^{-10}$	$1.2 \cdot 10^{-10}$	$1.3 \cdot 10^{-10}$

The adsorption mechanism of LAS onto LDH is ion exchange [6]. LAS molecules are exchanged with hydroxide ions in between the layers of the LDH. This is confirmed by an increase in pH from 7 to 10 during the experiment. Zagorodni (2007) [25] describes the steps of the ion exchange mechanism: (1) diffusion in the solution, (2) diffusion through the film around the particle, (3) diffusion in the particle and (4) ion exchange reaction. Three rate determining steps can be considered: diffusion through the film around the particle, diffusion in the particle and ion exchange reaction.

Figure 7 shows the LAS adsorption rate of LDH and the predictions of the adsorption model (equations 3 to 9) and ion exchange model (equations 8 to 17). The adsorption model is not suited to describe the experimental data of LDH. In order to reach the equilibrium concentration at the end of the experiment, the model predicts a curve which is far below the experimental data. The associated effective diffusion coefficient ($2.8 \cdot 10^{-8}$ m^2/s) is unrealistic because it is two orders of magnitude higher than the molecular diffusion coefficient of LAS in water ($4 \cdot 10^{-10}$ m^2/s [24]). The adsorption model is clearly not suitable. The adsorption mechanism of LAS onto LDH is based on ion exchange and therefore, the fit of the ion exchange model (IE model) is added to figure 7. From these results it is evident that the ion exchange model is also not able to describe the experimental data of LDH. The fits are better compared to the adsorption

model, because surface adsorption is added to the model which results in four diffusion coefficients to fit. At the start of the experiment the diffusion coefficient of OH^- is rate determining. Towards the end the uptake process is determined by the diffusion coefficient of LAS. To fit the ion exchange model to the experimental results the diffusion coefficient of OH^- should be decreased compared to the initial value to delay the initial adsorption rate and reach the experimental values. The diffusion coefficient of LAS should be increased compared to the initial value to accelerate the adsorption rate at the end and reach the experimental values. Following this explanation, the diffusion coefficient of OH^- would be lower compared to the diffusion coefficient of LAS, which is not expected. The best fit by hand does not give a satisfying result. It seems that the LAS adsorption rate onto LDH is not limited by diffusion in the particle.

Much research has been reported on the adsorption of anionic components onto LDH [10-17]. In these studies the first order model, pseudo second order model and Elovich model have been used to correlate the experimental results. In many studies the LAS adsorption rate onto LDH is very well described by the first order model, which is also the case in this work (R^2=0.99). The main conclusion postulated in literature is that the ion exchange reaction (chemisorption) is rate determining. These investigations were carried out with one particle size of LDH. Figure 8 shows the results of the LAS adsorption rate onto LDH with different particle sizes. It is very clear that the particle size has an influence on the LAS adsorption rate. Assuming that the ion exchange reaction would be the rate determining step, it is not expected that the particle size has an influence on the LAS adsorption rate.

Another possible rate determining step is film diffusion [25]. Diffusion through a film (external mass transfer) was not expected to be the rate determining step. The flow rate was sufficiently high and no difference in LAS adsorption rate was observed (figure 5B). However, it is well known that adsorption of ionic molecules onto an oppositely charged ionic surface form an electric double layer at the surface of the ion exchange material [25, 26]. Ionic surfactant molecules can form bilayers at an oppositely charged surface [3]. It is also known from literature that this bilayer can cause an extra resistance for example in liquid membranes [27, 28]. The resistance of an electric double layer of small ions at an ion exchange membrane is described by Park et. al. (2006) [29, 30]. The electric double layer causes a resistance especially at low concentrations. To further investigate the exact composition of a double layer with resistances, electrical impedance spectroscopy should be performed. To develop this method is outside the scope of this investigation and will therefore not be further investigated. Summarizing the above, it is plausible that a double layer or a bilayer of surfactants can cause a film layer resistance.

Double layer model

Zagorodni (2007) [25] describes mass transfer for ion exchange and states that the formation of a thin film of solution at the surface of an ion exchange material is unavoidable. Rigorous agitation can reduce the thickness of the film but can never take

it off completely. This so called electric double layer is described by equation 20 and replaces boundary condition (equation 6) in the adsorption model:

$$D_{eff}\left(\frac{\partial C_A}{\partial r}\right) = k_{DL}\left(C_{bulk} - C_A\right) \qquad (20)$$

where k_{DL} is the double layer mass transfer coefficient. The double layer model is based on the adsorption model and the double layer coefficient (k_{DL}) estimated. The diffusion coefficient was not rate determining and was estimated around $3.6 \cdot 10^{-7}$ m^2/s. The resistance is now totally situated in the double layer outside the particle. As illustrated by figure 7, the double layer model resulted in a very good fit.

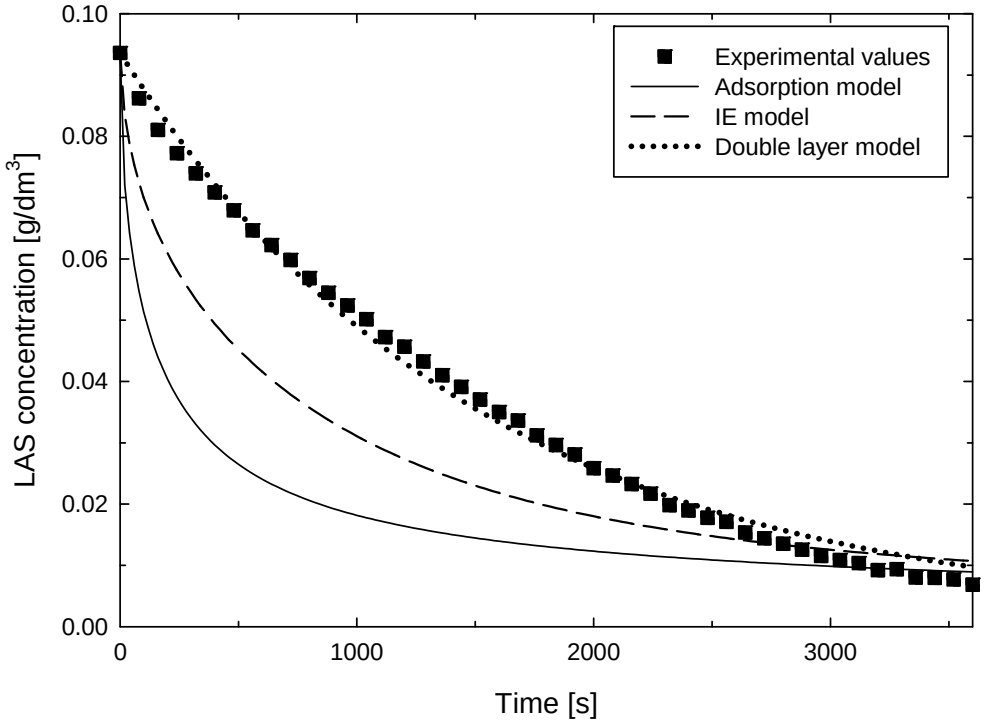

Figure 7: LAS concentration in time for LDH with results from different models (IE is ion exchange). The initial LAS concentration is 0.09 g/dm^3, the particle size is 500-800 µm and the flow rate is 60 ml/min.

Figure 8A shows the results for the LAS adsorption rate onto LDH with different particle sizes and the fits of the double layer model. The estimated double layer coefficients are listed in table 4. The estimated double layer coefficients are not related to the particle size (table 4). To confirm this figure 8B is added which shows the model simulations for an average double layer coefficient of $7.5 \cdot 10^{-5}$ m/s (average value calculated from table 4). The simulations follow the experimental results reasonably well. External mass transfer resistance caused by the flow rate is not expected, because in that case the double layer coefficient would be related to the particle size. This clearly supports that the resistance of LAS adsorption onto LDH is situated in a flow rate independent residual external film layer which can be the so-called (electric) double layer [25, 26].

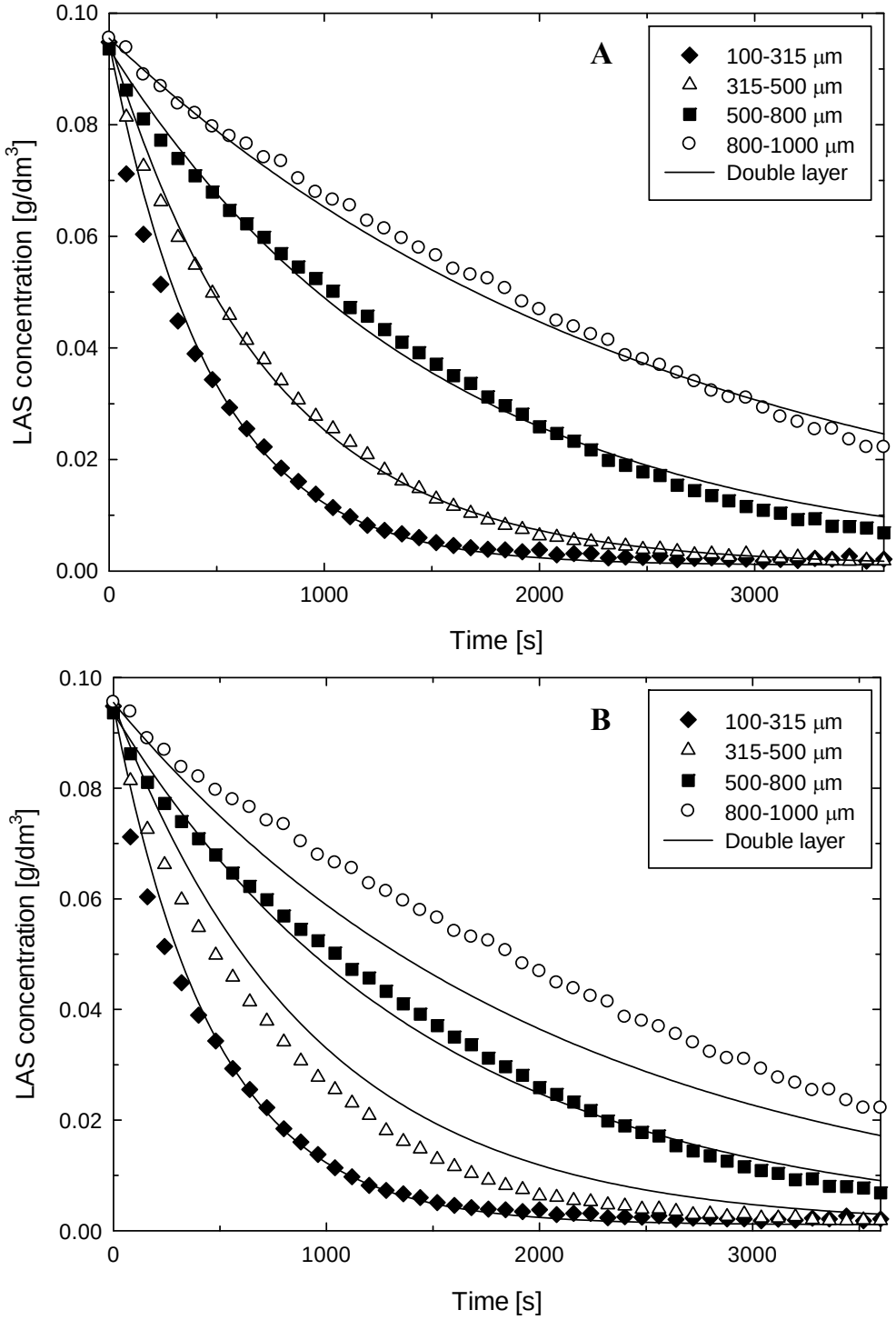

Figure 8: LAS concentration in time for LDH with different particle sizes. The double layer coefficients are estimated in 8A and shown in table 4, an average double layer coefficient ($7.5 \cdot 10^{-5}$ m/s) is used for the model simulations in figure 8B. The initial LAS concentration is 0.09 g/dm^3 and the flow rate is 60 ml/min. The solid lines represent the results of the double layer model.

Table 4: Double layer coefficients obtained from fitting experimental data with the double layer model for different particle sizes of LDH.

Particle size [μm]	100-315	315-500	500-800	800-1000
k_{DL} [m/s]	$7.5 \cdot 10^{-5}$	$9.3 \cdot 10^{-5}$	$7.2 \cdot 10^{-5}$	$5.9 \cdot 10^{-5}$

4.4.6. Influence of initial LAS concentration

The influence of the initial LAS concentration on the LAS adsorption rate for GAC-1240 and LDH is shown in figure 9A and B respectively. Table 5 shows the intra particle diffusion coefficient obtained by fitting the model to the experimental data for GAC-1240. The initial LAS concentration does not influence the value of the diffusion coefficient for GAC-1240 significantly. This means that the initial LAS concentration does not have an influence on the diffusion coefficient of LAS.

The double layer model is used to describe the LAS adsorption onto LDH (figure 9B). The model predictions describe the experimental results quite well. Table 5 gives the double layer coefficient obtained from fitting the model to the experimental data for LDH. The double layer coefficient hardly changes with different initial LAS concentrations. The surfactant molecules form a bilayer at low concentrations and this is apparently not influenced by the initial LAS concentration in the range investigated.

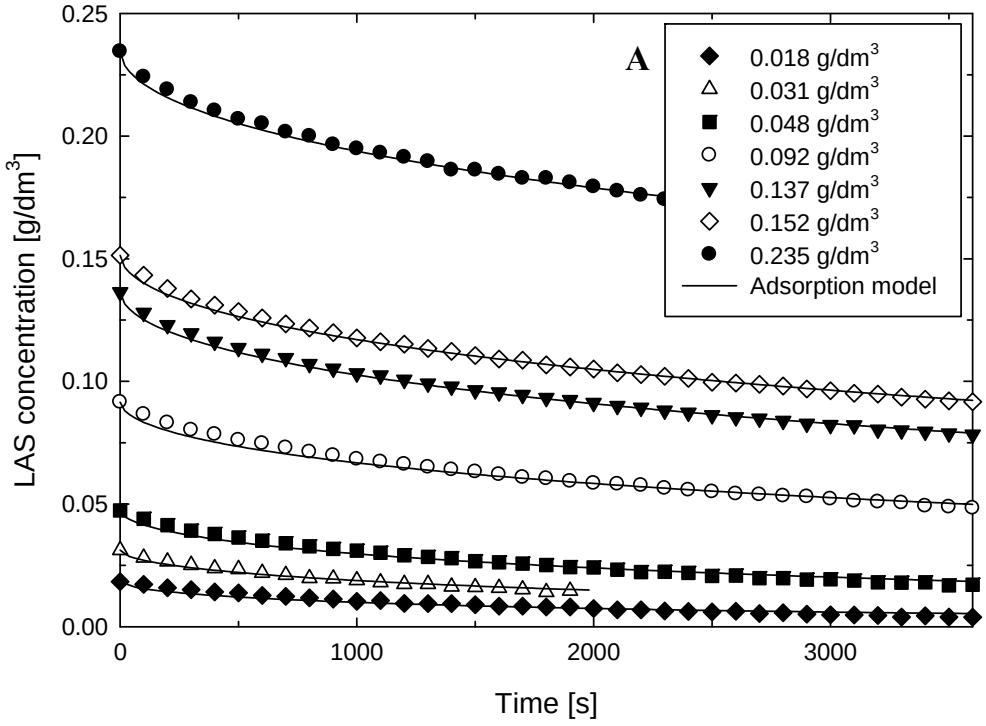

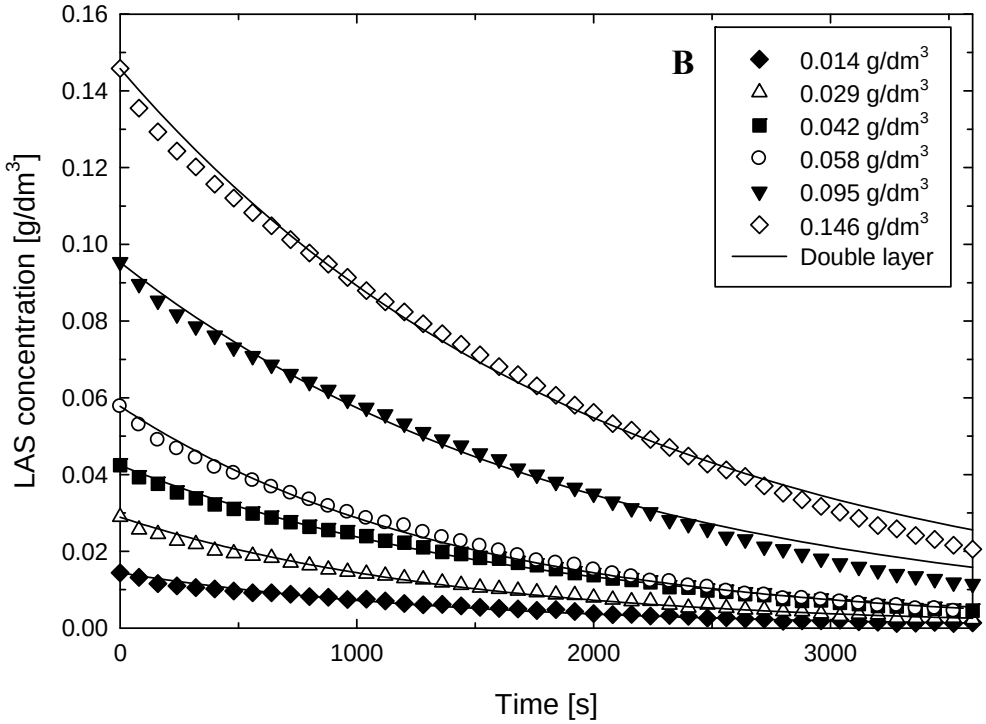

Figure 9: LAS concentration in time for GAC-1240 (A) and LDH (B) with different initial LAS concentrations. The particle size is 500-800 µm and the flow is 60 ml/min. The solid lines represent the results of the adsorption model, GAC-1240 (A) and double layer model, LDH (B).

Table 5: Effective diffusion coefficient obtained from fitting experimental data with the adsorption model for GAC-1240. Double layer mass transfer coefficient obtained from fitting experimental data with the double layer model for LDH.

Initial LAS concentration [g/dm^3] ***GAC-1240***	0.018	0.031	0.048	0.092	0.137	0.152	0.235
D_{eff} [m^2/s]	$1.1\cdot10^{-10}$	$1.1\cdot10^{-10}$	$1.4\cdot10^{-10}$	$1.5\cdot10^{-10}$	$1.2\cdot10^{-10}$	$1.5\cdot10^{-10}$	$1.2\cdot10^{-10}$
Initial LAS concentration [g/dm^3] ***LDH***	0.014	0.029	0.042	0.058	0.095	0.146	
k_{DL} [m/s]	$7.7\cdot10^{-5}$	$7.8\cdot10^{-5}$	$6.5\cdot10^{-5}$	$7.8\cdot10^{-5}$	$5.6\cdot10^{-5}$	$5.5\cdot10^{-5}$	

4.5. Conclusions

In this work the adsorption rate of LAS on activated carbon GAC-1240 and LDH is investigated with the ZLC method. The experimental results were described with several models to determine the rate limiting step and accompanying parameters. The following conclusions can be drawn from the experimental work:

- The adsorption of LAS onto GAC-1240 was well described by the adsorption model. The effective diffusion coefficient of GAC-1240 is $1.3\cdot10^{-10} \pm 0.2\cdot10^{-10}$ m^2/s and does not change with particle size or initial LAS concentration.
- The adsorption of LAS onto LDH was not sufficiently described by the adsorption model and the ion exchange model because the experimental results show a first order decline. The results cannot be explained by assuming chemisorption because an influence of particle size is found. Surfactants can

form a double layer or bilayer on oppositely charged surfaces resulting in a film layer resistance.

- The (electric) double layer model results in a good description of the experimental data for LDH. The resistance of LAS adsorption onto LDH is completely situated in the double layer outside the particle. The double layer coefficient is $7 \cdot 10^{-5} \pm 2 \cdot 10^{-5}$ m/s.

4.6. Symbols

b	affinity coefficient [dm^3_{water}/g_{LAS}]
C	LAS concentration in the liquid phase [g_{LAS}/dm^3_{water}]
C_{bulk}	LAS concentration in the bulk solution [g_{LAS}/dm^3_{water}]
C_{NRM}	LAS concentration with the non-recycle mode [g_{LAS}/dm^3_{water}]
C_{RM}	LAS concentration with the recycle mode [g_{LAS}/dm^3_{water}]
C_∞	LAS concentration at $t=\infty$ [g_{LAS}/dm^3_{water}]
D_{eff}	effective diffusion coefficient [m^2/s]
D_{HSDM}	diffusion coefficient calculated with the HSDM model [m^2/s]
D_m	molecular diffusion coefficient [m^2/s]
D_{pA}	diffusion coefficient of LAS in the pores [m^2/s]
D_{pB}	diffusion coefficient of OH^- in the pores [m^2/s]
D_{sA}	diffusion coefficient of LAS at the solid phase [m^2/s]
D_{sB}	diffusion coefficient of OH^- at the solid phase [m^2/s]
k_{DL}	double layer mass transfer coefficient [m/s]
m	mass of the adsorbate [$g_{adsorbent}$]
N_{pA}	flux of LAS in the pores [$g_{LAS} \cdot m^2/s$]
N_{sA}	flux of LAS at the solid phase [$g_{LAS} \cdot m^2/s$]
q	adsorption capacity of particle [$g_{LAS}/g_{adsorbent}$]
q_m	maximum adsorption capacity of particle [$g_{LAS}/g_{adsorbent}$]
$\bar{q}$	average adsorption capacity of particle [$g_{LAS}/g_{adsorbent}$]
r	radial position within the particle [m]
R	radius of the particle [m]
t	time [s]
V	volume of solution [m^3]
V_{ZLC}	volume of the ZLC set-up [m^3]
ε_p	porosity of particle [$m^3_{void}/m^3_{adsorbent}$]
ρ_s	solid density of particle [$g_{adsorbent}/m^3_{solid}$]
τ	tortuosity [-]

4.7. References

1. Schouten, N., et al., *Selection and evaluation of adsorbents for the removal of anionic surfactants from laundry rinsing water.* Water Research, 2007. **41**(18): p. 4233-4241 (Chapter 2).
2. Ho Tan Tai, L., *Formulating detergents and personal care products*. 1st ed. 2000, New York, USA: AOCS Press.

3. Holmberg, K., et al., *Surfactants and polymers in aqueous solution*. 2nd ed. 2003, West Sussex, UK: Wiley.
4. Adak, A., M. Bandyopadhyay, and A. Pal, *Removal of anionic surfactant from wastewater by alumina: a case study.* Colloids and Surfaces A: Physicochemical and Engineering Aspects, 2005. **254**(1-3): p. 165-171.
5. Sontheimer, H., J.C. Crittenden, and R.S. Summers, *Activated carbon for water treatment*. 2nd ed. 1988, Karlsruhe, Germany: DVGW-Forschungsstelle.
6. Pavan, P.C., G.d.A. Gomes, and J.B. Valim, *Adsorption of sodium dodecyl sulfate on layered double hydroxides.* Microporous and Mesoporous Materials, 1998. **21**(4-6): p. 659-665.
7. Eic, M. and D.M. Ruthven, *A new experimental technique for measurement of intracrystalline diffusivity.* Zeolites, 1988. **8**(1): p. 40-45.
8. Ruthven, D.M. and P. Stapleton, *Measurement of liquid phase counter-diffusion in zeolite crystals by the ZLC method.* Chemical Engineering Science, 1993. **48**(1): p. 89-98.
9. Dekic-Zickovic, T., *The reverse flow adsorption technology for the process integrated recyling of homogeneous catalysts*, in *Department of Chemical Engineering and Chemistry* 2008, Thesis Eindhoven University of Technology: Eindhoven.
10. Lv, L., et al., *Uptake of chloride ion from aqueous solution by calcined layered double hydroxides: Equilibrium and kinetic studies.* Water Research, 2006. **40**(4): p. 735-743.
11. Lazaridis, N.K. and D.D. Asouhidou, *Kinetics of sorptive removal of chromium(VI) from aqueous solutions by calcined Mg-Al-CO_3 hydrotalcite.* Water Research, 2003. **37**(12): p. 2875.
12. Lazaridis, N.K., T.D. Karapantsios, and D. Georgantas, *Kinetic analysis for the removal of a reactive dye from aqueous solution onto hydrotalcite by adsorption.* Water Research, 2003. **37**(12): p. 3023-3033.
13. Ni, Z.M., et al., *Treatment of methyl orange by calcined layered double hydroxides in aqueous solution: adsorption property and kinetic studies.* Journal of Colloid and Interface Science, 2007. **316**(2): p. 284-291.
14. Goh, K.-H., T.-T. Lim, and Z. Dong, *Application of layered double hydroxides for removal of oxyanions: A review.* Water Research, 2008. **42**(6-7): p. 1343-1368.
15. Das, J., et al., *Calcined Mg-Fe-CO_3 LDH as an adsorbent for the removal of selenite.* Journal of Colloid and Interface Science, 2007. **316**(2): p. 216-223.
16. Santosa, S.J., E.S. Kunarti, and Karmanto, *Synthesis and utilization of Mg/Al hydrotalcite for removing dissolved humic acid.* Applied Surface Science, 2008(In Press, Corrected Proof, Doi:10.1016/j.apsusc.2008.01.122).
17. Vreysen, S. and A. Maes, *Adsorption mechanism of humic and fulvic acid onto Mg/Al layered double hydroxides.* Applied Clay Science, 2008. **38**(3-4): p. 237-249.
18. Valverde, J.L., et al., *Model for the determination of diffusion coefficients of heterovalent ions in macroporous ion exchange resins by the zero-length column method.* Chemical Engineering Science, 2005. **60**(21): p. 5836-5844.

19. Serarols, J., J. Poch, and I. Villaescusa, *Determination of the effective diffusion coefficient of Zn(II) on a macroporous resin XAD-2 impregnated with di-2-ethylhexyl phosphoric acid (DEHPA): Influence of metal concentration and particle size.* Reactive and Functional Polymers, 2001. **48**(1-3): p. 53-63.
20. Ruthven, D.M., *Principles of adsorption and adsorption processes*. 1st ed. 1984, New York, USA: John Wiley & Sons, Inc.
21. Basar, C.A., et al., *Removal of surfactants by powdered activated carbon and microfiltration.* Water Research, 2004. **38**(8): p. 2117-2124.
22. Lide, D.R., *Handbook of Chemistery and Physics*. 85th ed. 2004, New York, USA: CRC Press.
23. Hou, X., et al., *Hydration, expansion, structure, and dynamics of layerd double hydroxides.* American Mineralogist, 2003. **88**: p. 167-179.
24. Aktkins, P.W., *Physical Chemistry*. 4th ed. 1990, Oxford, UK: Oxford Univesity Press.
25. Zagorodni, A.A., *Ion exchange materials*. 1st ed. 2007, Oxford, UK: Elsevier.
26. Shaw, D.J., *Colloid & Surface Chemistry*. 4th ed. 1992, Oxford, UK: Butterworth Heinemann.
27. Mortaheb, H.R., et al., *Study on a new surfactant for removal of phenol from wastewater by emulsion liquid membrane.* Journal of Hazardous Materials, 2008(In Press, Corrected Proof, Doi:10.1016/j.jhazmat.2008.03.095).
28. Sabry, R., et al., *Removal of lead by an emulsion liquid membrane: Part I.* Desalination, 2007. **212**(1-3): p. 165-175.
29. Park, J.S., et al., *An electrical impedance spectroscopic (EIS) study on transport characteristics of ion-exchange membrane systems.* Journal of Colloid and Interface Science, 2006. **300**(2): p. 655-662.
30. Park, J.S., et al., *An approach to fouling characterization of an ion-exchange membrane using current-voltage relation and electrical impedance spectroscopy.* Journal of Colloid and Interface Science, 2006. **294**(1): p. 129-138.

5. Influence of components present in laundry rinsing water on the adsorption of anionic surfactants onto activated carbon and layered double hydroxide

Abstract

Low cost adsorption technology offers high potential to clean up laundry rinsing water. From an earlier selection of adsorbents [1], layered double hydroxide (LDH) and activated carbon (GAC-1240) proved to be interesting materials for the removal of the anionic surfactant, linear alkyl benzene sulfonate (LAS), which is the main contaminant in laundry rinsing water. The main research question is to identify the influence of other components (sodium triphosphate (STP), sodium carbonate (Na_2CO_3) and sodium chloride (NaCl)) present in laundry rinsing water on the adsorption capacity and adsorption kinetics of LAS onto GAC-1240 and LDH. Equilibrium experiments are used to investigate the adsorption capacity and the zero length column (ZLC) method is used to investigate the adsorption kinetics. No large influence of STP, Na_2CO_3 and NaCl is found for the LAS adsorption capacity onto GAC-1240 and LDH. The LAS adsorption rate is increased by the addition of STP, Na_2CO_3 and NaCl for GAC-1240, because the ionic strength of the solution is increased by the added components. This also counts for the influence of NaCl on the LAS adsorption rate onto LDH. However, the LAS adsorption rate is decreased by the addition of STP and Na_2CO_3 for LDH, because STP and CO_3^{2-} compete with LAS for adsorption.

5.1. Introduction

Shortage of water is a growing global problem. One way of dealing with this problem is the development of technologies for wastewater clean-up and re-use. Laundry accounts often for more than half of the daily domestic water consumption in countries like India. The major part of laundry water is rinsing water. Laundry rinsing water is relatively clean and therefore highly suitable for clean-up and re-use. The main contaminant in laundry rinsing water is the anionic surfactant. Linear alkyl benzene sulfonate (LAS) is the most commonly used anionic surfactant in detergent powders [2].

Adsorption technology offers high potential to clean-up the laundry rinsing water. Adsorption can be low cost and can be applied in small devices and is therefore suitable for use on low-income household scale. Our previous research [1] on adsorbent selection showed that granular activated carbon (GAC) and layered double hydroxide (LDH) proved to be interesting adsorbents for the removal of LAS. The adsorption kinetics of LAS onto activated carbon GAC-1240 and LDH have been investigated with the (ZLC) method [3].

The main components of laundry rinsing water are the added detergents and dirt constituents released from fabrics during rinsing. The main ingredients of hand wash detergents are shown in table 1. Anionic surfactant, linear alkyl benzene sulfonate (LAS) is the active component of a detergent. Sodium triphosphate (STP) and sodium carbonate (Na_2CO_3) are builders and provide an alkaline environment in the water [4]. Other ingredients in detergents like anti-redeposition polymers, flow aids, fluorescensers, bleach and perfumes are present in very low quantities and are therefore not considered for further investigation. Sodium chloride (NaCl) is present in water and is assumed at an average concentration of 0.25 g/dm^3 [5].

Table 1: Composition of different detergents in mass% [4]. ABS is alkyl benzene sulfonate (branched), LAS is linear alkyl benzene sulfonate and STP is sodium triphosphate (builder). Main components investigated are printed bold.

Constituents	Typical laundry bar	Hand wash powder
ABS/LAS	**15-30**	**15-30**
Non-ionics		0-3
STP	**2-10**	**3-20**
Sodium carbonate	**2-10**	**5-10**
Aluminosilicate	0-5	
Sodium silicate	2-5	5-10
Calcite	0-20	
Aluminium sulphate	0-5	
Kaolin	0-15	
Sodium sulphate	5-20	20-50

Many investigations have been done on the influence of different components on surfactant adsorption. Most work is done on the addition of electrolytes. Bautista-

Toledo et. al. (2008) [6] explained that the presence of electrolytes in the solution modifies the strength of the surfactant-activated carbon electrostatic interaction. The electrolytes screen the surface charge of the adsorbent. When the ionic strength is increased this will decrease the LAS adsorption capacity when electrostatic interactions are attractive. The adsorption capacity is increased when the electrostatic interactions are repulsive. Pavan et. al. (1999) and Reis et. al. (2004) [7, 8] describe the influence of ionic strength on surfactant adsorption onto LDH. The increase in ionic strength causes an increase in adsorption capacity due to the reduced repulsion between the charged head groups of the surfactants. Paria and Khilar (2004) [9] explains that the presence of an electrolyte can enhance surfactant adsorption. Electrolytes increase the polarity of water and decrease the critical micelle concentration (CMC). The shape of the aggregates changes with increasing electrolyte concentration. The aggregates become more flat and can adsorb more easily. Furthermore, they also describe that ions shield the charged surfactant head group and decrease the columbic repulsion. The surfactants can approach each other closer.

To develop a low cost adsorption technique for recycling of laundry rinsing water, we have to gain insight in the influence of other components present in laundry rinsing water. Before the project is continued it is important to find out if there are components that dramatically influence the LAS adsorption. The main objective of this work is to investigate the influence of STP, Na_2CO_3 and NaCl on the LAS adsorption capacity and LAS adsorption rate onto GAC-1240 and LDH. The adsorption capacity was investigated with equilibrium experiments and the adsorption kinetics was investigated with the ZLC method.

5.2. Materials and Methods

5.2.1. Materials

The anionic surfactant, linear alkyl benzene sulfonate (LAS) was obtained from Unilever R&D, Vlaardingen, The Netherlands. Purity is around 92 wt% and the chain length is C_{10} to C_{13} (equally distributed; average molecular weight of LAS-acid is 312 g/mol). The critical micelle concentration (CMC) is 2 mM [10]. Sodium triphosphate ($Na_5P_3O_{10}$, molecular weight 368.7 g/mol), sodium carbonate (Na_2CO_3) and sodium chloride (NaCl) are analytically pure agents and obtained from Sigma-Aldrich (Steinheim, Germany) and Boom (Meppel, The Netherlands).

Granular activated carbon, GAC-1240 was supplied by Norit, Amersfoort, The Netherlands and extrudates of LDH was supplied by Akzo Nobel, Arnhem, The Netherlands. The activated carbon granules and LDH extrudates were grinded and sieved in fractions. The specific surface area, pore size and pore volume distribution were measured using nitrogen adsorption at -196^{o}C (liquid nitrogen temperature) with the Micromeritics Tristar 3000.

Table 2: Properties of adsorbents.

Material	Raw material	Activation method	Specific surface area (BET) [m^2/g]	Pore volume [cm^3/g]	Average pore size [nm]
GAC-1240	coal	steam	1131	0.64	4.2
LDH	-	-	131	0.33	8.6

5.2.2. Analysis of the different components

In table 3 the investigated components and their concentrations in laundry rinsing water are listed. The LAS concentration in rinsing water was found to be around 0.1-0.3 g/dm^3 [5]. The concentrations of the other components are calculated from table 1 proportionally to 0.1 g_{LAS}/dm^3. The concentration of LAS was measured with Total Organic Carbon – Total Carbon (TOC-TC) (Shimadzu TOC-V cph), STP was measured with Inductively Coupled Plasma (ICP) (Perkin Elmer Optima 5300 DV), Na_2CO_3 was measured with Total Organic Carbon – Inorganic Carbon (TOC-IC) (Shimadzu TOC-V cph) and NaCl was measured with Ion Chromatograph (IC) (Metrohm 761 Compact IC). Calibration curves are used to calculate the concentration of the components.

Table 3: The concentration of the main components in laundry rinsing water and the analysis methods applied.

Ingredient	Concentration [g/dm^3]	Concentration [$mmol/dm^3$]	Ionic strength* [$mmol/dm^3$]	Analysis method
Linear alkyl benzene sulfonate (LAS)	0.10	0.32	0.32	TOC-TC
Sodium triphosphate (STP)	0.15	0.41	6.12	ICP
Sodium carbonate (Na_2CO_3)	0.12	1.13	3.40	TOC-IC
Salt (NaCl)	0.25	4.28	4.28	IC

*Ionic strength is calculated with the Debye Hückel relation [11].

5.2.3. Adsorption equilibrium experiments

Adsorption equilibrium experiments were conducted to determine the influence of other components present in laundry rinsing water on the adsorption isotherm of LAS for two types of adsorbents. The adsorption experiments were conducted at different initial LAS concentrations ranging from 0.1 to 3 g/dm^3 milli-Q water. Each single component (STP, Na_2CO_3 and NaCl) was added to the LAS solution to obtain the fixed concentration presented in table 3. 0.1 gram of adsorbent and 80 ml of the solution was mixed in a screw capped flask and placed in a shaking bath (Julabo SW22) at 25°C. With a preliminary experiment the equilibrium time was determined to be 48 hours; equilibrium was reached well within this time. The water phase was sampled with a syringe equipped with a filter (Spartan 30/0.45RC (0.45μm)) to

remove suspended solids and the LAS concentration was measured by TOC-TC. The concentration of the components added were analysed with the methods described in table 3. The experiments were carried out in duplicate.

5.2.4. ZLC set-up

The zero length column (ZLC) set-up was used to determine the influence of other components present in laundry rinsing water on the adsorption kinetics of LAS for two types of adsorbents and is illustrated in figure 1. The set-up consists of a pump (Knauer Preparative HPLC Pump 1800), a UV detector (Knauer Smartline 2500) and a column (Omnifit chromatography column with a 6.6 mm internal diameter and two adjustable end-pieces).

The set-up can be operated in a non-recycle and recycle mode. In the non-recycle mode the inlet tube and outlet tube are placed in two separate beakers. This mode is used for calibration and cleaning purposes. In the recycle mode the inlet tube and outlet tube are place in the same beaker. The beaker is equipped with a stirrer to assure ideal mixing. This mode is used for the kinetic experiments.

The experiments were conducted according to the following procedure. The adsorbents were pre-treated to remove air from the pores in the following way: milli-Q water was added to the adsorbent and vacuum was applied. The time of pre-treatment depends on the material and was investigated in chapter 4 [3]. The pre-treatment time of GAC-1240 is 16 hours and the pre-treatment time of LDH is 30 minutes. The column was packed with the adsorbent up to a bed height of 4 mm (0.065 grams of GAC-1240 and 0.091 grams of LDH). Preceding the experiment, the column was equilibrated with nitrogen-sparged milli-Q water. After equilibration water was replaced with a 50 ml LAS solution and the LAS concentration was monitored with the UV detector at 223 nm. Each single component (STP, Na_2CO_3 and NaCl) was added to LAS solution and its effect was monitored. The component was added according to the concentration in table 3. The concentration of the component was analysed after one hour of experimenting. The experiments were conducted at room temperature.

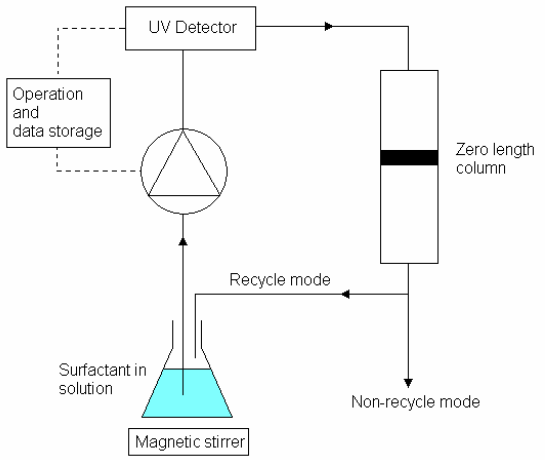

Figure 1: Schematic representation of the zero length column set-up.

The calibration of the ZLC set-up is described in chapter 4 [3]. The volume of the ZLC set-up needs to be known because the water in the set-up dilutes the initial solution. The calculated volume of the ZLC set-up was found to be 11.15 ml. The concentration of the recycle mode was taken as initial concentration C_0 in the experiments.

5.3. Results and discussion

5.3.1. Influence of components on the LAS adsorption capacity

The LAS adsorption isotherms of LAS only, LAS in combination with STP or Na_2CO_3 or NaCl onto GAC-1240 are shown in figure 2A and onto LDH in figure 2B. From the figures it is clear that there is no large effect of the different components on the LAS adsorption capacity for both GAC-1240 and LDH. At low LAS concentrations the isotherms are identical, but at higher concentrations differences occur. In both figures (2A and 2B) LAS only resulted in the highest adsorption capacity, closely followed by the LAS and NaCl combination. It seems that NaCl does not influence the LAS adsorption capacity. Both STP and Na_2CO_3 resulted in the lowest maximum adsorption capacity for both GAC-1240 and LDH. STP and Na_2CO_3 increase the pH of the solution. Increasing the pH promotes surface oxidation of activated carbons which makes the surface more negatively charged and decreases anionic surfactant adsorption [12]. Increasing the pH for LDH will also make the LDH surface less positive and this can decrease the LAS adsorption capacity [7].

Additional analysis of the concentration of STP, Na_2CO_3 and NaCl after LAS adsorption did not show any changes. This indicates that NaCl, Na_2CO_3 and STP are not adsorbed by GAC-1240 and LDH. It was expected that LDH would also adsorb STP, because like LAS, STP is a negatively charged organic molecule. Therefore, the adsorption of STP only is also investigated and the isotherm is shown in figure 3.

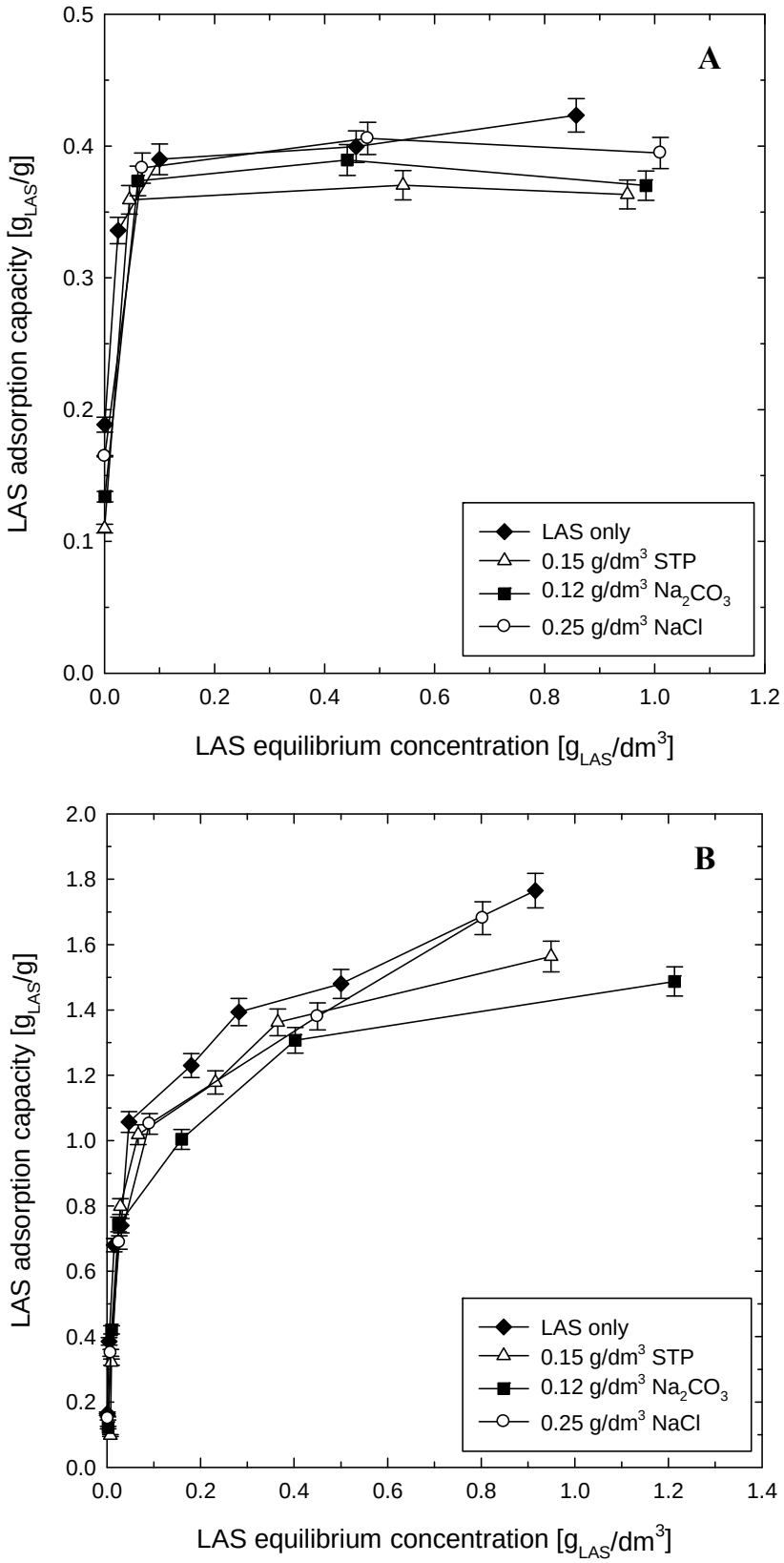

Figure 2: Adsorption isotherms of LAS only and LAS in combination with STP, Na_2CO_3 or NaCl for GAC-1240 (A) and LDH (B). Lines were only added to guide the eye.

Figure 3 shows the LAS adsorption isotherm and STP adsorption isotherm combined with the Langmuir isotherm [1]. The obtained Langmuir parameters are listed in

table 4. The figure is represented in mmols to compare the adsorption capacity of LAS and STP easily. It is clear that STP is adsorbed by LDH. The adsorption capacity is much lower compared to LAS. It must be taken into account that STP contains five negative charges where LAS contains only one. The adsorption capacity of STP is five times lower compared to LAS (see q_m in table 4). The amount of charges that is adsorbed by the LDH is equal for LAS and STP. The affinity (b in table 4) of STP is lower compared to LAS. The hydrophobic tail of LAS is expelled from the water and this results in a very high affinity to adsorb. STP is hydrophilic and therefore the tendency to adsorb is lower.

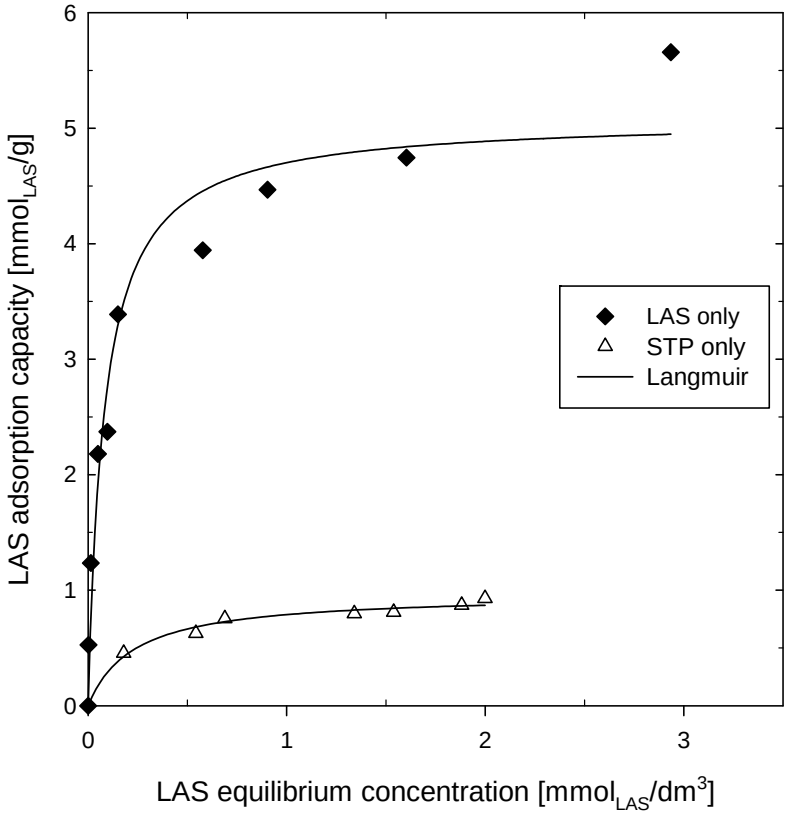

Figure 3: Adsorption isotherms of LAS only and STP only for LDH in mmols. Lines are the Langmuir isotherms.

Table 4: Langmuir isotherm parameters fitted from the experimental data in figure 3.

Component	b [dm^3/mmol]	q_m [mmol/g]
LAS	12.24	5.08
STP	4.35	0.97

5.3.2. Influence of components on the LAS adsorption kinetics

Figure 4 shows the relative LAS concentration in time for GAC-1240 (A) and LDH (B) with LAS only and LAS in combination with STP, Na_2CO_3 or NaCl. The LAS adsorption rate for GAC-1240 is only slightly influenced by the addition of STP, Na_2CO_3 or NaCl. By adding STP, Na_2CO_3 or NaCl the ionic strength of the solution is

increased. Paria et. al. (2004) [9] describes that the presence of an electrolyte can enhance surfactant adsorption. Electrolytes increase the polarity of water and decrease the CMC. Furthermore, the ions screen the charged surfactant head group and decrease the columbic attraction. The surfactants can approach each other closer. The ionic strength is decreased from STP>NaCl >Na_2CO_3 (see table 3) while the order in figure 4A is NaCl>STP>Na_2CO_3. This could be caused by the amount of NaCl ions which are much more compared to the STP ions (table 3).

Compared to GAC-1240, the LAS adsorption rate for LDH (figure 4B) is more influenced by the addition of STP, Na_2CO_3 or NaCl to the solution. The LAS adsorption rate is increased by the addition of NaCl compared to LAS only. This can be explained by the increase in ionic strength of the solution. The addition of STP and Na_2CO_3 results in a decrease of the LAS adsorption rate. STP and Na_2CO_3 compete with LAS for adsorption. The OH^- between the LDH layers can be replaced by CO_3^{2-}, STP or LAS. In equilibrium LAS wins the competition, because no adsorption of CO_3^{2-} and STP was observed at equilibrium (see paragraph 5.3.1). The strongest effect is found for STP. The STP concentration was analysed at time t=0 and t=3600 s and shows a STP concentration decrease of 85%. Apparently, STP is initially adsorbed by LDH but in time the STP molecules are expelled from LDH. LAS is adsorbed in the LDH structure and bilayers are formed resulting in desorption of other molecules.

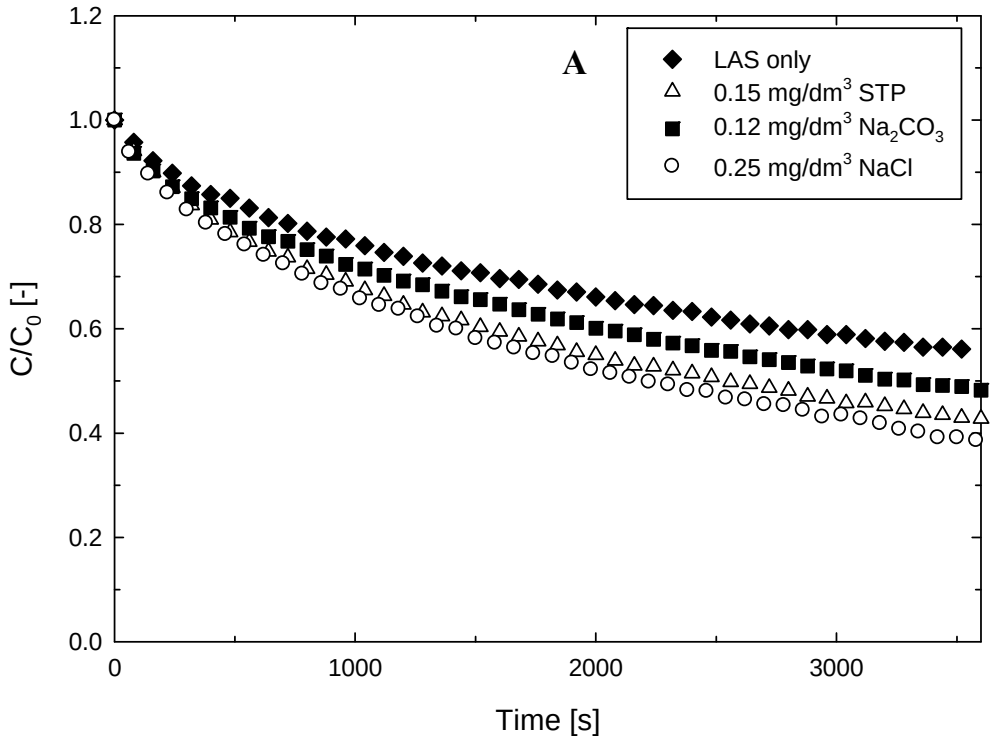

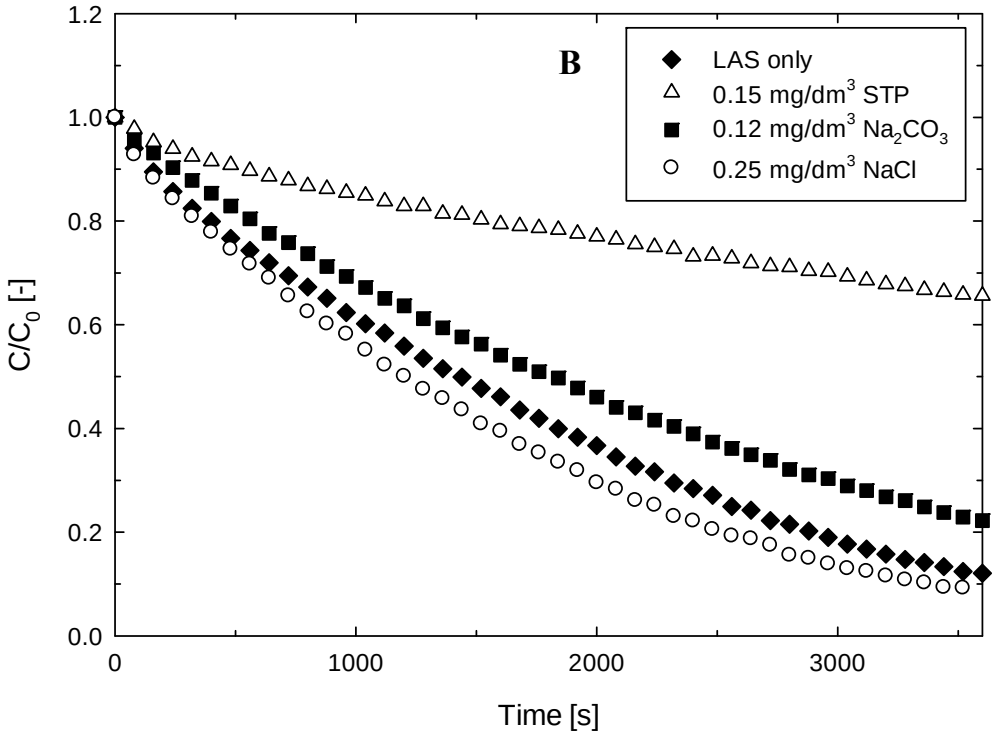

Figure 4: Relative LAS concentration in time for GAC-1240 (A) and LDH (B) with NaCl, Na_2CO_3 or STP added. The initial LAS concentration is 0.09 g/dm^3, particle size is 500-800 µm and the flow rate is 60 ml/min.

5.4. Conclusions

In this work the influence of other components (STP, Na_2CO_3 and NaCl) present in laundry rinsing water on the LAS adsorption onto GAC-1240 and LDH is investigated. The influence on the adsorption capacity and adsorption kinetics were investigated. The following conclusions can be drawn from the experimental work:

- There is no large influence of STP, Na_2CO_3 and NaCl on the adsorption capacity of LAS for GAC-1240 and LDH.
- STP, Na_2CO_3 and NaCl increased the LAS adsorption rate for GAC-1240. This is caused by an increase in ionic strength of the solution by the added components and this enhances the LAS adsorption.
- NaCl increased the LAS adsorption rate for LDH by increasing the ionic strength. Both STP and Na_2CO_3 decrease the LAS adsorption rate. CO_3^{2-} and STP compete with LAS for the adsorption onto LDH. In time LAS expels CO_3^{2-} and STP from the LDH.

5.5. References

1. Schouten, N., et al., *Selection and evaluation of adsorbents for the removal of anionic surfactants from laundry rinsing water.* Water Research, 2007. **41**(18): p. 4233-4241 (Chapter 2).
2. Holmberg, K., et al., *Surfactants and polymers in aqueous solution*. 2nd ed. 2003, West Sussex, UK: Wiley.

3. Schouten, N., et al., *Investigation of adsorption kinetics of anionic surfactant with the zero length column method.* Submitted, 2008: p. (Chapter 4).
4. Ho Tan Tai, L., *Formulating detergents and personal care products*. 1st ed. 2000, New York, USA: AOCS Press.
5. Unilever, *Personal communication*. December 2004: Hindustan Unilever Research India, 64 Main Road, Whitefield P.O. Bangalore 560066, India.
6. Bautista-Toledo, M.I., et al., *Adsorption of sodium dodecylbenzenesulfonate on activated carbons: Effects of solution chemistry and presence of bacteria.* Journal of Colloid and Interface Science, 2008. **317**(1): p. 11-17.
7. Pavan, P.C., et al., *Adsorption of sodium dodecylsulfate on a hydrotalcite-like compound. Effect of temperature, pH and ionic strength.* Colloids And Surfaces A-Physicochemical And Engineering Aspects, 1999. **154**(3): p. 399-410.
8. Reis, M.d., et al., *Effects of pH, temperature, and ionic strength on adsorption of sodium dodecylbenzenesulfonate into Mg-Al-CO3 layered double hydroxides.* Journal of Physics and Chemistry of Solids, 2004. **65**(2-3): p. 487.
9. Paria, S. and K.C. Khilar, *A review on experimental studies of surfactant adsorption at the hydrophilic solid-water interface.* Advances in Colloid and Interface Science, 2004. **110**(3): p. 75-95.
10. Basar, C.A., et al., *Removal of surfactants by powdered activated carbon and microfiltration.* Water Research, 2004. **38**(8): p. 2117-2124.
11. Atkins, P.W., *Physical Chemistry*. 6th ed. 1999, Oxford, UK: Oxford University Press. pages 249-250.
12. Wu, S.H. and P. Pendleton, *Adsorption of anionic surfactant by activated carbon: Effect of surface chemistry, ionic strength, and hydrophobicity.* Journal Of Colloid And Interface Science, 2001. **243**(2): p. 306-315.

6. Column performance of granular activated carbon for the removal of anionic surfactants (LAS)

Abstract

Based on equilibrium experiments, activated carbon proved to be a promising material for the adsorption of LAS from laundry rinsing water to allow re-use of the rinsing water [1]. The application of a suitable adsorbent is most practical in a column operation. In this work small scale column experiments are performed and the influence of flow rate, bed height, initial LAS concentration, external mass transfer and flow direction were investigated. The experimental results are explained with a mathematical model consisting of mass balances combined with an adsorption equilibrium isotherm and transport kinetics (linear driving force model). The model estimates the influence of flow rate and bed height well. The main deviation between the model and experimental results is caused by the particle size distribution of the adsorbent, where the model assumes only one particle size. Subsequently, the model is used to design the column for the rinsing water recycler (RWR) prototypes. This resulted in two designs for further tests; a column (D=0.06 m; H=0.18 m) with a flow rate of 50 ml/min and a column with a flow rate of 100 ml/min. The adsorbent cost of both columns is $12 and $15 per year.

6.1. Introduction

The current work is part of a project that aims to develop low cost technologies for the local decentralized recycling of laundry rinsing water. The basic idea is to clean-up the polluted rinsing water to allow multiple use cycles. When the main contaminants are removed from the rinsing water, it can be re-used for household or irrigation purposes. Main contaminants are the added detergent ingredients and the 'dirt' released from the fabrics during rinsing. The overall objective of the project is to develop a small scale rinsing water recycler (RWR).

The application of adsorption technology for clean-up of laundry rinsing water offers high potential. It can be low cost and applied in small devices and is therefore suitable for use on low-income household scale. Our previous research [1] on adsorbent selection showed that granular activated carbon (GAC) proved to be an interesting adsorbent for the removal of anionic surfactant, linear alkyl benzene sulfonate (LAS), which is the main contaminant in rinsing water. Activated carbon showed a high adsorption capacity per dollar of material. Norit GAC-1240 was characterized with equilibrium batch experiments to obtain the adsorption capacity of LAS at different equilibrium concentrations. The experimental results were described with the Langmuir isotherm model [2].

Batch adsorption experiments provide useful information on the application of adsorbents for the removal of LAS from laundry rinsing water. However, the application of a suitable adsorbent is most practical in a continuous column operation [3]. Fixed-bed columns are widely used at different scales and for various applications [4-7] because of their simple operation. Fixed-bed adsorption has been applied to remove organic contaminants for many years with good results. The main reason is the high adsorption capacity of the bed since it is in equilibrium with the influent concentration rather than the effluent concentration [8]. Therefore, column operation will be used for the prototypes of the rinsing water recycler (RWR).

The dynamic behaviour of a column operation gives a changing effluent concentration in time which is commonly referred to as the breakthrough curve. The time at which the effluent concentration reaches a specified concentration is called the breakthrough time. For the design of adsorption systems accurate estimations of breakthrough curves are needed for specified conditions. Some work has been done on the adsorption of surfactants onto activated carbon in a column operation. Saleh (2006) [9] described the adsorption of cationic surfactants by granular charcoal, Weinberg and Narkis (1987) [10] described the adsorption of non-ionic surfactants onto activated carbon and Gupta et. al. (2003) [11] described the adsorption of anionic surfactants onto activated carbon produced from waste materials. More work has been done on the adsorption of dyes [12-14] and other contaminants [15-17] onto activated carbon in a column operation. Guelli U. de Souza et. al. (2008) [13] compared the experimental breakthrough curves of dye adsorption onto activated carbon with a mathematical model. The model consists of an adsorption equilibrium and adsorption kinetic models combined with mass balances. The experimental results were explained with the model simulations.

Many researchers described their experimental results with these mathematical models based on mass balances; for example the adsorption of heavy metals onto activated carbon [18, 19]. Hardly any work has been done on the mathematical modelling of the fixed bed adsorption of anionic surfactants onto activated carbon.

The main objective of this work is to design the column of the RWR prototypes. Small column experiments were preformed and breakthrough curves were measured for the adsorption of LAS onto GAC-1240. The influence of flow rate, bed height, initial LAS concentration, external mass transfer and flow direction on the breakthrough curve was investigated. A mathematical model from literature is used to simulate the experimental data. This mathematical model is used to design a column for the RWR prototypes.

6.2. Mathematical model

The equations that describe the dynamic behaviour of the adsorption process are the macroscopic equation (mass balance of the adsorption bed), microscopic equations (the rate equations corresponding to the various mass-transfer steps) and the equilibrium equation (adsorption of the overall uptake process) with its appropriate initial and boundary conditions. The general model is the most complicated model to solve mathematically and is therefore simplified with suitable assumptions. This significantly reduces the complexity of the model. The following assumptions are made:

- the system is isothermal
- there is only one solute adsorbed from the liquid
- liquid flow does not change during the experiments
- the axial liquid velocity is constant in the radial direction
- the solute concentration is constant in either phase in the radial direction.

The differential mass balance equation for a solute in a fixed bed adsorption column is given by Ruthven (1984) [20]. The equations are presented in the following variables; the concentration in the liquid phase C in [g_{LAS}/dm^3] and concentration on the solid phase, referred to as the adsorption capacity q in [$g_{LAS}/g_{adsorbent}$]:

$$-D_L\left(\frac{\partial^2 C_{bulk}}{\partial z^2}\right)_t + v_{int}\left(\frac{\partial C_{bulk}}{\partial z}\right)_t + \left(\frac{\partial C_{bulk}}{\partial t}\right)_z + \left(\frac{(1-\varepsilon_b)\rho_p}{\varepsilon_b}\right)\left(\frac{\partial \bar{q}}{\partial t}\right)_z = 0 \qquad (1)$$

where the first term is axial dispersion (D_L is the axial dispersion coefficient, C_{bulk} is the bulk concentration in the fluid phase and z is the axial position in the column), the second term is the flow term (v_{int} is the average axial velocity of the fluid through interstitial spaces), the third term is the concentration change term (t is time) and the fourth term is the adsorption rate expression (ε_b is the bed porosity, ρ_p is the particle density and $\bar{q}$ is the average adsorption capacity).

For the adsorption rate expression the linear driving force model (LDF) is used to represent the mass transfer into the solid pellets. The LDF model with the Glückauf approximation [21] (see appendix 6.8) is given by:

$$\frac{\partial \bar{q}}{\partial t} = \frac{15 D_{LDF}}{R^2}\left(q_S - \bar{q}\right) \quad (2)$$

where D_{LDF} is the effective diffusion coefficient, R is the radius of the adsorbent particle and q_S is the adsorption capacity at the outer surface of the adsorbent. External mass transfer is described by:

$$\frac{\partial \bar{q}}{\partial t} = \frac{3 k_L}{R \rho_P}\left(C_{bulk} - C_S\right) \quad (3)$$

where k_L is the film layer mass transfer coefficient and C_S is the concentration at the surface of the adsorbent. Equilibrium between LAS on the solid phase and in the liquid phase is described with the Langmuir isotherm model:

$$\frac{q_S}{q_m} = \frac{b C_S}{1 + b C_S} \quad (4)$$

where q_m is the maximum capacity of the particle and b is the affinity coefficient.

The initial model conditions are:

For t=0, C_{bulk}=0, $\bar{q}$=0 (5)

The boundary conditions are:

For t>0 and z=0: $C_0 = C_{bulk} - \frac{D_L}{v_{int}} \frac{\partial C_{bulk}}{\partial z}$ (6)

For t>0 and z=L: $\left(\frac{\partial C_{bulk}}{\partial z}\right) = 0$ (7)

where C_0 is the initial concentration at the inlet of the column and L is the length of the adsorption bed.

6.2.1. Dimensionless model

For the simulation it is often advantageous to make the model dimensionless. The following variables are introduced:

$$X = \frac{C_{bulk}}{C_0} \qquad X_S = \frac{C_S}{C_0} \quad (8)$$

$$Y = \frac{\bar{q}}{q_0} \qquad Y_S = \frac{q_S}{q_0} \quad (9)$$

$$\xi = \frac{z}{L} \qquad \theta = \frac{t v_{int}}{L} \quad (10)$$

where X is the dimensionless bulk concentration, X_S is the dimensionless concentration at the surface of the adsorbent, Y is the dimensionless average adsorption capacity, q_0 is the adsorption capacity in equilibrium with C_0, Y_S is the dimensionless adsorption capacity at the surface of the adsorbent, ζ is the dimensionless distance in the adsorption bed and θ is the dimensionless time. The differential mass balance equation is now rewritten to:

$$\frac{\partial X}{\partial \xi} + \frac{\partial X}{\partial \theta} + \frac{\left(1 - \varepsilon_b\right)}{\varepsilon_b}\left(\frac{q_0 \rho_P}{C_0}\right)\frac{\partial Y}{\partial \theta} = \frac{1}{Pe}\frac{\partial^2 X}{\partial \xi^2} \quad (11)$$

where *Pe* is the Peclet number:

$$\mathrm{Pe} = \frac{v_{int} L}{D_L} \tag{12}$$

At high Peclet numbers the effect of axial dispersion becomes negligible and the flow can be assumed as plug flow. The constants in equation (11) result in a dimensionless parameter, the dimensionless loading τ:

$$\tau = \frac{\varepsilon_b}{(1-\varepsilon_b)} \frac{C_0}{\rho_P} \frac{\theta}{q_0} \tag{13}$$

The loading is the amount of LAS that passed through the column at time t divided by the maximum amount of LAS that can be adsorbed by the column. The linear driving force (LDF) model is rewritten to:

$$\frac{\partial Y}{\partial \theta} = \frac{15 D_{LDF} L}{R^2 v_{int}} (Y_S - Y) \tag{14}$$

The external mass transfer equation is rewritten to:

$$\frac{\partial Y}{\partial \theta} = \frac{3 k_L L}{R v_{int}} \left(\frac{C_0}{q_0 \rho_P} \right) (X - X_S) \tag{15}$$

The Langmuir isotherm model is rewritten to:

$$Y_S = \frac{X_S}{r + X_S} \tag{16}$$

where *r* is the separation factor given by

$$r = \frac{1}{1 + bC_0} \tag{17}$$

The initial and boundary conditions are rewritten to:

At $\theta = \tau = 0, X = 0, Y = 0$ (18)

At θ>0 and ξ=0: $X(0) - \frac{1}{\mathrm{Pe}} \frac{\partial X(0)}{\partial \xi} = 1$ (19)

For θ>0 and ξ=L: $\frac{\partial X(L)}{\partial \xi} = 0$ (20)

The results of the simulations with different flow rates, bed heights and initial concentrations can be compared by plotting the relative LAS concentration *X* as a function of the loading τ.

6.2.2. Parameters

The equations (11), (12), (14) – (17) with initial conditions (18) and boundary conditions (19) and (20) are implemented in g-PROMS 3.0.3 (Process Systems Enterprise) and solved numerically to obtain the concentration profile in the bed and to estimate the breakthrough curves. The value of the LDF diffusion coefficient is obtained from zero length column experiments [2]. The value of the axial dispersion coefficient and the external film mass transfer coefficient are obtained from empirical correlations which are described below.

Estimation of the axial dispersion coefficient

In the model the effects of all mechanisms which contribute to axial dispersion are combined into one axial dispersion coefficient. To investigate the influence of axial dispersion, the axial dispersion coefficient is calculated with empirical correlations. The two main mechanisms that contribute to axial dispersion are molecular diffusion and turbulent mixing arising from the splitting and recombination of flows around the adsorbent particles. These effects are described by Ruthven (1984) [20]:

$$\frac{1}{Pe'} = \frac{\gamma_1 \varepsilon_b}{Re\,Sc} + \gamma_2 \qquad (21)$$

where γ_1 and γ_2 are experimental constants, *Pe'* is the particle based Peclet number, *Re* the Reynolds number and *Sc* is the Schmidt dimensionless number:

$$Pe' = \frac{v_{int} 2R}{D_L} \qquad (22)$$

$$Sc = \frac{\upsilon}{D_m} \qquad (23)$$

$$Re = \frac{\varepsilon_b v_{int} 2R}{\upsilon} \qquad (24)$$

where v_{int} is the interstitial velocity, D_m is the molecular diffusion coefficient and υ is the kinematic viscosity. The molecular diffusion coefficient is calculated with the Wilke-Chang method [22]:

$$D_m = \frac{7.4 \cdot 10^{-8} (\varphi M_B)^{0.5} T}{\mu V_A^{\,0.6}} \qquad (25)$$

where φ is the association factor, M_B is the molecular weight of the solvent, T is the temperature, μ is the viscosity of the solvent and V_A is the molecular volume of the solute at its normal boiling point. For the first term of equations (21) Wicke suggested [20]:

$$\gamma_1 = 0.45 + 0.55\varepsilon_b \qquad (26)$$

For the second term Edwards and Richardson suggested [20]:

$$\gamma_2 = \frac{1}{2\left(1 + \frac{13\gamma_1 \varepsilon_b}{Re\,Sc}\right)} \qquad (27)$$

The value of the axial dispersion coefficient is calculated within the model in gPROMS and a representative value is given in paragraph 6.4.3.

Estimation of the external film mass transfer coefficient

To estimate the external mass transfer coefficient, the most widely used correlation is from Wakao and Funazkri [20]:

$$Sh = \frac{k_L 2R}{D_m} = 2.0 + 1.1 Re^{0.6} Sc^{1/3} \qquad \text{for } 3<Re<10^4 \qquad (28)$$

Wilson and Geankoplis reported the correlation for low Reynolds numbers [20]:

$$Sh = \frac{k_L 2R}{D_m} = \frac{1.09}{\varepsilon_b} Re^{1/3} Sc^{1/3} \qquad \text{for } 0.0015<Re<55 \qquad (29)$$

The value of the external mass transfer coefficient is calculated within the model in gPROMS and a representative value is given in paragraph 6.4.3.

Pressure drop over the column

The pressure drop over the column is calculated with the Ergun equation [3]:

$$\frac{\Delta P}{L} = \frac{150(1-\varepsilon_b)^2}{\varepsilon_b^3 (2R)^2}\mu v_{sup} + \frac{1.75(1-\varepsilon_b)}{\varepsilon_b^3 2R}\rho_{liq} v_{sup}^2 \qquad (30)$$

where ΔP is the pressure drop over the bed, v_{sup} is the superficial velocity and ρ_{liq} is the liquid density. The liquid height needed to overcome the pressure drop is calculated with the following equation:

$$\Delta h = \frac{\Delta P}{\rho_{liq} g} \qquad (31)$$

where Δh is the liquid height and g is the gravitational acceleration. The pressure drop and liquid height are calculated within the model in gPROMS and representative values are given in paragraph 6.4.3.

6.3. Materials and Methods

6.3.1. Materials

The anionic surfactant, linear alkyl benzene sulfonate (LAS) was obtained from Unilever R&D, Vlaardingen, The Netherlands. Purity is around 92 wt% and the chain length is C_{10} to C_{13} (equally distributed; average molecular weight of LAS-acid is 312 g/mol). The critical micelle concentration (CMC) is 2 mM (0.6 g_{LAS}/dm^3) [23]. Granular activated carbon, GAC-1240 was supplied by Norit, Amersfoort, The Netherlands.

6.3.2. Characterization

The activated carbon granules were grinded and sieved to obtain the 315-500 μm fraction. The specific surface area, pore size and pore volume distribution were measured using nitrogen adsorption at -196^{o}C (liquid nitrogen temperature) with the Micromeritics Tristar 3000. Samples were pre-treated overnight to remove water and other contaminants from the pores. During the pre-treatment, a nitrogen flow was applied and the samples were heated to 105^{o}C.

6.3.3. Adsorption equilibrium experiments

The adsorption equilibrium experiments were conducted at different initial LAS concentrations ranging from 0.05 to 3 g/dm^3 milli-Q water. GAC-1240 (0.065 gram) and 80 ml of LAS solution were mixed in a screw capped flask and placed in a shaking bath (Julabo SW22) at 25^{o}C. In a preliminary experiment the equilibrium time was determined to be 48 hours; equilibrium was reached well within this time. The water phase was sampled with a syringe equipped with a filter (Spartan 30/0.45RC (0.45μm)) to remove suspended solids and the LAS concentration was measured by spectrophotometry at 223 nm with an accuracy of 2% (Shimadzu UV-1650PC).

6.3.4. Experimental set-up

The experimental set-up used to determine the column characteristics of the LAS adsorption on GAC-1240 is shown in figure 1. The set-up consists of a peristaltic pump (Masterflex L/S), a UV detector (Knauer Smartline 2500) and a column (Omnifit chromatography column with a 15 mm internal diameter and two adjustable end-pieces). The set-up can be operated up flow and down flow by exchanging the inlet and outlet tube of the column.

The experiments were conducted according to the following procedure. First, the adsorbents were pre-treated to remove air from the pores; milli-Q water was added to the adsorbent and vacuum was applied for 16 hours. Second, the column was packed with the adsorbent and equilibrated with vacuum filtrated milli-Q water (Whatman membrane filter (0.45 μm)) to prevent air bubbles in the column. After equilibration, water was replaced with a LAS solution and the LAS concentration at the outlet was monitored with the UV detector at 223 nm. The influence of bed height, flow rate, initial LAS concentration, external mass transfer and flow direction on the breakthrough curve was investigated. The LAS solution was also prepared with vacuum filtrated milli-Q water. The experiments were conducted at room temperature.

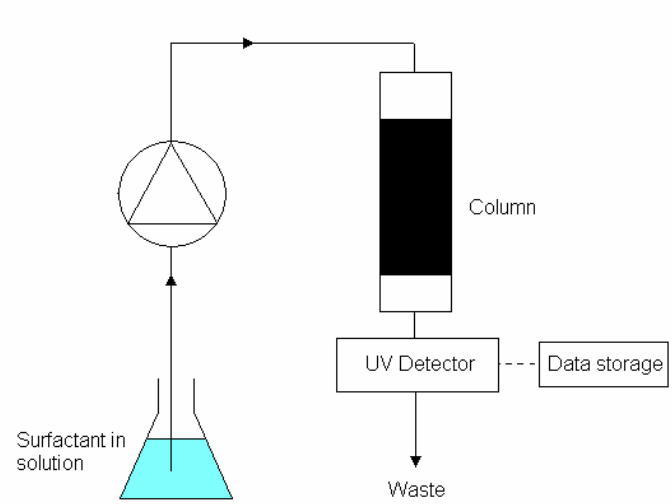

Figure 1: Schematic representation of the experimental set-up.

6.4. Results and discussion

6.4.1. Characterization of GAC-1240

Table 1 shows the properties of GAC-1240. Specific surface area, pore volume and average pore size were measured. The particle and bed density (420 g/dm^3) were obtained from the supplier Norit. The bed porosity was calculated from the particle and bed density.

Table 1: Material properties of GAC-1240.

Material	Raw material	Activation method	Bed porosity ε_b [-]	Particle density ρ_P [g/dm^3]	Specific surface area (BET) [m^2/g]	Pore volume [cm^3/g] at p/p_0=0.99	Average pore size [nm]
GAC-1240	coal	steam	0.49	830	1159	0.65	4.1

6.4.2. Adsorption equilibrium experiments

The LAS adsorption isotherm of GAC-1240 is shown in figure 2. The data is fitted with the well-known Langmuir isotherm model, which was selected because of its simplicity and previously demonstrated ability to describe surfactant adsorption [1]. The Langmuir parameters were obtained by fitting the experimental data and shown in the table in figure 2. The high value of the affinity coefficient b indicates a high affinity of LAS for GAC-1240. The maximum capacity q_m is 0.37 g LAS per gram GAC-1240.

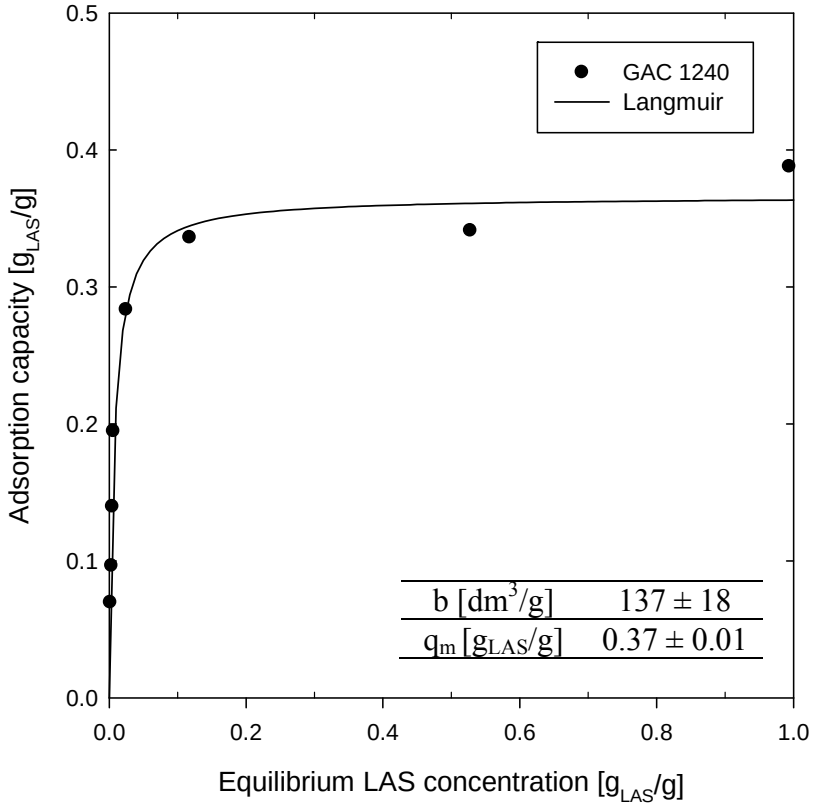

Figure 2: Adsorption isotherm of LAS for GAC-1240. The symbols are experimental data and the line is the fitted Langmuir isotherm model. The obtained Langmuir parameters are shown in the inserted table.

6.4.3. Determination of the parameters

The LDF diffusion coefficient was determined with the Glückauf approximation (appendix 6.8) and the experimental results of the zero length column set-up (ZLC) were used [2]. The ZLC experiments were performed for short times and the adsorption capacity at the end of the experiment was around 30% of the maximum

adsorption capacity. An additional experiment was performed with a longer operation time and a larger volume of LAS solution to obtain an adsorption capacity close to the maximum adsorption capacity. This experiment is performed to check if the diffusion coefficient is not affected by the adsorption capacity. The result of the additional experiment is shown in figure 11 (appendix 6.8). Two LDF diffusion coefficients were found: one initially fast D_{LDF}=1.2·10^{-13} m^2/s and one slower D_{LDF}=2.1·10^{-14} m^2/s. The initial LDF diffusion coefficient is different from the diffusion coefficient estimated with ZLC set-up. This difference is caused by a factor, which is the result of the difference in definition of the driving force: a concentration difference respectively an adsorption capacity difference. When the ZLC diffusion coefficient is corrected for dimensions it is similar to the LDF diffusion coefficient. The lower diffusion coefficient at a higher capacity can be explained by competition between the LAS molecules in the adsorbent. This lower diffusion coefficient is used as a first estimation for the mathematical model. The LDF diffusion coefficient was determined more accurately by comparing the simulation results of the column model with the experimental breakthrough curves. The simulation with a LDF diffusion coefficient of 3.2·10^{-14} m^2/s resulted in a good description of the experimental data ("base case" in figure 4). A preliminary calculation of the model is performed to obtain all the parameters. The results are shown in table 2. The Reynolds number is low, which means that the flow is laminar. The high Peclet number indicates a negligible effect of axial dispersion which was confirmed by model simulations; the flow can be assumed as plug flow. The pressure drop over the bed was calculated for an ideal situation (uniform, spherical particles) and resulted in a very low pressure drop.

Table 2: Parameters and calculated results.

Parameter	Symbol	Value	Unit
Adsorbent properties			
Particle diameter	2R	$4.07 \cdot 10^{-4}$	[m]
Particle density	ρ_p	830	[g/dm^3]
Solvent properties			
Dynamic viscosity	μ	$0.8904 \cdot 10^{-3}$	[Pa·s]
Kinematic viscosity	υ	$0.8904 \cdot 10^{-6}$	[m^2/s]
Molecular weight	M_B	18	[g/mol]
Density	ρ_{liq}	1000	[g/dm^3]
Association factor	φ	1	[-]
Solute properties			
Molar volume of LAS*	V_A	$227 \cdot 10^{-6}$	[m^3/mol]
Geometry of the bed			
Length	L	0.043	[m]
Diameter	D	0.015	[m]
Bed porosity	ε_b	0.49	[-]
Process parameters			
Flow rate	F	$7.98 \cdot 10^{-8}$	[m^3/s]
Inlet concentration	C_0	0.1015	[g_{LAS}/dm^3]
Temperature	T	298	[K]
Langmuir parameters			
Affinity coefficient	b	137	[dm^3/g_{LAS}]
Maximum capacity	q_m	0.37	[g_{LAS}/$g_{adsorbent}$]
Calculated parameters			
LDF diffusion coefficient	D_{LDF}	$3.2 \cdot 10^{-14}$	[m^2/s]
Adsorption capacity at C_0	q_0	0.345	[g_{LAS}/$g_{adsorbent}$]
Superficial velocity	v_{sup}	$4.52 \cdot 10^{-4}$	[m/s]
Interstitial velocity	v_{int}	$9.16 \cdot 10^{-4}$	[m/s]
Molecular diffusion coefficient	D_m	$3.6 \cdot 10^{-10}$	[m^2/s]
Schmidt number	Sc	2474	[-]
Reynolds number	Re	0.207	[-]
Peclet number	Pe	213	[-]
Axial dispersion coefficient	D_L	$1.85 \cdot 10^{-7}$	[m^2/s]
Sherwood number	Sh	17.7	[-]
Film layer mass transfer coefficient	k_L	$1.56 \cdot 10^{-5}$	[m/s]
Pressure drop over bed	ΔP	33.7	[Pa]
Liquid height	Δh	$3.44 \cdot 10^{-3}$	[m]

* Estimated from ACD/Chemsketch version 5.12.

6.4.4. Breakthrough curves

Reproducibility

Figure 3 shows the reproducibility of the breakthrough curve measurement. Both curves are almost identical. The small difference between the curves can be caused by a slight variation in packing of the adsorbent in the column for each experiment. Furthermore, the experiments run for two to five days and this can cause a small variation in the pump flow rate and a small variation in UV absorbance.

The total adsorption capacity of the column can be calculated from the experimental results with equation (32) [12]:

$$q_{total} = F \int_{t=0}^{t=t_{end}} (C_0 - C_t) dt \qquad (32)$$

where q_{total} is the total adsorbed quantity of LAS and C_t is the concentration at the outlet of the column (ζ =1). When the total adsorbed quantity is divided by the adsorbent mass in the column, the result can be compared to the expected adsorption capacity q_0 which is calculated from the adsorption isotherm (see figure 2). Results show that the actual adsorption capacity is around 80% of the expected ideal equilibrium adsorption capacity q_0. This deviation is more often found in literature and can be explained by non-ideal flow through the column [12]. Another investigation points out the difference between the equilibrium experiments and column experiments. The LAS concentration continuously decreases in the batch experiments while the LAS concentration continuously increases in the column operation [8]. Furthermore, Tan et. al. (2008) [12] stated that the effective surface area of the activated carbons packed in a column is lower compared to surface area in the stirred batch experiments.

An additional test was performed to investigate the difference between the actual adsorption capacity and equilibrium adsorption capacity. A breakthrough test was performed until the inlet concentration was reached. The maximum adsorbent capacity reached was again 80% of the expected ideal equilibrium adsorption capacity q_0. The column was dismantled and the adsorbent was repacked in the column. The flow was started again and the outlet concentration was measured. The outlet concentration decreased to 75% of the inlet concentration and increased in a few hours to the inlet concentration. This indicates that in the first run part of the adsorbent was not used because the solution did not contact all the adsorbent particles packed in the column. Another effect is caused by the residence time, if the residence time is increased the adsorbent capacity is increased as well (4.8 ml/min 80% and 1.1 ml/min 85%).

The experimental results will be plotted as a function of τ (equation (13)) in which q_0 is replaced by q_{total}/M resulting in:

$$\tau = \frac{\varepsilon_b}{(1-\varepsilon_b)} \frac{C_0}{\rho_P} \frac{tv_{int}}{L} \frac{M}{q_{total}} \qquad (33)$$

where M is the mass of adsorbent in the column. By doing this the experimental results and simulation results can be compared in a relative manner.

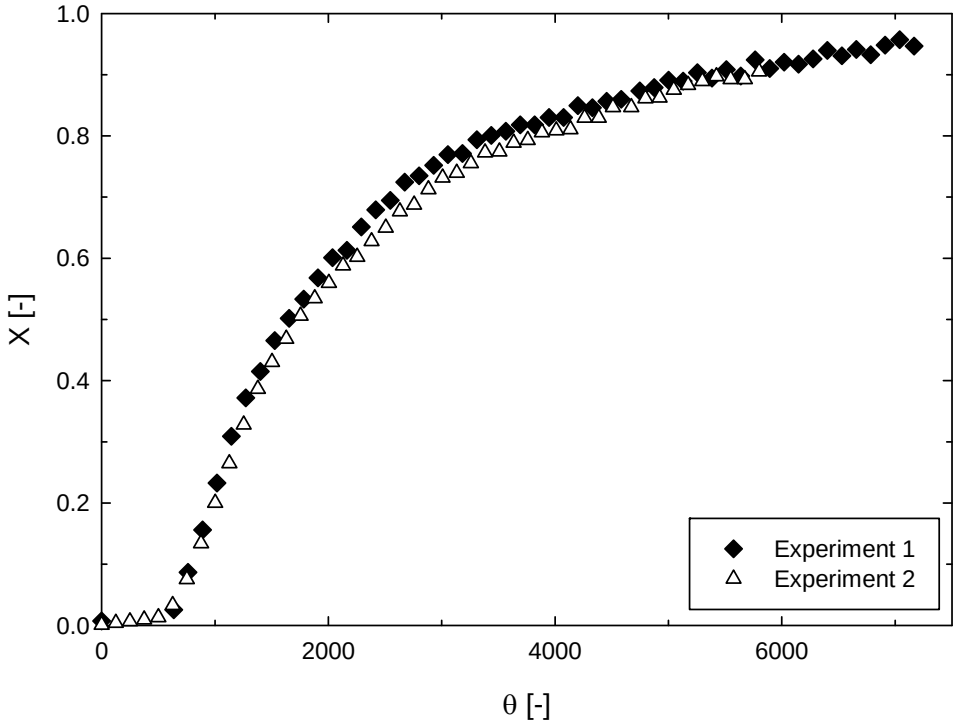

Figure 3: Reproducibility of the experimental breakthrough curves (bed height 43 mm; flow rate 4.8 ml/min; initial concentration 0.1 g_{LAS}/dm^3; particle size 315-500 µm).

Figure 4 shows a typical breakthrough curve combined with the simulation results obtained from the model for different particle diameters. The solid line is the result of the model simulation with the average particle diameter and the parameters as presented in table 2. The model with average particle size (407 μm) shows a close fit to the experimental results. It mainly deviates from the experimental results at the start of the experiment. In practice the particle size of the adsorbent ranges from 315 to 500 μm. Therefore, two model simulations for the smallest and largest particle size are added in figure 4. The initial shape of the breakthrough curve is well described by the smallest particle size, but overestimates the point of breakthrough. The point of breakthrough is set at *X=0.1* because the maximum allowed LAS concentration in the effluent is 0.01 g_{LAS}/dm^3 (see chapter 1: general introduction). The shape of the experimental curve at the end is well described by the largest particle size but underestimates the point of breakthrough in comparison to the experimental results. This indicates that the smaller particles contribute mainly at the start of the experiment and the larger particles at the end of the experiment which is as expected. The influence of the particle size can, in principle, be incorporated in the model by taking the particle size distribution into account. However, the experimental results are sufficiently described by the model simulation with an average particle size. Furthermore, there are additional reasons for the deviation between the model and experimental results. For example, the model assumes spherical adsorbent particles while in practice the granular activated carbon in not spherical at all. Therefore, the average particle size of 407 μm is used in the subsequent model simulations.

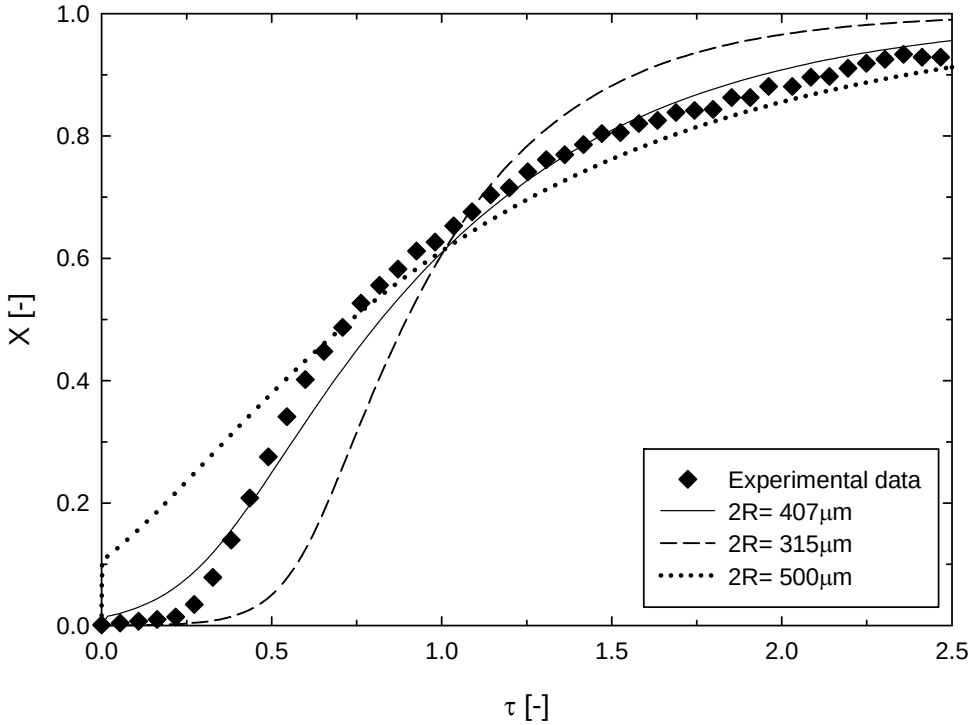

Figure 4: Experimental breakthrough curve ("base case": bed height 43 mm; flow rate 4.7 ml/min (0.62 BV/min); initial concentration 0.1 g_{LAS}/dm^3; particle size 315-500 μm) and model simulations with particle size 407, 315 and 500 μm.

Flow rate

Figure 5 shows the effect of a changing flow rate on the breakthrough curve. To help compare the results of different flow rates and bed heights, the residence time is added to the legend in bed volumes per minute (BV/min). The point of breakthrough at *X=0.1* is at the highest loading (τ) for the lowest flow rate and also shows the steepest breakthrough curve. At low flow rates the residence time is longer and the LAS molecules have more time to adsorb. This is in agreement with previous research [9, 12]. The lines in figure 5 are the model simulations for the different flow rates. The overall picture of the experimental results is well described by the model. At lower flow rates the breakthrough point appears at higher loadings and the breakthrough curve is steeper. The model overestimates the experimental results of 1.1 and 2.3 ml/min. To describe the experimental data better, the average particle size in the model should be increased; the breakthrough curve becomes shallower. At lower flow rates, the residence time is increased and the LAS molecules have more time to diffuse into the activated carbon particles. Under these conditions the larger particles can contribute more to the adsorption of LAS. The influence of residence time can also be investigated by changing the bed height of the column and is described in the next paragraph.

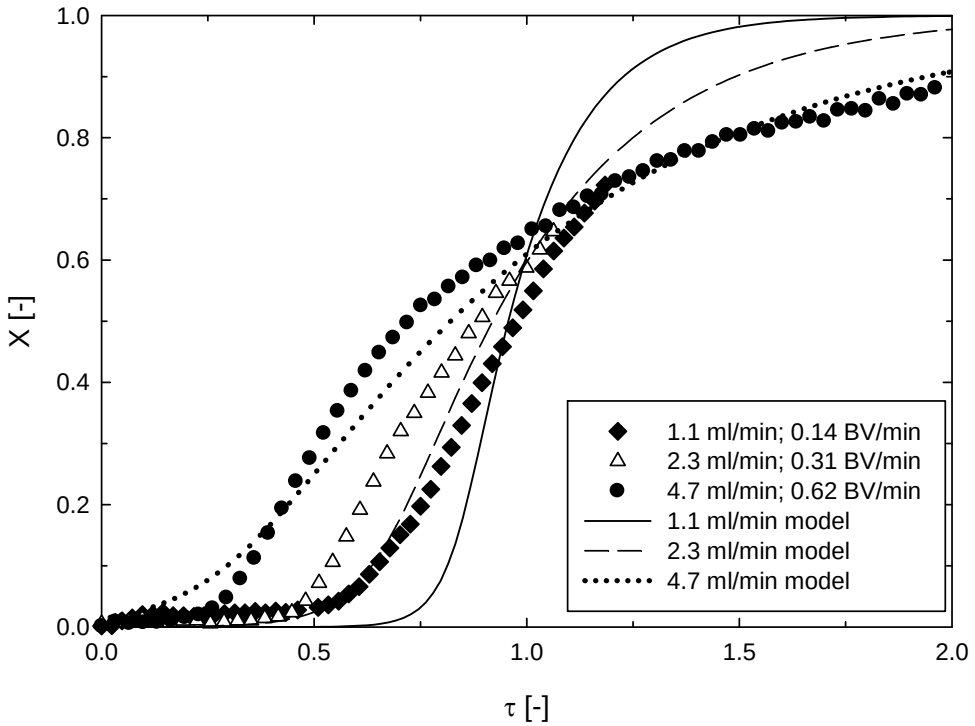

Figure 5: Influence of flow rate on the experimental breakthrough curve (bed height 43 mm; starting concentration 0.1 g_{LAS}/dm^3; particle size 315-500 µm). The lines are the model simulations of different flow rates with particle size 407 µm.

Bed height

Figure 6 shows the influence of different bed heights on the breakthrough curve. The breakthrough point (at *X=0.1*) appears at a higher loading with increasing bed height. The breakthrough curve becomes also steeper with increasing bed height. In a higher bed, the amount of activated carbon is larger and the residence time is longer. This trend is equal to the trend found for a decreasing flow rate and is also found in literature [9, 12]. The simulation results of the model for different bed heights are added in figure 6. The overall picture of the experimental results is well described by the model. When the bed height is increased the breakthrough point appears at higher loadings and the breakthrough curve is steeper. The model underestimates the initial experimental results at small bed length (43 mm). If the particle size would be decreased for the experiments with bed length 43 mm, the modelled breakthrough curve will be steeper and will fit the experimental data well. At shorter residence times, the smaller particles contribute more to the adsorption of LAS. The model overestimates the experimental results at large bed lengths (65 and 111 mm). If the particle size would be increased in the model for 65 and 111 mm bed length the breakthrough curve will be shallower and will fit the experimental data much better. At longer residence times, the larger particles contribute more to the adsorption of LAS. These results are in agreement with the results shown for changing flow rate.

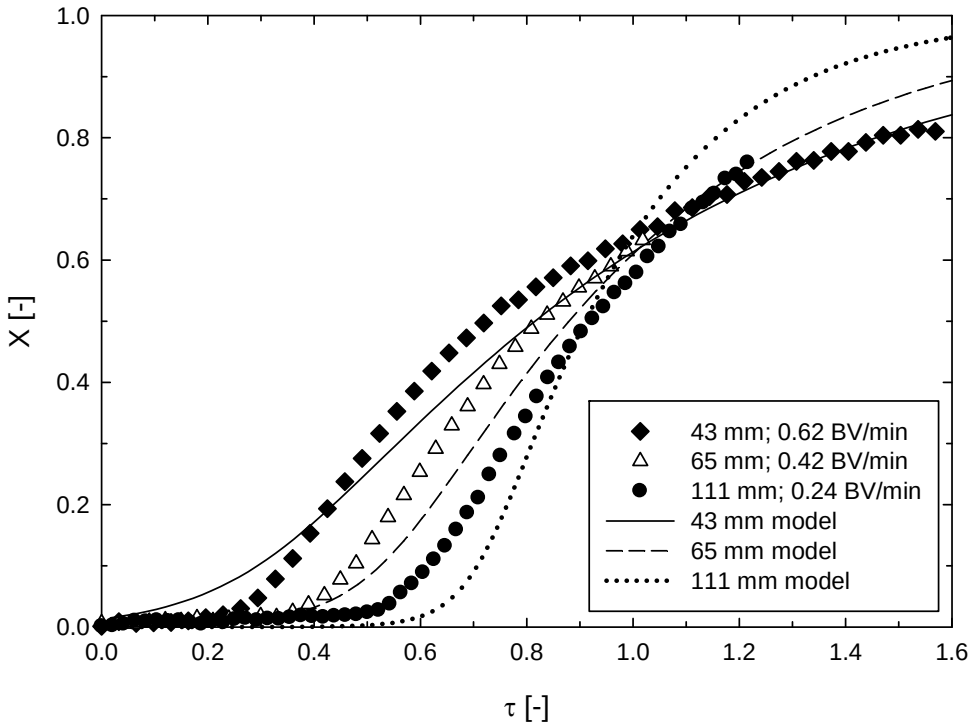

Figure 6: Influence of bed height on the breakthrough curve (flow rate 4.8 ml/min; starting concentration 0.1 g_{LAS}/dm^3; particle size 315-500 µm). The lines are the model simulations of different bed heights with particle size 407 µm.

External mass transfer

The contribution of external mass transfer can be investigated by increasing the flow rate and increasing the bed height with the same factor. In this way the flow rate is increased but the amount of bed volumes in time is not changed. Figure 7 shows two pairs of experiments with equal relative flow rates (expressed in BV/min) but different absolute flow rates (expressed in ml/min). Both pairs show a slightly earlier breakthrough point at the lower flow rate compared to the higher flow rate. This is the result of a decreased external mass transfer coefficient at lower flow rates (k_L $1.55 \cdot 10^{-5}$ m/s for 4.8 ml/min compared to k_L $1.23 \cdot 10^{-5}$ m/s for 2.3 ml/min). The model descriptions fit the trend well. The deviations are caused by the particle size distribution as explained before.

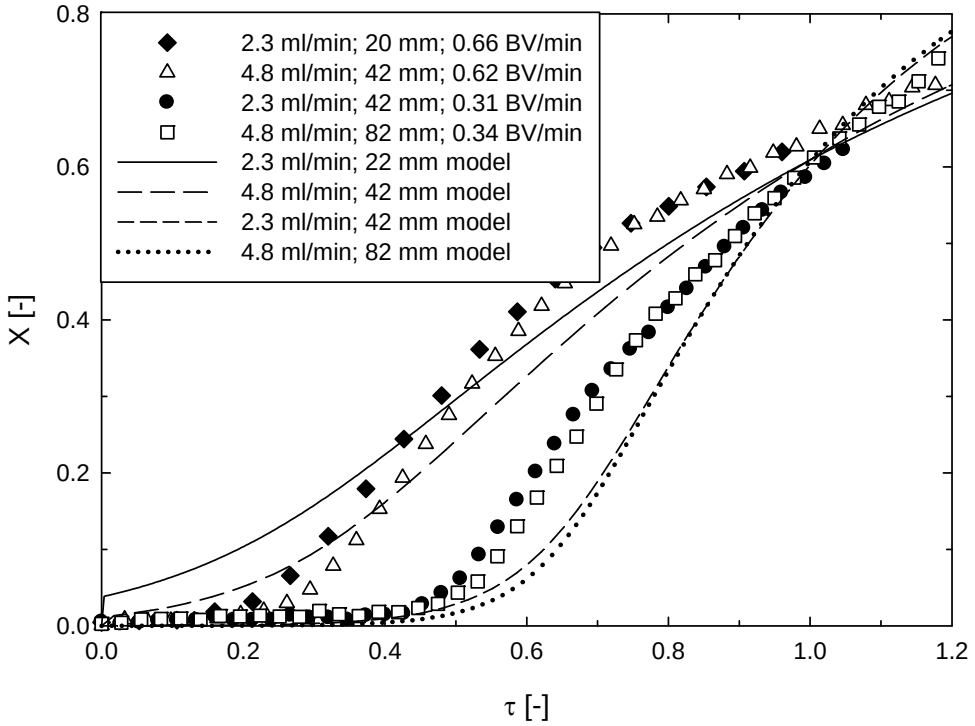

Figure 7: Influence of external mass transfer (starting concentration 0.1 g_{LAS}/dm^3; particle size 315-500 µm). The lines are the model simulations (particle size 407 µm).

Initial LAS concentration

Figure 8 represents the influence of the initial LAS concentration on the breakthrough curve. Experimental results show a small influence of the initial LAS concentration on the experimental breakthrough curve. The simulation results (see lines added in figure 8) predict a much larger effect. The model underestimates the experimental results for 0.2 g_{LAS}/dm^3 and overestimates the experimental results for 0.05 g_{LAS}/dm^3. Sperlich et. al. (2008) [24] investigated the validity of different kinetic expressions in mathematical models for breakthrough curve simulation. The LDF model is compared to the homogeneous surface diffusion model (HSDM) which is described in more detail as the adsorption model in chapter 4 [2]. Hand et. al. (1984) [25] defined three categories of breakthrough curves corresponding to different Biot numbers which can be seen in figure 9. The Biot number is defined according to equation (34):

$$Bi = \frac{k_L R C_0}{D_{LDF} \rho_p q_0} \qquad (34)$$

The Biot numbers for C_0=0.05, 0.1 and 0.2 g_{LAS}/dm^3 are 20, 35 and 66 respectively. It is clear that the initial concentration 0.1 g_{LAS}/dm^3 is just beyond the limit of the second category and the initial concentration 0.2 g_{LAS}/dm^3 is clearly in category three. The LDF model is not valid in this situation which explains the deviation of the breakthrough curve simulation. The deviation of the model from the experimental results of initial concentration C_0=0.05 g_{LAS}/dm^3 is not understood yet. Fortunately, the model gives a good simulation of the breakthrough curve with initial concentration C_0=0.1 g_{LAS}/dm^3. Therefore, the model can be used in the final design of the column for the RWR.

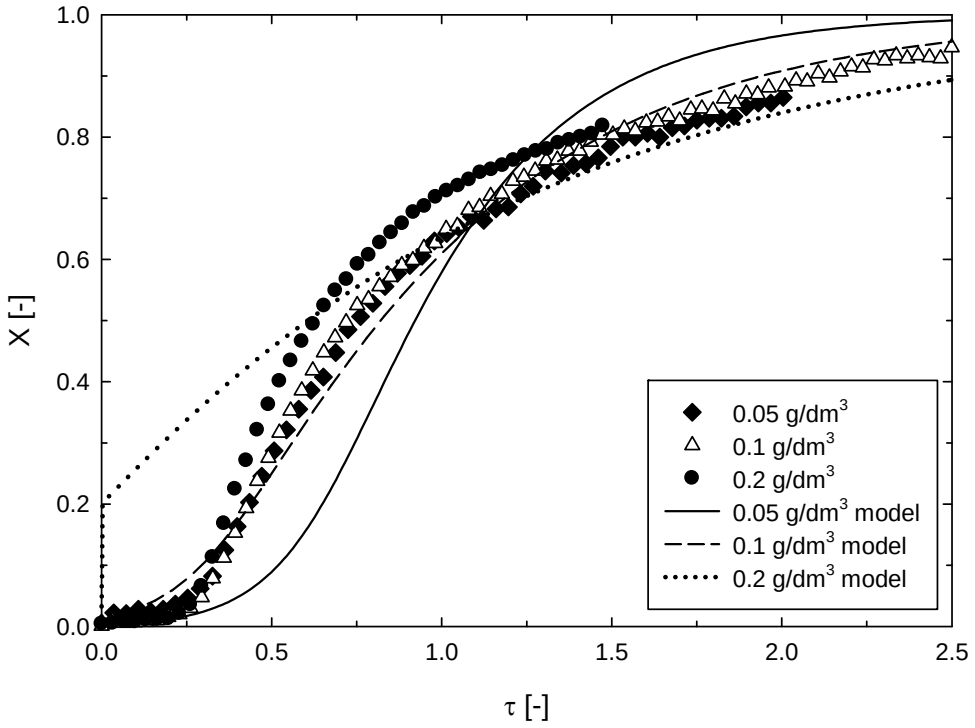

Figure 8: Influence of initial concentration on the breakthrough curve (bed height 43 mm; flow rate 4.8 ml/min; particle size 315-500 µm). The lines are the model simulations of different initial concentrations (particle size 407 µm).

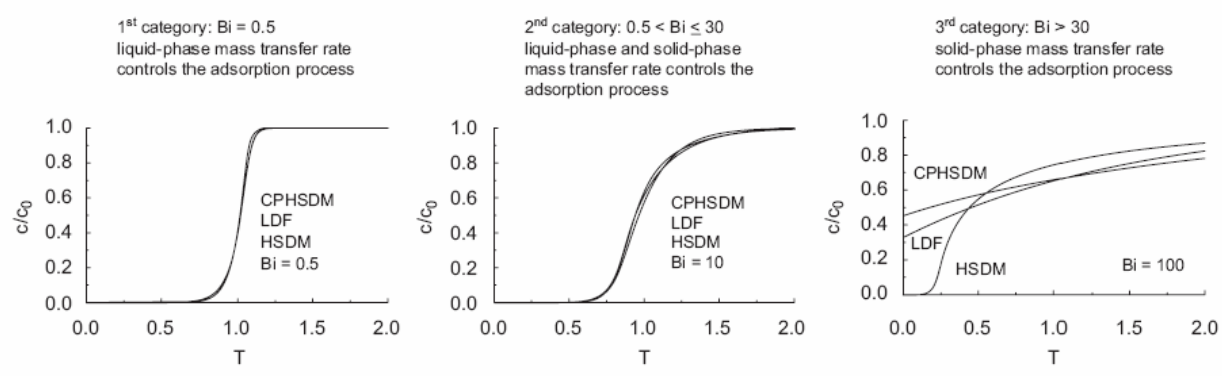

Figure 9: Categories defined by Hand et. al. (1984) [25] and corresponding model simulations Sperlich et. al. (2008) [24] (CPHSDM=constant pattern homogeneous surface diffusion model, LDF=linear driving force model, HSDM= homogeneous surface diffusion model).

Flow direction

The influence of up flow or down flow is shown in figure 10. Results show that the influence of the flow direction is small. During the up flow experiments it was observed that the packing of the bed is essential. If the bed was not tightly packed channelling takes place and an increased LAS concentration is immediately measured at the outlet of the column. In a down flow operation this is not that critical, because gravity helps packing the bed tightly. The small difference in the experimental results of the up flow and down flow operation is probably caused by the packing of the bed which was tighter in the up flow operation. This decreases the bed porosity and delays the breakthrough point [12]. For the RWR design it is important to know that the column can be operated in up flow and down flow mode and can be simulated with the same mathematical model.

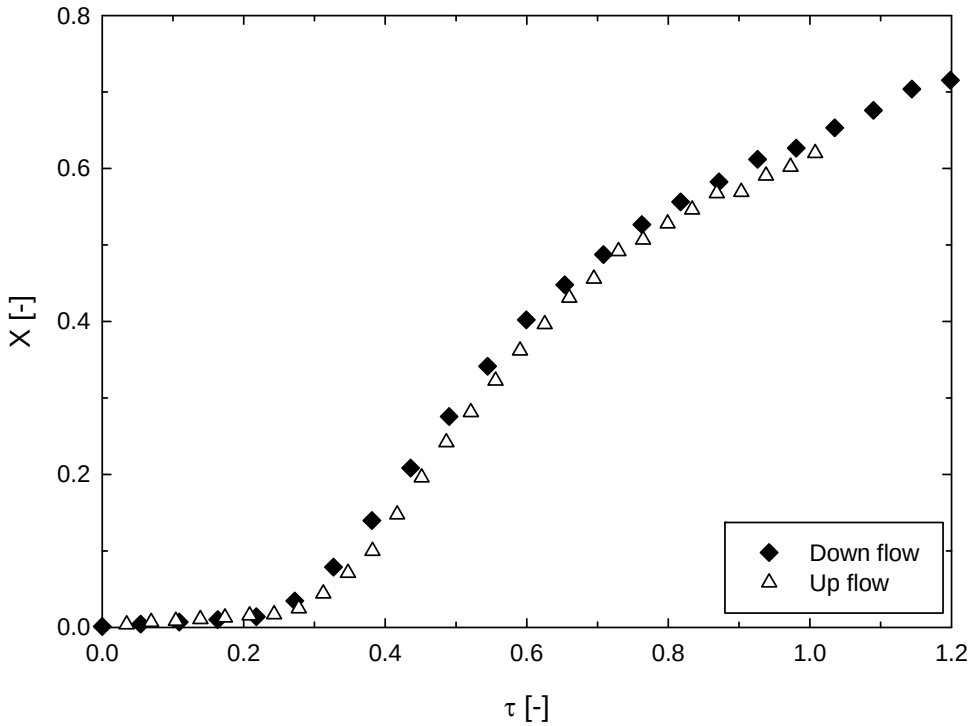

Figure 10: Influence of flow direction on the breakthrough curve (bed height 43 mm; flow rate 4.8 ml/min; initial concentration 0.1 g_{LAS}/dm^3; particle size 315-500 µm).

The model will be used to design a column for the RWR. To achieve the highest adsorption capacity of the adsorbent in the column the residence time should be as long as possible. For the final design of the RWR column a residence time of 0.14 BV/min (figure 5, flow rate 1.1 ml/min) will be used. To prevent an overestimation at *X=0.1* by the model (see figure 5, 1.1 ml/min model); the particle size in the model will be adjusted to 500 μm so that the model describes the experimental results well. This 'model' particle size and residence time were used for the final design of the column of the RWR.

6.4.5. Design of the RWR column

The simulation results of the model are used to design the column of the RWR. For the design of the RWR column some laundry conditions are set (see also chapter 1: general introduction):

- the RWR should be able to treat the laundry rinsing water produced by one average household (around 25 dm^3 per day) [26]
- the concentration of LAS in laundry rinsing water is 0.1 g/dm^3 [26]
- the maximum effluent LAS concentration allowed is 0.01 g/dm^3

The main consideration in the design of the RWR column is the ratio between two parameters, the flow rate and the amount of adsorbent necessary per litre of rinsing water. The flow rate should be high to treat relative large volumes of rinsing water in a short period of time. On the other hand the amount of adsorbent per litre of rinsing water should be low to reduce the operation cost of the RWR. The model is used to find an optimum between flow rate, adsorbent mass and other important factors which are described in this paragraph.

Table 3 shows the results of model simulations for different RWR column designs. The calculations started with a flow rate of 50 ml/min and a column with diameter of 0.05 m and length of 0.15 m (L=3D) [27] (case 1). In practice the column operation will be stopped when the outlet concentration exceeds 0.01 g_{LAS}/dm^3. The time period until this point of breakthrough is referred to as the operation time. When the operation time is multiplied with the flow rate the treated volume is obtained. The operation time corresponds to a column operated for 24 hours per day. In practice the column will operate only for a limited period per day to treat 25 dm^3. The run time is the total treated volume divided by the daily treated volume (25 dm^3). The adsorbent efficiency can be calculated by dividing the treated volume by the adsorbent mass.

Table 3: Simulation results and additional calculations for different RWR column designs (initial concentration 0.1 g_{LAS}/dm^3).

	Case 1	Case 2	Case 3	Case 4	Case 5
Diameter [m]	**0.05**	**0.06**	0.06	**0.1**	0.1
Length [m]	**0.15**	**0.18**	0.18	**0.3**	0.3
Adsorbent mass [g]	123	214	214	991	991
Particle size [µm]	315-500	315-500	315-500	315-500	**300**
Flow rate [ml/min]	50	50	**100**	**500**	500
Flow [BV/min]	0.17	0.10	0.20	0.21	0.21
Operation time* [days]	3.42	6.71	2.67	2.38	4.13
Treated volume [dm^3]	246	483	384	1709	2669
Run time** [days]	9.8	19.3	15.4	68.4	118.8
Adsorbent efficiency [dm^3/g]	1.98	2.25	1.79	1.72	2.99
Adsorbent cost per year [$/y]	13.3	11.7	14.8	15.3	8.8
Liquid height [m]	0.019	0.016	0.031	0.094	0.104

*Operation time is full time operation (24 hours/day). **Run time is the operation time with 25 dm^3 of rinsing water per day.

Case 1 (see table 3) would result in a run time of 9.8 days. Replacing the adsorbent every 9.8 days is quite demanding. Therefore, a second case is simulated with a larger column diameter (0.06 m), the L=3D ratio is maintained and therefore the column length is 0.18 m. The run time for case 2 is increased to 19.3 days. This makes the replacement of the adsorbent less demanding. The flow rate of 50 ml/min is quite low, for a daily load of 25 dm^3 this means more than 8 hours of operation. In case 3 the flow rate is increased to 100 ml/min. The run time is decreased to 15.4 days which is still acceptable. The adsorbent efficiency also decreased slightly compared to case 2 but is also still acceptable.

The column operations of case 1 to 3 were designed for long batch times. The rinsing water is added to the column and the column can operate for several hours. The cleaned rinsing water can be re-used afterwards or the next day. In case 4 the flow rate is increased to 500 ml/min. This means that the total amount of rinsing water per day (25 dm^3) is treated within one hour batch time. The size of the column is adjusted to maintain the residence time of case 3 (0.2 BV/min). Modelling shows that the run time is increased to 68 days which is very promising. On the other hand the adsorbent efficiency decreases to 1.72 dm^3/g, but is still acceptable. The main drawback of this column (case 4) is the size of 0.1 m in diameter and 0.3 m in length which is quite large for a small scale household device. This could be improved by using multiple smaller columns in parallel. Another disadvantage of such a large column and long operation time is its sensitivity to fouling and clogging. This might be prevented by filters at the entrance of the column. Cases 2 and 3 will be used as prototypes of the RWR and tested with consumers in India.

The operation cost of the RWR column is mainly replacement of the adsorbent. The bulk price of GAC-1240 is 2.9 $/kg [28]. In table 3 the adsorbent cost is calculated for all cases per year (assuming 365 days per year). The adsorbent cost ranges from $11.7 to 15.3 per year for cleaning 9.1 m^3 of laundry rinsing water.

The liquid height is calculated with the Ergun equation (30) and equation (31). This liquid height is necessary to overcome the pressure drop of the column for a given flow rate. The smallest particle size (315 μm) of the particle size distribution is used for the calculations to obtain the worst case scenario. A liquid height of 0.094 m is found for case 4, which is still acceptable. Therefore, an extra case (5) is added with a uniform particle size of 300 μm.

In case 5, the run time and adsorbent efficiency is increased significantly with a particle size of 300 μm (table 3). The adsorbent cost per year decreased to 8.8 $/year which is very promising. A drawback of the small particle size is a initial higher pressure drop that will increase during operation because of fouling of the column.

6.5. Conclusions

In this work small column experiments were performed to investigate the adsorption of LAS with GAC-1240 in a column application. The influence of flow rate, bed height, initial LAS concentration, external mass transfer and flow direction on the breakthrough curve was investigated. Parallel a mathematical model was developed that describes the experimental results. The main deviation between the model and experimental results is caused by neglecting the effect of particle size distribution of the adsorbent. The model assumes one particle size, where in practice the adsorbent consists of particles ranging from 315 to 500 μm. When the residence time is increased, by decreasing the flow rate or increasing the bed height, larger particles contribute relative more to the adsorption of LAS. When the residence time is decreased, by increasing the flow rate or decreasing the bed height, smaller particles contribute relative more to the adsorption of LAS. The model is used to design a column for the rinsing water recycler (RWR) to treat 25 litres of laundry rinsing water per day during an extended period. This resulted in two designs for further tests; a column (D=0.06 m; H=0.18 m) with a flow rate of 50 ml/min and a column with a flow rate of 100 ml/min. The adsorbent cost of both columns is $12 and $15 per year which is acceptable.

6.6. Symbols

b affinity coefficient [dm^3/g_{LAS}]
Bi Biot number [-]
C_{bulk} bulk concentration in fluid phase [g_{LAS}/ dm^3]
C_S concentration at the surface of the adsorbent [g_{LAS}/ dm^3]
C_t concentration at time t at the outlet of the column (ζ=1) [g_{LAS}/ dm^3]
C_0 concentration of the inlet stream [g_{LAS}/dm^3]
D_L axial dispersion coefficient [m^2/s]

D_m molecular diffusion coefficient [m^2/s]
D_{LDF} LDF diffusion coefficient [m^2/s]
F flow rate [dm^3/s]
g gravitational acceleration [m/s^2]
Δh liquid height [m]
k_L film layer mass transfer coefficient [m/s]
L length of the adsorption bed [m]
M adsorbent mass [$g_{adsorbent}$]
M_B molecular weight of the solvent [g/mol]
ΔP pressure drop over the bed [Pa]
Pe Peclet number [-]
Pe' particle based Peclet number [-]
$\bar{q}$ average adsorption capacity in the pores of particle [$g_{LAS}/g_{adsorbent}$]
q_0 adsorption capacity in equilibrium with C_0 [$g_{LAS}/g_{adsorbent}$]
q_m maximum adsorption capacity of particle [$g_{LAS}/g_{adsorbent}$]
q_S adsorption capacity of particle at the surface of the adsorbent [$g_{LAS}/g_{adsorbent}$]
q_{total} total adsorbed quantity [g_{LAS}]
q* adsorption capacity in equilibrium with the bulk of the fluid [$g_{LAS}/g_{adsorbent}$]
r separation factor [-]
R radius of the particle [m]
Re Reynolds number [-]
Sc Schmidt number [-]
t time [s]
T temperature [K]
V_A molecular volume of the solute at its normal boiling point [m/s]
v_{int} interstitial velocity [m/s]
v_{sup} superficial velocity [m/s]
X dimensionless bulk concentration [-]
X_S dimensionless concentration at the surface of the adsorbent [-]
Y dimensionless average adsorption capacity [-]
Y_S dimensionless adsorption capacity at the surface of the adsorbent [-]
z the axial position in the column [m]

γ_1, γ_2 experimental constants as described in equation (26) and (27) [-]
ε_b bed porosity [m^3_{void}/m^3_{bed}]
ζ dimensionless distance in the adsorption bed [-]
θ dimensionless time [-]
μ viscosity of the solvent [Pa*s]
υ kinematic viscosity [m^2/s]
ρ_{liq} liquid density [g/dm^3]
ρ_p particle density [$g_{adsorbent}/dm^3_{adsorbent}$]
τ loading [-]
φ association factor [-]

6.7. References

1. Schouten, N., et al., *Selection and evaluation of adsorbents for the removal of anionic surfactants from laundry rinsing water.* Water Research, 2007. **41**(18): p. 4233-4241 (Chapter 2).
2. Schouten, N., et al., *Investigation of adsorption kinetics of anionic surfactant with the zero length column method.* Submitted, 2008: p. (Chapter 4).
3. Sontheimer, H., J.C. Crittenden, and R.S. Summers, *Activated carbon for water treatment*. 2nd ed. 1988, Karlsruhe, Germany: DVGW-Forschungsstelle.
4. Warwick, T.P., *Does point of use for the developing world really work?* Water Conditioning & Purification, 2002: p. 66-69.
5. Devi, R., et al., *Removal of fluoride, arsenic and coliform bacteria by modified homemade filter media from drinking water.* Bioresource Technology, 2008. **99**(7): p. 2269-2274.
6. Schroeder, D.M., *Field experience with SONO filters.* https://www.dwc-water.com/fileadmin/images/PDF_files/SIM_Reports.pdf, 2007.
7. Clasen, T., S. Nadakatti, and S. Menon, *Microbiological performance of a water treatment unit designed for household use in developing countries.* Tropical Medicine and International Health, 2006. **11**(9): p. 1399.
8. Dwivedi, C.P., et al., *Column performance of granular activated carbon packed bed for Pb(II) removal.* Journal of Hazardous Materials, 2008. **156**(1-3): p. 596-603.
9. Saleh, M.M., *On the removal of cationic surfactants from dilute streams by granular charcoal.* Water Research, 2006. **40**(5): p. 1052-1060.
10. Weinberg, H. and N. Narkis, *Physico-chemical treatments for the complete removal of non-ionic surfactants from effluents.* Environmental Pollution, 1987. **45**(4): p. 245-260.
11. Gupta, S., et al., *Performance of waste activated carbon as a low-cost adsorbent for the removal of anionic surfactant from aquatic environment.* Journal of Environmental Science and Health - Part A Toxic/Hazardous Substances and Environmental Engineering, 2003. **38**(2): p. 381-397.
12. Tan, I.A.W., A.L. Ahmad, and B.H. Hameed, *Adsorption of basic dye using activated carbon prepared from oil palm shell: batch and fixed bed studies.* Desalination, 2008. **225**(1-3): p. 13-28.
13. Guelli U. de Souza, S.M.A., L.C. Peruzzo, and A.A. Ulson de Souza, *Numerical study of the adsorption of dyes from textile effluents.* Applied Mathematical Modelling, 2008. **32**(9): p. 1711-1718.
14. Attia, A.A., B.S. Girgis, and N.A. Fathy, *Removal of methylene blue by carbons derived from peach stones by H_3PO_4 activation: Batch and column studies.* Dyes and Pigments, 2008. **76**(1): p. 282-289.
15. Diban, N., et al., *Granular activated carbon for the recovery of the main pear aroma compound: Viability and kinetic modelling of ethyl-2,4-decadienoate adsorption.* Journal of Food Engineering, 2007. **78**(4): p. 1259-1266.
16. Pelech, R., E. Milchert, and R. Wróbel, *Adsorption dynamics of chlorinated hydrocarbons from multi-component aqueous solution onto activated carbon.* Journal of Hazardous Materials, 2006. **137**(3): p. 1479-1487.

17. Gupta, V.K., I. Ali, and V.K. Saini, *Defluoridation of wastewaters using waste carbon slurry.* Water Research, 2007. **41**(15): p. 3307-3316.
18. Sperlich, A., et al., *Breakthrough behavior of granular ferric hydroxide (GFH) fixed-bed adsorption filters: modeling and experimental approaches.* Water Research, 2005. **39**(6): p. 1190.
19. Schneider, R.M., et al., *Adsorption of chromium ions in activated carbon.* Chemical Engineering Journal, 2007. **132**(1-3): p. 355-362.
20. Ruthven, D.M., *Principles of adsorption and adsorption processes*. 1st ed. 1984, New York, USA: John Wiley & Sons, Inc.
21. Glueckauf, E., *Theory of chromatography: Part 10. - Formula for diffusion into spheres and their application to chromatography.* Transactions of the Faraday Society, 1955. **51**: p. 1540-1551.
22. van der Wielen, L.A.M., et al., *Diffusivities of organic electrolytes in water.* Chemical Engineering Journal, 1997. **66**(2): p. 111-121.
23. Basar, C.A., et al., *Removal of surfactants by powdered activated carbon and microfiltration.* Water Research, 2004. **38**(8): p. 2117-2124.
24. Sperlich, A., et al., *Predicting anion breakthrough in granular ferric hydroxide (GFH) adsorption filters.* Water Research, 2008. **42**(8-9): p. 2073-2082.
25. Hand, D.W., J.C. Crittenden, and W.E. Thacker, *Simplified models for design of fixed-bed adsorption systems.* Journal of Environmental Engineering, 1984. **110**(2): p. 440-446.
26. Unilever, *Personal communication*. December 2004: Hindustan Unilever Research India, 64 Main Road, Whitefield P.O. Bangalore 560066, India.
27. Sinnott, R.K., *Coulson & Richardson's Chemical Engineering*. 3rd ed. Vol. volume 6. 1999, Oxford, UK: Butterworth-Heinemann.
28. Norit, *Nijverheidsweg Noord 72, 3812 PM Amersfoort, The Netherlands.* June 2008.

6.8. Appendix 1: Glückauf approximation

The differential mass balance in a sphere is [20]:

$$\frac{\partial q}{\partial t} = \frac{D_{LDF}}{r^2}\frac{\partial}{\partial r}\left(r^2\frac{\partial C}{\partial r}\right) \quad (1)$$

The average intra particle concentration is given by:

$$\bar{q} = \frac{3}{R^3}\int_0^R r^2 q dr \quad (2)$$

Differentiating the above equation with respect to time:

$$\frac{\partial \bar{q}}{\partial t} = \frac{3}{R^3}\int_0^R \left(\frac{\partial q}{\partial t}\right) r^2 dr \quad (3)$$

Substituting (1) into (2) results in:

$$\frac{\partial \bar{q}}{\partial t} = \frac{3}{R^3}\int_0^R \left(\frac{D_{LDF}}{r^2}\frac{\partial}{\partial r}\left(r^2\frac{\partial q}{\partial r}\right) r^2\right) dr \quad (4)$$

This can be solved by fill in the limits of the integral:

$$\frac{\partial \bar{q}}{\partial t} = \frac{3}{R^3}\left(D_{LDF} R^2 \left(\frac{\partial q}{\partial r}\right)_{r=R}\right) \quad (5)$$

$$\frac{\partial \bar{q}}{\partial t} = \frac{3D_{LDF}}{R}\left(\frac{\partial q}{\partial r}\right)_{r=R} \quad (6)$$

Assuming the concentration profile inside the solid particle is parabolic:

$$\left(\frac{\partial q}{\partial r}\right)_{r=R} = \frac{5}{R}\left(q_R - \bar{q}\right) \quad (7)$$

where q_R is the value of q at r=R.

Substituting (7) in (6) results in:

$$\frac{\partial \bar{q}}{\partial t} = \frac{15D_{LDF}}{R^2}\left(q_R - \bar{q}\right) \quad (8)$$

Integrating the equation with limit t=0 to t=t results in:

$$\ln\left(\frac{q^*}{q^* - \bar{q}}\right) = \frac{15D_{LDF}}{R^2} t \quad (9)$$

where q* is the adsorption capacity in equilibrium with the bulk of the fluid. The plot of $\ln\left(\frac{q^*}{q^* - \bar{q}}\right)$ versus t should result in a straight line and the LDF diffusion coefficient can be calculated.

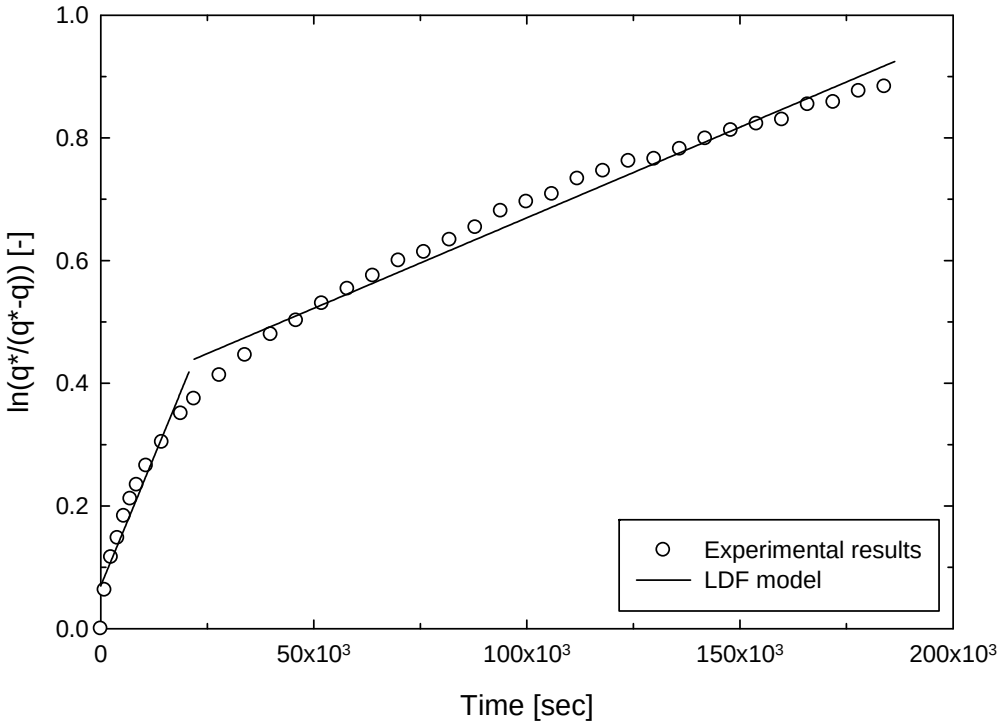

Figure 11: Estimation of the LDF diffusion coefficient. Experiment performed in ZLC with 0.065 grams of GAC-1240 with particle size 500-800µm and 0.2 dm^3 of LAS solution with a concentration of 0.1 g_{LAS}/dm^3.

7. Development of the Rinsing Water Recycler (RWR) and early consumer tests in India

Abstract

The current work is part of a project that aims to develop low cost technologies for the local decentralized recycling of laundry rinsing water. The basic idea is to clean-up the polluted rinsing water to allow multiple use cycles. Two prototypes of the rinsing water recycler (RWR) were tested with model rinsing water. In the bucket-to-bucket and siphon prototype activated carbon, Norit GAC-1240 was applied in a column operation. During the tests with model rinsing water, the particulate soil present clogged the column. An additional step is necessary to remove the particulate soil. Coagulation with poly aluminium chloride (PAC+) proved to be the easiest method to remove the particulate soil. The combination coagulation and adsorption was suitable to clean-up the model rinsing water for re-use. The operational cost of the prototypes is around $1.7 per cubic metre of water which is higher compared to the local water price of $1 per cubic metre of water. Early consumer tests with the bucket-to-bucket and siphon prototype were carried out in Phulera, Rajasthan, India. The response of the consumers on the quality of the treated water was very positive. The consumers preferred the siphon prototype because it is small and easy to use. The flow rate is an important point for improvement. Finally, the amount of money that consumers are willing to spend on the RWR prototypes is higher then the actual cost of the prototypes.

7.1. Introduction

The UN estimates that between 2000 and 2030 the urban population of developing countries will nearly double in size from 2 billion to about 4 billion people. This population growth will dramatically intensify the economical and physical water scarcity already existing in these countries [1]. One way of dealing with this increasing water scarcity is the development of technologies for wastewater clean-up and re-use. However, in large parts of the developing world, incomes are only around one US dollar a day. Therefore, water re-use technologies can only be implemented successfully if they are of low cost.

Many small scale water technologies are developed for safe drinking water, for example for the removal of arsenic from drinking water. Arsenic problems are a concern of small communities in rural areas around the world, where groundwater is the main source of drinking water. Devi et. al. (2008) [2] describes a system where filtration and adsorption are combined in a tank. The tank is filled with layers of sand, crushed brick, gravel and drain stone to remove fluoride, arsenic and coliform bacteria from drinking water. Sarkar et. al. (2005) [3] describes an adsorption column mounted on top of an existing well-head hand pump. The column contains a splash distributor for the oxidation of dissolved iron and below a fixed-bed of activated alumina and graded gravels is present to adsorb arsenic. The SONO filter consists of two buckets placed above each other [4]. The top bucket contains river sand and composite ion matrix, the lower bucket contains sand and activated carbon. The composite ion matrix adsorbs inorganic arsenic components and the activated carbon adsorbs organic arsenic components.

Other small scale treatment techniques have been developed to treat water and obtain safe drinking water. More than one billion people do not have access to safe water. Diarrhoeal diseases resulting from a lack of safe water remain a leading cause of illness and death in the developing world, with about two million children dying every year due to these diseases [5]. Many drinking water filters combine filtration and colloidal silver to kill the bacteria. Another method is a combination of filtration and chlorination to kill the bacteria and adsorption to remove the chlorination products and excess of chlorine. DSM developed a filter consisting of silicium oxide impregnated with silver, which kills 99.99% of all bacteria [6]. Potters for peace use the same treatment method with a ceramic pot filter. Clay is mixed with sawdust and water and baked in an oven. Due to the heat the sawdust burns and leaves a porous structure behind. The pot is submerged in a solution of colloidal silver [5]. Unilever developed the Pure-it system which combines filtration, disinfection and adsorption [7]. The system is gravity driven and uses siphons to treat the water step by step. Warwick (2002) [8] described two two-bucket systems. In the top bucket the water is filtered with a ceramic filter and in the lower bucket it is chlorinated. A second system consists of filtration and chlorination in the top bucket and adsorption by activated carbon in the lower bucket. An up-flow water filter was developed by UNICEF and tested by Singh and Chaudhuri (2006) [9]. The system consists of two tanks. In the upper tank the untreated water is stored and the lower tank contains gravel, sand, crushed charcoal

and fine sand. The water in the upper tank is introduced at the bottom of the lower tank and the water flows upwards through the layers in the lower tank.

Small scale systems for the treatment of water to obtain safe drinking water are very common, but a large part of the daily water consumption is not used for drinking. About half of the daily water consumption in India is used for doing laundry where it is used for washing and rinsing [10]. The major part of laundry water is rinsing water, which is relatively clean compared to the main wash liquor. Therefore, rinsing water is highly suitable for clean-up and re-use. Although this water is an attractive source, the treatment of laundry rinsing water in small scale systems is not very common.

The current work is part of a project that aims to develop low cost technologies for the local decentralized recycling of laundry rinsing water. The basic idea is to clean-up the polluted rinsing water to allow multiple use cycles. When the main contaminants from the rinsing water are removed, it can be re-used for household or irrigation purposes. Main contaminants are the added detergent ingredients and the 'dirt' released from the fabrics during rinsing [10].

The objective of this study was to develop a small scale rinsing water recycler (RWR). The criteria for the design were determined. Previous research, a literature survey and many discussions resulted in three RWR prototypes. These RWR prototypes were tested using a solution of anionic surfactant in water and model rinsing water. With the results from the tests the prototypes were developed further or rejected. Finally, the selected RWR prototypes were tested with consumers in India. The consumer tests took place in Phulera, Rajasthan, where water scarcity is common. The consumers were asked for their feedback and suggestions for improvement.

7.2. Rinsing water recycler (RWR) specifications and design

To design a rinsing water recycler (RWR) with an optimal performance, the following criteria need to be fulfilled:

- removal of the main components in model rinsing water; the treated water should be suitable for doing laundry, cleaning and irrigation
- household scale; the RWR should be able to treat laundry rinsing water produced by one average household (around 25 litres per day) [10]
- low cost; the investment and operating costs for the RWR should be low compared to the local water price ($0.75-1.00 per cubic meter water) [11]
- no power source; in developing countries power is not always available and therefore the RWR should not depend on electricity or other power sources
- the RWR should be easy to use, easy to maintain, portable and safe
- low amount of waste; the amount of waste should be minimized
- attractive to culture; the RWR should not interfere with the consumer habits.

The first priority is to remove the main components from laundry rinsing water. In previous research [12], adsorption technology proved to be suitable for the removal of the main components, namely anionic surfactants. Adsorption technology has the

potential to become a suitable low cost technology because it can be applied in small devices and is applicable on household scale. Our research showed that activated carbon (GAC-1240) and layered double hydroxide (LDH) are suitable for the removal of anionic surfactants (linear alkyl benzene sulfonate (LAS)) from laundry rinsing water. The LAS adsorption capacity compared to the adsorbent cost make GAC-1240 and LDH suitable materials for application in a RWR. A disadvantage of LDH is its instability [13]. LDH is not very stable in water and therefore only suitable for short time application in a RWR.

Adsorption in column operation is often used in small scale devices for local drinking water treatment (as described in paragraph 7.1: the introduction;). A suitable adsorbent in column operation meets many of the mentioned criteria. A suitable adsorbent contains a high adsorption capacity to remove the main components. A high adsorption capacity minimizes the amount of adsorbent necessary and therefore minimizes the cost, size of the column and amount of waste. A column operation is applicable on a household scale and is easy to use. The flow is driven by gravity and no electricity is needed.

Three Rinsing Water Recycler prototypes (RWR) were developed. Pictures of two prototypes and their schematic drawings are shown in figure 1. In both prototypes the GAC-1240 is applied in a packed bed. At the top and bottom of the column, cloth filters and foam filters are present to filter large particulates and keep the adsorbent bed in position. Data from chapter 6 is used to calculate the column dimensions for a concentration of LAS of 0.1 g_{LAS}/dm^3 and 25 litres of rinsing water per day. For the preliminary tests with model rinsing water the columns are slightly smaller to reduce the amount of GAC-1240 consumed for each test. The column diameter is 0.036 m and the length is 0.11 m. The amount of GAC-1240 in the column is around 45 grams. The flow rate is 50 ml/min. The presented column operation is simulated with the mathematical model from chapter 6 and resulted in a breakthrough at 0.01 g_{LAS}/dm^3 after 27.5 hours. For the tests in this chapter the presented column should perform well.

A column operation is often introduced in a bucket-to-bucket system [3], [8]. In our set-up two buckets are placed above each other and a column filled with adsorbent is fixed in the bottom of the top bucket (figure 1A). The column consists of cloth filters, foam filters, and 45 grams of GAC-1240 (particle size: 315-500 μm). The flow rate through the column can be adjusted by a tap at the bottom of the column. Laundry rinsing water is poured in the top bucket and flows through the column were soluble contaminants are adsorbed. With a rubber ring the entrance of the column is slightly higher than the bottom of the bucket. Dirt and sand present in laundry rinsing water will settle at the bottom of the upper bucket preventing the column from clogging.

Based on the idea of the UNICEF up-flow water filter [9] the siphon prototype was developed (figure 1B). The siphon is placed in a bucket filled with laundry rinsing water, which is placed at an elevated level. The siphon consists of a column filled with cloth filters, foam filters, a support plate with holes (diameter 2 mm) and 45 grams of

GAC-1240 (particle size 315-500 μm). The bottom of the siphon is closed and holes (diameter 2 mm) are drilled at the side of the tube two centimetres above the bottom and about one cm below the support plate. This will make sure that the settled dirt and sand stay behind in the bucket to prevent the column from clogging. The top of the siphon is connected to a tube. After placing the siphon in a bucket with rinsing water, the flow is started with a hand pump and a tap is used to control the flow. The difference in water level between the top bucket and lower bucket is the driving force for the flow rate. The tube length can be adjusted to make sure that the flow rate does not exceed the designed value.

The bucket-to-bucket and siphon clean the rinsing water after laundry. The third prototype is a permeable bag containing adsorbent and is operated in batch mode. It cleans the laundry rinsing water during the rinsing process. The permeable bag is added during the rinse and directly adsorbs the released soluble contaminants from the clothes. Rinsing water is cleaned instantly and no additional water for rinsing is necessary. The adsorbent in the permeable bag is discharged after use. The process of rinsing only takes a few minutes and adsorption of the main contaminants should take place within this time period. The short operation time allows both GAC-1240 and LDH as suitable adsorbents.

The adsorbent is present in a ‘micro porous’ bag to remove it easily from the water while keeping it accessible for the adsorbate (LAS). To investigate the feasibility of the permeable bag a ´best case´ scenario was taken. The adsorbent is added directly to the rinse water (without a permeable bag) and the smallest available particle size (<100 μm) is used. The adsorption should take place within 10 minutes, because the process of rinsing only takes a few minutes. Agitation during rinsing was simulated with a stirrer.

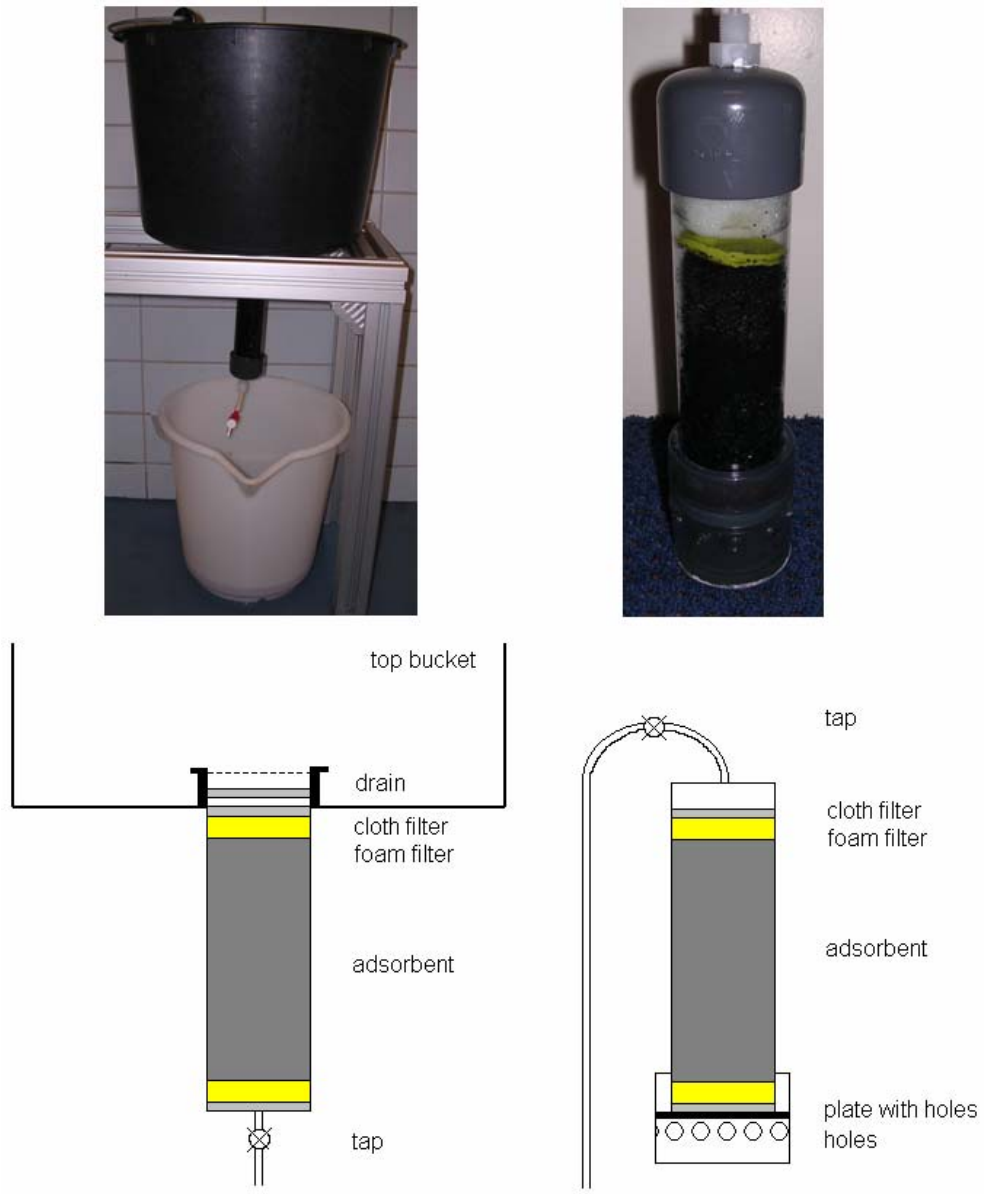

Figure 1: Pictures and schematic drawing: A. Bucket-to-bucket prototype and B. Siphon prototype. The dimension of both columns is identical: diameter 0.036 m and length 0.11 m.

7.3. Materials and Methods

7.3.1. Materials

Model rinsing water is made according to the specifications given by Hindustan Unilever [10]. The ingredients are Surf Excel obtained from Unilever R&D, Vlaardingen, The Netherlands and model soil obtained from Hindustan Unilever R&D, Bangalore, India. Demi water is used to make model rinsing water. $CaCl_2$ was added to obtain average Indian water hardness (table 1). A Surf Excel concentration of 0.5 g/dm^3 results in a LAS concentration of 0.1 g/dm^3.

Table 3: The concentration of the main ingredients in model rinsing water [10].

Ingredient	Concentration [g/dm^3]
Surf Excel	0.5
Model soil*	0.5
Salt (NaCl)	0.1
$CaCl_2$	0.25

* Model soil consists of 90% kaolinite, 5% carbon, 2.5 % Fe_3O_4, 2.5% SiO_2.

The adsorbent in the prototypes of the rinsing water recyclers (RWR) was granular steam-activated carbon (GAC). GAC-1240 was supplied by Norit, Amersfoort, The Netherlands. The permeable bag is tested with both GAC-1240 and extrudates of layered double hydroxide (LDH). LDH was supplied by Akzo Nobel, Arnhem, The Netherlands.

7.3.2. Characterization

Model rinsing water and the treated water were analyzed with different methods as shown in table 2. The samples are filtered to remove particulate soil (Spartan 30/0.45RC (0.45μm)). Furthermore, the treated water was examined by sight and smell to understand the perception of the consumers.

The model soil was characterized by particle size distribution and morphology (see table 2). The suspension is treated in an ultrasonification bath for 10 minutes (Bandelin Sonorex Digitec).

The activated carbon granules and LDH extrudates were grinded and sieved in fractions. The specific surface area, pore size and pore volume distribution of these fractions were measured using nitrogen adsorption at -196^{o}C (liquid nitrogen temperature) with the Micromiretics Tristar 3000. The samples are pre-treated overnight to remove water and other contaminants from the pores. During the pre-treatment, a nitrogen flow is applied and the samples are heated to 105^{o}C.

Table 2: Characterization of model rinsing water: analysis techniques and corresponding components.

Analysis liquid phase	Components
Total carbon (TC) (Shimadzu TOC-V CPH)	Total carbon Total organic carbon (TOC)
Inorganic carbon (IC) (Shimadzu TOC-V CPH)	Carbonate (CO_3^{2-})
Dr Lange (anionic surfactant) (Lange LDK332 Anionic surfactant Hach Lange GMBH)	Linear alkyl benzene sulfonate (LAS)
UV absorption at 223nm (Shimadzu UV-1650PC)	LAS only when no other contaminants are present in water
Inductively Coupled Plasma (ICP) (Perkin Elmer Optima 5300 DV)	Phosphorus, measure for sodium triphosphate (STP) Calcium (Ca^{2+})
pH (pH/Cond 340i WTW)	OH^-, CO_3^{2-}
Analysis solid phase	**Property**
Scanning Electron Microscope (SEM) Jeol SEM JSM-6480LV	Morphology
Particle size distribution (Eyetech Ankersmid LFC 101 Time of transmission method)	Particle size distribution

7.3.3. Operation of the RWR prototypes

Pictures of the two Rinsing Water Recycler prototypes (RWR) and their schematic drawings are shown in figure 1. In both prototypes the GAC-1240 is present as a packed bed. The GAC-1240 in the prototypes was pre-treated to remove entrapped air from the pores and to prevent air bubbles in the column. Therefore, milli-Q water was added to the adsorbent and vacuum was applied for 16 hours.

Bucket-to-bucket

Five litres of model rinsing water were added to the top bucket. The model rinsing water was allowed to settle for five minutes. Subsequently, the tap was opened and a flow rate of 50 ml/min was maintained. The model rinsing water and the treated water were analysed, see table 2.

Siphon

The siphon is placed in the bucket and placed at an elevated level. The model rinsing water was allowed to settle for five minutes. The flow was started with a hand pump and a flow rate of 50 ml/min was maintained with the tap. The model rinsing water and treated water were analysed, see table 2.

Permeable bag

To investigate the feasibility of the permeable bag a ´best case´ test was preformed. GAC-1240 or LDH with the smallest particle size (<100 μm) was added directly (without a permeable bag) to a solution of 0.1 g LAS per litre and the suspension was stirred with 300 rpm. Every minute a sample was taken from the solution and the LAS concentration was measured with UV-detection (see table 2). The LAS concentration should decrease to 0.01 g/dm^3 within 10 minutes. The amount of adsorbent was adjusted to reach this objective.

7.4. Results and discussion

7.4.1. Characterization of model soil

The morphology of the model soil was observed using a Scanning Electron Microscope (SEM) and the picture is shown in figure 2. Model soil consists of very small plate shaped particles which are aggregated to larger particles.

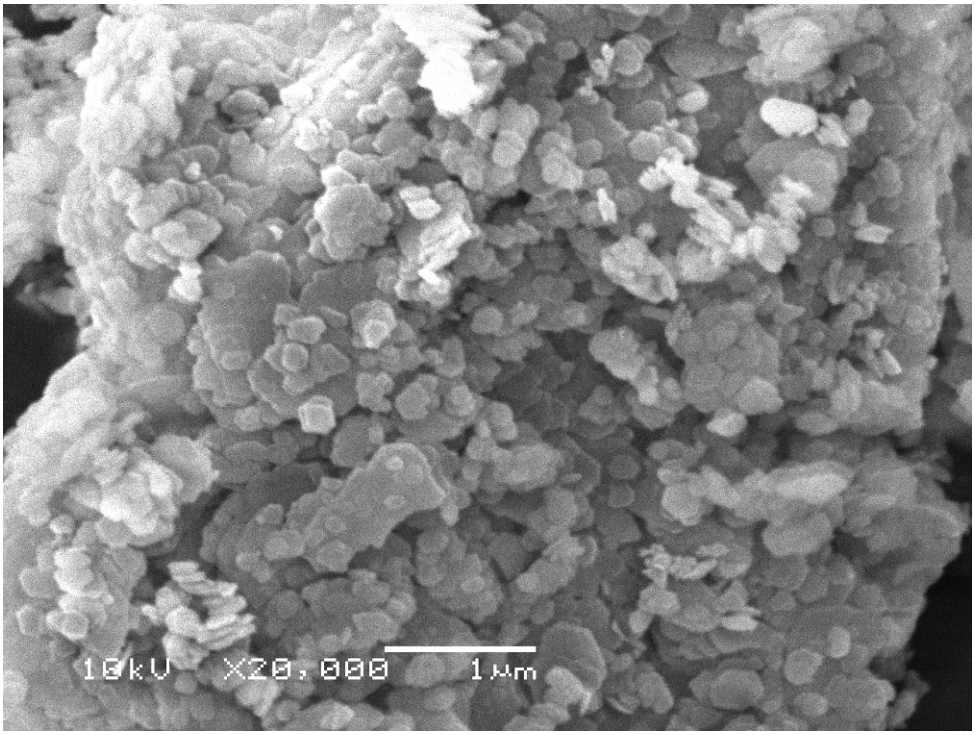

Figure 2: SEM picture of the model soil.

Table 3 gives the size distribution of the particulates present in model soil. The solution was sonified to break down the aggregates into smaller particulates. This simulates the agitation during laundry which will also break down the aggregates. The particulates are very small with an average particle size of 1.07 μm.

Table 3: Particle size distribution (number based).

	D10 [μm]	D50 [μm]	D90 [μm]
Model soil	0.62	1.07	3.89

7.4.2. Characterization of the adsorbents

Table 4 shows the properties of GAC-1240 and LDH. GAC-1240 is used in the RWR column prototypes and the permeable bag. LDH is only used in the permeable bag, because of its instability in water it is suitable for short term application only.

Table 4: Material properties of GAC-1240 and LDH.

Material	Specific surface area (BET) [m^2/g]	Pore volume [cm^3/g] at p/p_0=0.99	Average pore size [nm]	Particle porosity ε_p [-]	Apparent density ρ_{app} [g/cm^3]	Cost [$/kg]
GAC-1240	1159	0.65	4.1	0.57	0.42	2.9
LDH	136	0.35	8.6	0.51		6.0

7.4.3. Tests with linear alkyl benzene sulfonate (LAS) in water

The prototypes were first tested with a solution of the main component in laundry rinsing water, namely linear alkyl benzene (LAS). All prototypes are evaluated in this investigation: the bucket-to-bucket prototype, the siphon prototype and the permeable bag. The first two prototypes were operated in column operation. The operation conditions for the column were tested extensively with solutions of LAS in water and are described in chapter 6. Therefore, only the results of the experiments with the permeable bag are described here. The 'best case' test was performed to investigate the feasibility of the permeable bag. During the 'best case' test the permeable bag was not used to obtain the most optimal mixing of the adsorbent with the LAS solution. Furthermore, the smallest particle size (<100 μm) of the adsorbent was used for the fastest adsorption kinetics.

Table 5 shows the amount of adsorbent necessary to decrease the LAS concentration of one litre solution from 0.1 to 0.01 g/dm^3 during the 'best case' test. For both adsorbents one gram is necessary to decrease the LAS concentration of one litre solution within five to ten minutes. In the 'best-case' test the costs for GAC-1240 per cubic meter treated water is $2.9 and the cost for LDH is $6 (see table 5). The costs for both adsorbents are much higher compared to the local water price of $0.75 to $1 per cubic meter water [11]. During the experiments with GAC-1240 it was observed that adding GAC-1240 to the LAS solution, the water became grey because fines leached into the water. Even when larger particles were used and were kept in a permeable bag this grey colour occurs. Therefore, adding GAC-1240 to clean clothes in rinsing water is not an option.

Table 5: Time needed and costs involved to reduce the initial LAS concentration of 0.1 g_{LAS}/dm^3, to 0.01 g_{LAS}/dm^3, at a stirring speed of 300 rpm with a particle size <100 μm.

Adsorbent	Time [min]	Amount [$g_{adsorbent}/dm^3_{rinsing\ water}$]	Costs [$/$m^3_{rinsing\ water}$]
GAC-1240	3	1	2.9
LDH	10	1	6.0

When the adsorbent is added to the rinsing water in a permeable bag, the following considerations should be taken into account. The minimum particle size of the adsorbent must be larger than the size of the pores in the permeable bag. However, fast adsorption needs small particles. To keep the small particles in the bag, the bag needs small pores. However, this decreases the permeability of the bag and results in an additional barrier for the adsorbate adsorption. There are two options: i) to increase the particle size of the adsorbent or ii) decrease the pore size of the permeable bag. In both options the adsorption rate decreases which need to be compensated by increasing the amount of adsorbent to adsorb the same amount of LAS in the same time. Consequently, the amount of adsorbent per bucket of laundry rinsing water is considerable and will result in large amounts of waste.

Based on the 'best-case' test and the above considerations it is concluded that the feasibility of the permeable bag is very low, due to the high amounts of adsorbent needed to treat one litre of laundry rinsing water. These high amounts of adsorbent result in a large amount of waste and high costs, therefore the permeable bag is not evaluated any further.

7.4.4. Tests with model rinsing water

RWR with adsorption

Two prototypes: the bucket-to-bucket prototype and the siphon prototype were tested with model rinsing water. Figure 3 shows a picture of the model rinsing water (A) and the water treated with the bucket-to-bucket prototype (B). The model rinsing water looks very turbid, because of the model soil present. The particulates do not settle because LAS and sodium triphospate (STP) keep the small particulates in dispersion. There is a clear difference between the model rinsing water (A) and treated water (B). There is no foam present at the interface of the treated water and most of the particulate soil is removed. Furthermore, the detergent smell clearly present in the model rinsing water is not present in the treated water. However, a haze is still present in the treated water, due to a small amount of particulate soil.

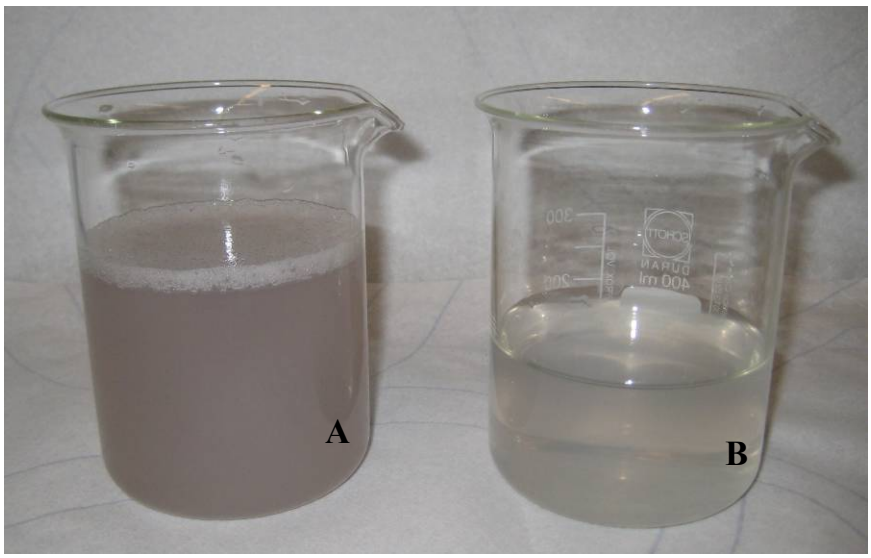

Figure 3: A. model rinsing water and B. treated water with the bucket-to-bucket prototype.

The analysis results of the model rinsing water and the treated water of both prototypes is shown in figure 4. The main difference between the bucket-to-bucket and the siphon is their design and flow direction through the column. GAC-1240 is used in both prototypes and no difference is expected between the analyses of the treated water. The results of the water treated with the bucket-to-bucket and siphon are indeed very similar (figure 4). The TOC concentration is significantly reduced for the treated water compared to the model rinsing water. Inorganic carbon (IC) is only slightly lower for the treated water. Carbonate is not removed from the model rinsing water by adsorption, which was expected because GAC-1240 only removes organic components from the water. LAS is totally removed from the model rinsing water and STP is partly removed. The pH of the model rinsing water and treated water is around 10. OH^- and CO_3^{2-} are not removed by the prototypes.

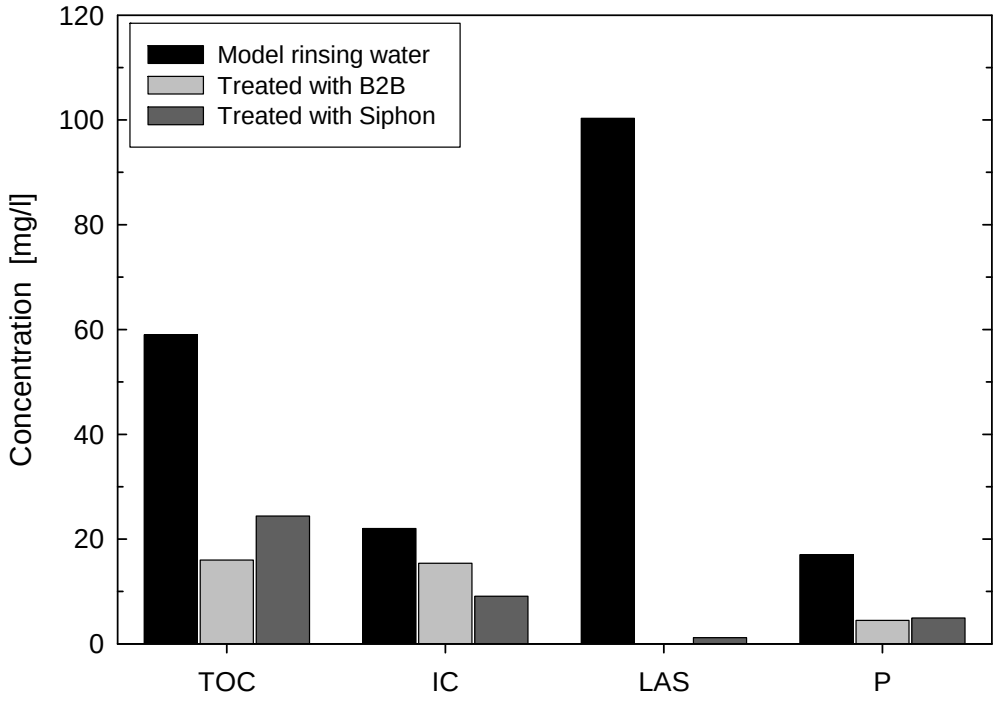

Figure 4: Total organic carbon (TOC), inorganic carbon (IC), linear alkyl benzene (LAS) and phosphorus (P) concentrations model rinsing water and the treated water with the bucket-to-bucket (B2B) and siphon prototype.

Figure 5 shows the decrease in flow rate through the column and water height in the top bucket during a test run of the bucket-to-bucket prototype. The initial flow rate was around 50 ml/min and decreased dramatically. The column was clogged by the particulates from the model soil. From figure 3B it was already clear that the particulates are not completely removed from the model water and cause a haze in the treated water. Similar results were obtained with the siphon which was also clogged by the particulates (not shown). An additional step is necessary to remove the particulates from the rinsing water before passing the water through the column.

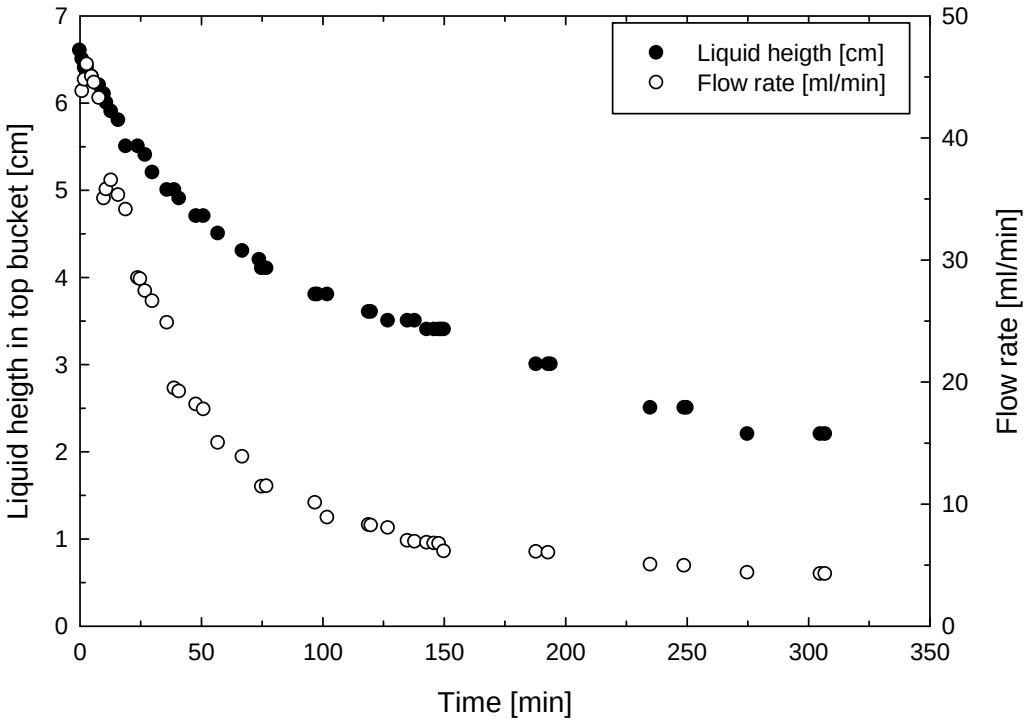

Figure 5: Flow rate and water height during run of bucket-to-bucket prototype.

Removal of particulate soil

The particulate soil that consists of clays and other minerals, is mainly released from clothes and ends up in the laundry rinsing water. Particulate soil is usually removed from clothes by a wetting and dispersing process. Anionic surfactants (LAS) and sodium triphosphate (STP) present in detergents are responsible for these processes [14]. Another source of particulate soil is a laundry bar, which contains up to 20% of calcite and 15% of kaolin [15]. The total particulate concentration in laundry rinsing water is around 0.5 g/dm^3 [10].

Coagulation/flocculation and sedimentation seems to be the most easy and effective method to remove particulate soil from laundry rinsing water. Filtration is not suitable, because the filter clogs easily due to the small particulates. Furthermore, gravity is used as driving force since no electricity will be used. This limits the pressure difference that can be reached and limits the use of filtration. The disadvantage of coagulation/flocculation is that it requires chemical additives and produces a sludge that requires disposal.

There is no general agreement about the meaning of the terms coagulation and flocculation. In this research we assume that coagulation is the destabilization of particulates by simple salts or charge neutralization to form larger flocks (the flocks tend to be small and dense). Flocculation is polymer bridging to form larger flocks (the flocks tend to be large and have a more open structure) [16]. Most of the particulate soil is negatively charged and therefore coagulants and flocculants are often positively charged. In model rinsing water 90% of the model soil is kaolinite ($Al_2Si_2O_5(OH)_4$) which is negatively charged. In this research we do not investigate

coagulation/flocculation intensively, but we aim to find a suitable coagulant/flocculant for laundry rinsing water.

Several coagulants/flocculants were tested on their ability to coagulate/flocculate the particulate soil present in the model rinsing water. The concentration of coagulant/flocculant necessary to treat one litre of model rinsing water was determined with the 'waste water jar test' [17]. A small amount of coagulant/flocculant was added to 400 ml of model rinsing water and stirred for 15 seconds with 250 rpm, stirred for 30 seconds with 50 rpm and was allowed to settle for four minutes. Subsequently, the turbidity of the supernatant was measured with an Eutech Instruments portable Turbidimeter TN-100. The steps were repeated and the amount of coagulant was increased each cycle until the turbidity was below 50 NTU. Table 6 lists the tested coagulants that were able to coagulate the particulate soil and reduce the turbidity below 50 NTU.

Table 6: Overview of investigated coagulants and their concentration necessary to coagulate one litre of model rinsing water. The obtained turbidity after coagulation is shown and can be compared to model rinsing water.

Coagulant	Concentration [$g_{coagulant}$/ $dm^3_{model\ rinsing\ water}$]	Turbidity [NTU]	Supplier
Model rinsing water	-	455	-
Calcium chloride* ($CaCl_2$)	1	46.0	BOOM
Poly aluminium chloride and cationic polymer* (PAC+)	0.72	28.2	Hindustan Unilever
Chitosan**	0.125	15.5	Nalco

* is a powder and ** is a solution of 10 gram chitosan, 10 ml acetic acid and 1000 ml demi water.

Calcium interacts with the negatively charged particulates (kaolinite) and flocks are formed. Furthermore, the Ca^{2+} interacts with the negatively charged STP and LAS. STP and LAS partly precipitate with Ca^{2+} and stay behind with the flocks. The amount of $CaCl_2$ to coagulate one litre of model rinsing water is significant. Adding Ca^{2+} is not a very sustainable solution and not preferred if the water will be re-used for doing laundry.

The positive charged PAC+ interacts with the negatively charged particulates and flocks are formed. PAC+ is a combination of coagulation and flocculation, whereas calcium is only coagulation.

At low concentrations, chitosan is able to reduce the turbidity of model rinsing water enormously. However, much research has been done by Hindustan Unilever on PAC+ and laundry rinsing water and therefore, PAC+ was used in the subsequent experiments as a suitable coagulant for the pre-treatment of rinsing water.

RWR combining coagulation and adsorption

The tests are continued with an additional coagulation step. PAC+ will be added to the model rinsing water (0.72 gram per litre of model rinsing water) and allowed to settle for five minutes. Subsequently, the flow is started and the adsorption of the soluble components can take place.

Figure 6 shows a picture of the model rinsing water and the treated water using coagulation and adsorption. The difference between both samples is very clear. The particulate soil and foam are totally removed from the treated water. Furthermore, the detergent smell clearly present in the model rinsing water was not present in the treated water.

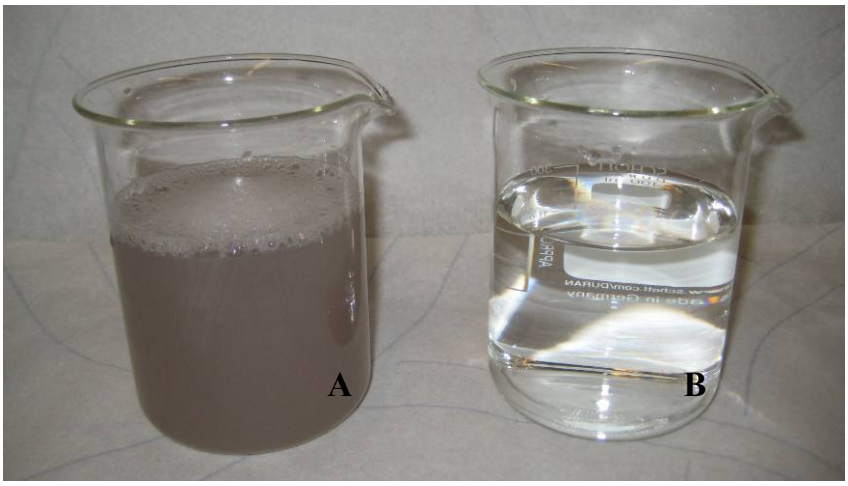

Figure 6: A. model rinsing water and B. treated water. Tests performed with siphon and coagulation with PAC+.

The analysis results of the model rinsing water, treated water after coagulation and treated water after adsorption is shown in figure 7. During the coagulation part TOC, LAS and STP are removed. Apparently, these components are trapped or adsorbed to the flocks and stay behind. After coagulation and adsorption LAS and STP are both totally removed from the rinsing water. The TOC concentration is significantly reduced for the treated water compared to the model rinsing water. Inorganic carbon (IC) is only slightly reduced.

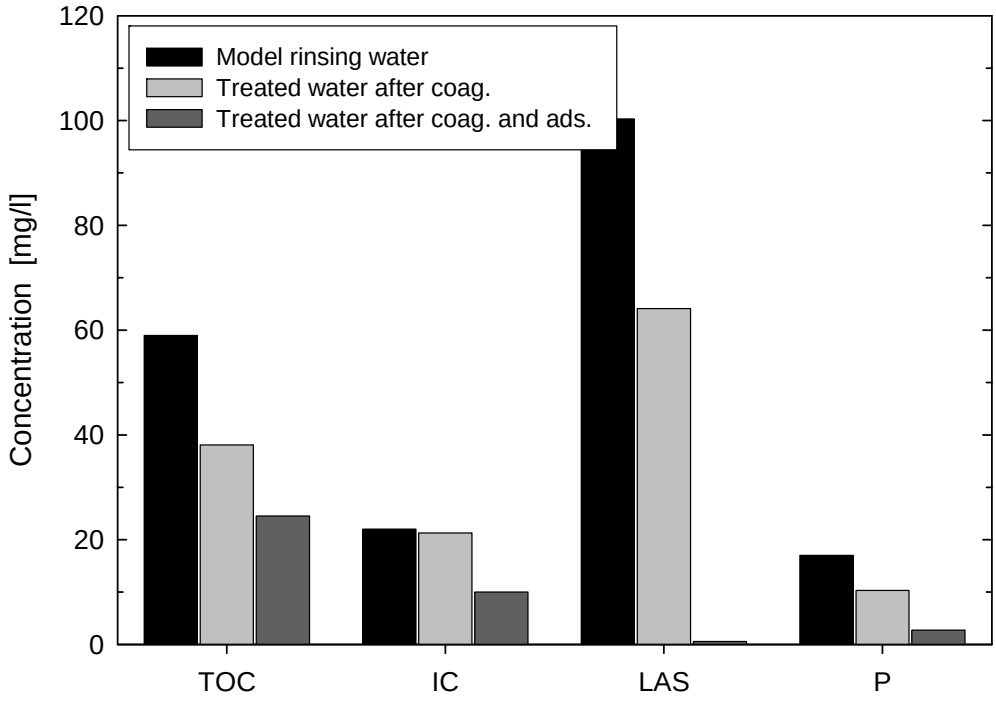

Figure 7: Total organic carbon (TOC), inorganic carbon (IC), linear alkyl benzene (LAS) and phosphorus (P) concentrations of model rinsing water, water treated with coagulation and water treated with coagulation and adsorption (siphon prototype).

Figure 8 shows the flow rate through the column and water height in the top bucket during a test run of the bucket-to-bucket prototype. The flow rate was constant around 60 ml/min. The slight decrease in flow rate is caused by a decreasing water head in the top bucket. Tests with the siphon gave similar results; the column did not clog (not shown).

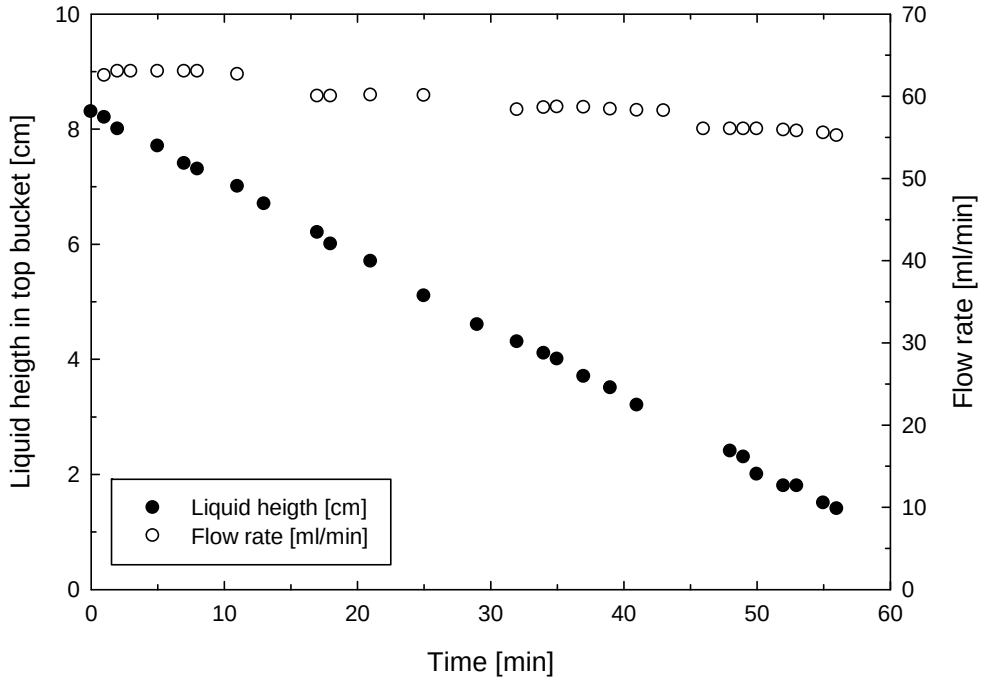

Figure 8: Flow rate and water height during run of bucket-to-bucket prototype.

7.4.5. Costs

The cost of both prototypes consists of the device itself, the adsorbent and coagulant powder. Both prototypes were prepared from generally available plumbing materials. The cost of the device will depend on the production country but will be very low. The operation cost consists of the adsorbent and coagulation powder. The adsorbent cost is calculated in chapter 6.4.5. The amount of the adsorbent to clean 25 dm^3 of rinsing water per day (9.1 m^3 per year) is estimated and with the bulk price of GAC-1240 (2.9 $/kg) the adsorbent cost is calculated. The adsorbent cost ranges from $11.7 to 15.3 per year for cleaning 9.1 m^3 of laundry rinsing water. This results in $1.31 per cubic meter water. The cost of the coagulant powder is around 0.5 $/kg [17] and this results in $3.28 per year and $0.36 per cubic meter water. The total operational cost is estimated at $1.67 per cubic meter water which is higher than the local water price of $0.75 to $1 per cubic meter water [11].

7.5. Early consumer tests

7.5.1. Introduction

The objective of the early consumer tests is to obtain a first insight in the consumers view on the developed prototypes. The aim was to find out what the consumers think about the prototypes and ask for their additional ideas and feedback. This valuable information can be used for further research. The consumer tests were carried out in Phulera, Rajasthan, India in February 2008. Phulera is situated in Rajasthan which is an arid area (see figure 9) and water scarcity is a daily returning problem for the inhabitants. The consumers were selected according to a socio-economic classification (SEC) by Hindustan Unilever (appendix 1). The consumers were selected in SEC A and B. Within these classes the consumers were chosen randomly. The consumer tests consisted of two group discussions and four individual consumer tests. Each group consisted of eight women. In the group discussions two prototypes of the rinsing water recycler were demonstrated: the siphon and the bucket-to-bucket prototype. The discussion was carried out with the help of a discussion guide (appendix 2). The discussion guide was written by Consumer Technical Insight Department (CTI) of Hindustan Unilever, Mumbai, India and consists of five parts: general discussion about water availability, present solutions, introduction to the concept and preliminary feedback, feedback after the demonstration and interest in purchase of the concept. The consumer groups were asked to give their preference for one of the prototypes. The preferred prototype was used in the individual consumer tests. During the individual consumer tests a hand wash was done and the laundry rinsing water was saved. The laundry rinsing water was treated with the prototype and the discussion guide was used to ask for feedback from the consumer.

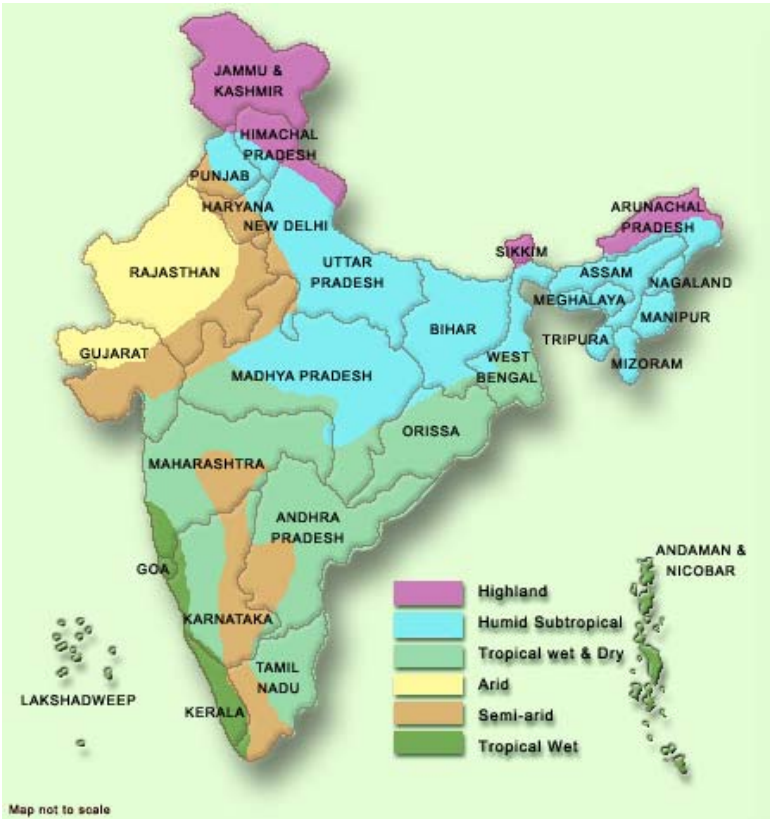

Figure 9: Map of climates in India.

7.5.2. General discussion about water availability and present solutions

In Phulera water shortage is a daily returning problem throughout the year. A household receives water from the tap. Water is not supplied continuously and may take place every other day, once a week or even once a month for about 30 minutes. This unpredictable supply of water results in the inconvenience of having to be present at home when tap water is available and also of being confined to the tap. Often the supply of electricity is interrupted when the municipality delivers water from the tap. This is to prevent that electrical pumps will draw large amounts of water from the taps compared to people without pumps. The amount of water received is approximately 200 to 500 litres. This is insufficient for one household and extra water is bought from a water tanker. The water tanker visits every 15 days and an amount of approximately 5000 litres is delivered for $0.75-1.00 per cubic metre water [11]. If space allows, households have 5000 litre storage tanks underground, close to their house. The tanker water is not potable and the water source is often unknown. The water is very hard and causes white deposits on kitchenware. Alum (aluminium sulphate) is often added to the tank to coagulate particulate soil ($0.05 average per week).

Additionally, it must be mentioned that the monsoons of the last two years were very good. In the years before the monsoons were worse and water was much scarcer. The infrastructure is also improved in the last years and there are many tanker water suppliers. This makes the consumers critical towards ideas to solve water related problems. In time of water scarcity people are much more open towards new ideas [18].

During the discussion the consumers were asked to explain their way of dealing with water scarcity. In periods of water scarcity the consumers prioritize the household activities as follows:

1. drinking/cooking
2. washing kitchenware
3. bathing
4. washing clothes
5. washing floors/toilets etc.

Furthermore, many alternatives are used to avoid excessive water consumption. Examples of these adaptations are: cleaning of kitchenware with mud or ash instead of water, washing of clothes in larger lots, reducing the amount of detergent to save on rinsing water, bathing with half a bucket of water and avoid watering any gardens or plants.

7.5.3. Introduction to the concept and preliminary feedback

The concept of re-using rinsing water and the prototypes were explained, at first without showing the prototypes of the rinsing water recycler. The spontaneous reaction of the consumers to the concept was positive. It was felt that they would probably use the recycled water for everything except drinking/cooking, washing kitchenware and bathing. They trust that science is evolving and assume that the rinsing water recycler would be a step towards solving their water related problems. Furthermore, they prefer to have a second source of water that makes them less dependent on the tanker water. This also prohibits the tanker water firm to increase their water prices without any reason.

7.5.4. Demonstration and feedback

The prototypes were demonstrated and the consumers were asked for their feedback and their preference for one of the prototypes (figure 10). It was noticed that the consumers were very outspoken. Instinctively, the consumers felt that the first step coagulation/flocculation was insufficient to clean laundry rinsing water. They do not like the idea of “clean” water that has been in contact with the waste (flocks) at the bottom of the bucket. After the second step (adsorption) they imagined that the treated water was of good quality. The amount of surfactant/detergent left in the treated water was estimated by sight, smell and by hand. They did not see, smell or feel surfactant/detergent in the treated water, it looked as clean as bottled drinking water and they would drink it if they did not know that it had been used for rinsing laundry. They would like to use the treated water for everything except drinking and cooking.

The consumers responded that the flow rate of both prototypes is too low. They would like to use the treated water the same day, or during the same laundry session. The flow rate should be increased to four buckets of laundry rinsing water per hour.

The consumers preferred the siphon prototype, because the siphon is small and easy to handle compared to the bucket-to-bucket prototype. Furthermore, only one additional bucket is necessary to operate the siphon. The bucket-to-bucket approach is less convenient because it is large and heavy when the upper bucket is filled with rinsing water. Therefore, the siphon prototype is selected for the individual consumer tests.

7.5.5. Results of the individual consumer tests

Four consumers performed their hand wash and saved the rinsing water for the demonstration with the siphon. The feedback from the individual consumer tests (figure 10) on the siphon prototype was both positive and negative. The feedback of two individual consumers was very positive. The quality of the water was very good and both individual consumers were interested in purchasing the prototype. Their suggestion for improvements was to increase the flow rate. One consumer had a hand water pump in front of the house. She explained that getting water from the hand water pump is less effort than using the siphon prototype. During the demonstration at the fourth consumer the coagulation/flocculation step was not successful. This could be caused by over dosage of the coagulant. Overdosing changes the charge of the negative kaolinite particulates to a positive charge because they are surrounded by the positive charged coagulant. Reliable dosing of the coagulant is a challenge in the concept of the RWR.

Figure 10: Group discussions and individual consumer tests.

7.5.6. Interest in purchase of prototype

70% of the consumers would like to purchase the siphon prototype. Necessary improvements would be an increase in flow rate and replacement of the adsorption column only once a year. Table 7 roughly indicates the amount of money (in $) that the consumers would like to spend on the siphon prototype. The consumers in the second group (SEC A) are willing to spend more on the prototype than the first group (SEC B). This is caused by the difference in SEC; SEC A can spent more compared to SEC B (see appendix 1). The consumers were asked for who they think this concept would be useful. Their response was that the concept would be interesting for middle class people facing water scarcity.

Table 7: Amount of money that consumer are willing to spend on the siphon prototype in $.

	Group 1 (SEC B)	Group 2 (SEC A)
Device	$ 3.00	$ 37 – 74
Replacement of adsorption column	$ 3.70 – 9.90 per month*	$ 12 - 25 per month*
Coagulant powder	$ 0.75 per month*	$ 0.30 – 3.96 per month*

*In one month approximately 750 litres of laundry rinsing water is produced.

7.5.7. Conclusions early consumer tests

The RWR prototypes were successfully tested by consumers resulting in a clear preference for the siphon type. The response of the consumers on the quality of the treated water was very positive. The flow rate is an important point for improvement. In general, coagulation worked well however during the tests it failed once. Therefore, the robustness of the coagulation and the dosing of coagulant needs improvement. Finally, the amount of money that consumers are willing to spend for a RWR prototype is higher than estimated earlier.

7.6. Conclusions and future work

The RWRs were tested with model laundry rinsing water and the permeable bag was tested with a LAS solution. The following conclusions can be drawn from the experimental data:

- The permeable bag is discarded, because the amount of GAC-1240 and LDH to clean one litre of rinsing water is high and therefore the cost and amount of waste are too high.
- Model rinsing water contains a high concentration of particulate soil that does not settle and clogs the filters and the columns.
- Combination of coagulation and adsorption in the RWRs is very effective in removing LAS, STP, perfumes and model soil. The column is not clogged by the soil since it is effectively removed by the coagulant.

The developed RWRs prototypes are exposed to early consumer tests. The overall conclusions of the consumer tests are:

- The bucket-to-bucket and siphon concepts combine adsorption and coagulation and clean the rising water to a satisfactory quality.
- The flow rate of both prototypes is too low.
- The money that the consumers are willing to spend on the RWR is higher than the roughly estimated cost of the RWR prototypes.

To make the RWR applicable for the consumer market some improvements need to be made:

- Improve the flow rate of the RWRs by adjusting the size of the column or increase the adsorption kinetics by decreasing the particle size of the adsorbent.
- Improve coagulation robustness and dosing; it should work with different water qualities.

- Find other methods to remove small particulates to exclude coagulation.
- Combine adsorption with removal of particulates in one step, this will make the concept more convenient for the users.

7.7. References

1. UnitedNations, *Water for People Water for Live. World Water Development Report. UNESCO WWAP*. 2003, United Nations.
2. Devi, R., et al., *Removal of fluoride, arsenic and coliform bacteria by modified homemade filter media from drinking water.* Bioresource Technology, 2008. **99**(7): p. 2269-2274.
3. Sarkar, S., et al., *Well-head arsenic removal units in remote villages of Indian subcontinent: Field results and performance evaluation.* Water Research, 2005. **39**(10): p. 2196.
4. Schroeder, D.M., *Field experience with SONO filters.* https://www.dwc-water.com/fileadmin/images/PDF_files/SIM_Reports.pdf, 2007.
5. Halem van, D., et al., *Assessing the sustainability of the silver-impregnated ceramic pot filter for low-cost household drinking water treatment.* Physics and Chemistry of the Earth, Parts A/B/C, 2008(In Press, Corrected Proof, Doi:10.1016/j.pce.2008.01.005).
6. DSM, *Van rietje tot waterzuiveraar.* Chemisch 2weekblad, 2008.
7. Clasen, T., S. Nadakatti, and S. Menon, *Microbiological performance of a water treatment unit designed for household use in developing countries.* Tropical Medicine and International Health, 2006. **11**(9): p. 1399.
8. Warwick, T.P., *Does point of use for the developing world really work?* Water Conditioning & Purification, 2002: p. 66-69.
9. Singh, V.P. and M. Chaudhuri, *A performance evaluation and modification of the UNICEF upward flow water filter.* Waterlines, 1993. **12**(2): p. 29-31.
10. Unilever, *Personal communication*. December 2004: Hindustan Unilever Research India, 64 Main Road, Whitefield P.O. Bangalore 560066, India.
11. Phulera, *Personal communication: Local water prices in Phulera, Rajasthan, India.* January/February 2008.
12. Schouten, N., et al., *Selection and evaluation of adsorbents for the removal of anionic surfactants from laundry rinsing water.* Water Research, 2007. **41**(18): p. 4233-4241 (Chapter 2).
13. Schouten, N., et al., *Optimization of layered double hydroxide stability and adsorption capacity for anionic surfactants.* Adsorption, 2007. **13**: p. 523-532 (Chapter 3).
14. Holmberg, K., et al., *Surfactants and polymers in aqueous solution*. 2nd ed. 2003, West Sussex, UK: Wiley.
15. Ho Tan Tai, L., *Formulating detergents and personal care products*. 1st ed. 2000, New York, USA: AOCS Press.
16. Gregory, J., *Particles in water. Properties and processes*. 2006: IWA Publishing.
17. Nalco, *Ir. G. Tjalmaweg 1, 2342 BV Oestgeest, The Netherlands.* 2004.

18. Unilever, *Personal communication*. January/February 2008: Unilever Research India, 165/166, Backbay Reclamation, Mumbai - 400020, India.

7.8. Appendix

7.8.1. Appendix 1: Socio-economic classification (SEC)

Socio-economic classification (SEC) classifies households based on the occupation and education of the chief wage earner. Table 8 and 9 shows the SEC for urban and rural areas. For urban areas E2 is lower class and A1 is upper class. For rural areas R4 is lower class and R1 is upper class.

Table 8: SEC for urban areas.

EDUCATION OCCUPATION	Illiterate	School up to 4yrs	School up to 5-9yrs	S.S.C./ H.S.C.*	Some college but not graduate	Graduate/ Post Graduate	Graduate/ Post Graduate profes-sional
Unskilled Workers	E2	E2	E1	D	D	D	D
Skilled workers	E2	E1	D	C	C	B2	B2
Petty Traders	E2	D	D	C	C	B2	B2
Shop Owners	D	D	C	B2	B1	A2	A2
Businessmen/ Industrialists with No of employees:							
● None	D	C	B2	B1	A2	A2	A1
● 1 – 9	C	B2	B2	B1	A2	A1	A1
● 10+	B1	B1	A2	A2	A1	A1	A1
Self employed professionals	D	D	D	B2	B1	A2	A1
Clerical /Salesman	D	D	D	C	B2	B1	B1
Supervisory Level	D	D	C	C	B2	B1	A2
Officers/ Executives							
● Juniors	C	C	C	B2	B1	A2	A2
● Mid/Sen	B1	B1	B1	B1	A2	A1	A1

* S.S.C./H.S.C.=Secondary and Higher Secondary school

Table 9: SEC for rural areas.

TYPE OF HOUSE EDUCATION	Brick and mortar home	Brick walls with thatched roof	Mud walls with thatched roof
Illiterate	R4	R4	R4
Literate but no formal school	R3	R4	R4
Up to 9th standard	R3	R3	R4
S.S.C. / H.S.C.*	R2	R3	R3
Some College or above	R1	R2	R3

* S.S.C./H.S.C.=Secondary and Higher Secondary school

7.8.2. Appendix 2: Discussion guide

General

What are the problems faced by you concerning water availability?
When do you face water problems? Are the water problems throughout the year or only during summers?
During water shortage, how much water do you get?
What is the frequency of water in the taps during water shortage?

Present solutions

What do you do during water shortage? How do you manage?
Which household chore gets a priority?
Which is the chore you would avoid in case water is scarce?
What is it you are not prepared to compromise on?
What are you prepared to compromise?
If you were to get different qualities of water? How would you use it? Best quality of water will be used for which chores and the worst for which?

Introduction to the concept of recycling: re-use of rinsing water

What if I present to you a product which could recycle your laundry rinsing water? You could re-use your laundry rinsing water. All that you are required to do is: add a powder, stir and leave the soil to settle at the bottom. Then open the tube grip/tap to release water in the lower bucket. In the lower bucket you collect the treated water.
What are your views on this technology?
What are your concerns about this technology?
What will you use this treated water for fabric wash, dish wash or? At what stage? Why?

Actual live demonstration of the technology

What are your views about this technology, now that you have seen it yourself?
What do you think about its (a) efficiency (b) effectiveness?
What is it that you particularly liked about this technology? Why?
What is it that you particularly disliked about this technology? Why?
What are the concerns you have about this technology?
What are the questions that are coming to your mind about this technology?
What are the main disadvantages? Advantages?
How can we improve this for your convenience? If you could change one thing on this technology, what would it be?
If I give you three additional benefits, what should I focus on?

Changes demanded in (a) design and (b) methodology

According to you how and where could it be used?
Who are the people who will benefit from this technology?
When do you think you will use this technology? How often?
Under which circumstances would you use this technology?
What will force you to use this product routinely?

Post-demonstration discussion

What do you think about this technology, now that you have tried it yourself?
How would you rate its efficiency?
How would you describe the purified water? How do you compare it with the fresh water?
According to you how and where could it be used?
Who are the people who will benefit from this technology?
When do you think you will use this technology?
Under which circumstances would you use this technology?
What will force you to use this product routinely?
What are the benefits you/these people will get on using this technology?
What are the disadvantages according to you?
What are the improvements you would like to have?
What are your particular likes / dislikes?

Changes demanded in (a) methodology and (b) efficiency

How do you think we can make it more user-friendly, so that anybody facing water shortage would be motivated to use it?
How would you like to use this product? When and where?
When and under which circumstances will you use this technology?
For which purposes would you use the treated water? Why?
How will you use this treated water?

Interest in purchase

What would you spend for this technology?
What would you spend for the device?
What would you spend for the powder and replacement of the content of the device?

8. Conclusions and outlook

8.1. Conclusions

The objective of this thesis was to design a rinsing water recycler (RWR) for low cost decentral recycling of laundry rinsing water. Important criteria were: removal of the main components from rinsing water, household scale, low cost, no power source needed, easy to use, portable, safe, attractive to culture, no recycling of the adsorbent and low amount of waste. Prototypes of the RWR were developed by a systematic procedure and tested in the laboratory to clean-up laundry rinsing water. Two RWR prototypes (bucket-to-bucket and siphon) were used in early consumer tests in Phulera, India. The prototypes cleaned the rising water to a satisfactory quality. The consumers preferred the siphon prototype because it is small and easy to handle. They also suggested the flow rate as most important point for improvement.

Crucial in the design of the RWR was the selection of the adsorbent. It determines the adsorption capacity and consequently the operating cost of the RWR and the amount of waste. The adsorption of the main component in laundry rinsing water, namely the anionic surfactant, linear alkyl benzene sulfonate (LAS) was investigated with equilibrium experiments. Layered double hydroxide (LDH) was found to be very promising, because of its high LAS adsorption capacity. Also activated carbons (AC) were suitable because of their relatively low cost. LDH is only suitable for short contacting times.

Adsorption only was not sufficient to clean the laundry rinsing water. Particulate soil present in rinsing water clogs the filters and the adsorption column. Therefore, an additional step appeared necessary to remove the particulate soil. The combination of coagulation and adsorption in the RWRs was very effective in removing anionic surfactant, sodium triphosphate (STP), perfumes and model soil.

The presence of other soluble contaminates in laundry rinsing water could influence the LAS adsorption. Fortunately, experiments showed that STP, Na_2CO_3 and NaCl do not influence the adsorption capacity of LAS onto activated carbon (GAC-1240) and LDH. They even increased the LAS adsorption rate onto GAC-1240. This is caused by an increase in ionic strength of the LAS solution by addition of the components. For LDH, NaCl increased the LAS adsorption rate also by increasing the ionic strength. Both STP and Na_2CO_3 decrease the LAS adsorption rate. CO_3^{2-} and STP compete with LAS for the adsorption onto LDH.

The RWR operating time depends on the adsorption kinetics. The LAS adsorption rate on activated carbon and LDH was investigated with the zero length column (ZLC) method. The adsorption of LAS onto granular activated carbon (GAC-1240) was well described by the adsorption model. The resistance is completely situated inside the particle. The resistance of LAS adsorption onto LDH is situated completely in the

double layer outside the particle. The double layer model results in a good description of the experimental results for LDH.

Small column experiments were performed to investigate the adsorption of LAS onto GAC-1240 in a column application. The experimental breakthrough curves were simulated with a mathematical model giving good results. Finally, the model is used to design a column for the rinsing water recycler (RWR). This resulted in two designs; a column (D=0.06 m; H=0.18 m) with a flow rate of 50 ml/min and a column with a flow rate of 100 ml/min. The adsorbent cost of both columns is around $12-15 per year which is acceptable for the targeted consumer community.

8.2. Outlook

The bucket-to-bucket and siphon prototype of the RWR fulfilled all the initially determined criteria. They were successfully tested in early consumer tests in India. These tests and our own experience from laboratory tests resulted in several ideas for future improvements.

8.2.1. Improvements of the RWR prototypes

Early consumer tests pointed out that the flow rate was an important point for improvement. The flow rate can be improved by increasing the column diameter. Another option is to increase the LAS adsorption rate which is possible by decreasing the particle size of the adsorbent. Initial model simulations showed promising results for a large column (D=0.1 m; H=0.3 m) with a flow rate of 500 ml/min. Model simulations with a similar column and smaller particles (300 μm) were even more promising: the run time and adsorbent efficiency increased significantly (120 days and 3 dm^3 rinsing water per gram of adsorbent) and the adsorbent cost per year decreased to $9 per year ($1 per m^3 of laundry rinsing water).

Correct dosing of the coagulant is a great challenge. The particulate soil concentration in laundry rinsing water can vary enormously. The dosing should be adjusted to the particulate soil concentration and the concentration of other contaminants that can influence coagulation. Therefore, other methods to remove particulate soil should be investigated. Interesting options are the application of ceramic membranes or electrostatic coalescence. Some initial tests were performed with a ceramic membrane (hollow fibre ceramic membrane, Hyflux Ceparation, pore size 200 nm). The membrane was able to remove the particulate soil, but the flow rate decreased due to clogging of the pores. The clogging was solved with forward flushing, but the effect of forward flushing after a long operation time needs to be investigated. An additional challenge is the fragility of the ceramic membranes; a RWR device should be shockproof and fall proof. Another method to remove particulates could be electrostatic coalescence, an effective method to coalescence charged particles. Only a small power source (for example a battery) is necessary to operate such a system.

When the RWR prototype is successful in India, the amount of waste from the spent adsorbent will be considerable. Therefore, recycling of the adsorbent should be investigated. The column of the RWR can be designed as a cartridge. When the consumer purchases a new cartridge, the spent cartridge can be returned. The same supply chain for distribution can be used for collecting the spent cartridges. The loaded adsorbent is reactivated in a process similar to the production process [1]. The recycling of the adsorbent needs some investigation, for example the effect of reactivation on adsorption capacity, handling of spent cartridges (smell, safety and bacterial growth) and the cost should be considered.

8.2.2. Improvements of the adsorbent

LDH proved to be a promising material for the removal of anionic surfactants. The main restriction of this material is its limited stability in water. This is caused by the rearrangement of the nano size crystallites of which a LDH aggregate exists. The stability can be increased by binding the crystallites to each other. Some initial tests were performed with different "glues" at different concentrations. Positive charged clays (bentonite and kaolinite) can function as glue between the negative charged LDH crystallites, also polymers (polyvinylalcohol and sodium carboxymethylcellulose) or waterglass (Na_2SiO_3) could be an option. Promising results were obtained with low concentrations of kaolinite. Thorough research must be done to completely understand the governing mechanisms. Furthermore, companies that produce LDH have a high knowledge about LDH stability. Collaboration with such a company can be really helpful. Finally, the precipitation of LDH on a support, for example a cellulose support [2], to increase stability is another interesting option to investigate.

Surface modification and pore size tailoring of activated carbons can be promising to increase the surfactant adsorption capacity and adsorption rate. Initial tests were performed in collaboration with dr. C.O. Ania from the National Institute for Carbon in Spain [3]. Impregnation of the surface with amine did not result in a higher LAS adsorption capacity. The pH of the laundry rinsing water is around 10. At this pH the charge of amine groups is neutral and does not result in higher adsorption capacities compared to untreated carbon [4]. Another option is to modify the surface with quaternized ammonium groups which have a point of zero charge above 10. This requires an extensive procedure with high concentrations of alkaline solutions [5], but it can still be interesting. Additionally, to increase the pore volume to meso pores can improve the LAS adsorption capacity and LAS adsorption rate. Finally, the cost relative to adsorption capacity should be investigated to make a balanced decision about feasibility of the improvements.

8.2.3. Investigation of other concepts

This research was focussed on removing the main contaminant in laundry rinsing water, namely an anionic surfactant. Another approach is to re-use water *and* to save chemicals. For example by removing all the other (useless) components but not the surfactants from laundry rinsing water. Water and surfactants can now be re-used.

Another idea is to save chemicals by removing the surfactants from rinsing water and recycle the surfactants. This method would be a very interesting application for washing machines. The surfactants are adsorbed when the waste water is drained off and the surfactants are desorbed when the fresh water enters the washing machine. This could save large amounts of chemicals.

8.3. References

1. Sontheimer, H., J.C. Crittenden, and R.S. Summers, *Activated carbon for water treatment*. 2nd ed. 1988, Karlsruhe, Germany: DVGW-Forschungsstelle.
2. Mandal, S. and S. Mayadevi, *Cellulose supported layered double hydroxides for the adsorption of fluoride from aqueous solution.* Chemosphere, 2008. **72**(6): p. 995-998.
3. Ania, C.O., *Consejo Superior de Investigationes Cientificas, Instituto National del Carbon, Energy and Environment Department, Apartado 73, 33080 Oviendo, Spain*. 2007: www.incar.csic.es.
4. Schouten, N., et al., *Selection and evaluation of adsorbents for the removal of anionic surfactants from laundry rinsing water.* Water Research, 2007. **41**(18): p. 4233-4241 (Chapter 2).
5. Wartelle, L.H. and W.E. Marshall, *Quaternized agricultural by-products as anion exchange resins.* Journal of Environmental Management, 2006. **78**(2): p. 157.

Dankwoord

De sneeuwpop was minstens een meter of twee, met een wortel als neus en stokken als armen. André steekt zijn hoofd buiten het raam en roept: “Als je gaat promoveren dan heb je de vrijheid om nog eens zo’n pop te maken”. Dat was in de tijd van piekeren over mijn toekomst (wel/niet promoveren of toch het bedrijfsleven in?) het leukste argument dat ik heb gehoord om te gaan promoveren. En inderdaad als promovendus heb je meer vrijheid om alles naar eigen inzicht te plannen, als na vier jaar je proefschrift maar af is. Toen André me een project voorstelde over het schoonmaken van waswater in India was ik gelijk enthousiast. Dat het bij Wetsus (voor mij toen nog onbekend) in Leeuwarden was, nam ik op de koop toe. Die sneeuwpop hebben we inderdaad nog een keer gemaakt in Leeuwarden.

Zo begon mijn leventje als promovendus in Leeuwarden, een geweldige tijd en daarvoor wil ik graag een aantal mensen bedanken. Allereerst natuurlijk André de Haan, bedankt voor jouw vertrouwen dat ik een promotie tot een goed einde kan brengen. En ik moet eerlijk zeggen, tijdens mijn afstuderen leerde ik je kennen en daarom durfde ik een promotie onder jouw begeleiding wel aan. Je manier van werken heb ik als heel prettig ervaren, we hebben regelmatig contact gehad en jouw interesse, enthousiasme en input hebben mij gemotiveerd en geïnspireert. Ik heb de afgelopen vier jaar een geweldig team om me heen gehad: André de Haan, Louis van der Ham, Paul Birker, Philip van der Hoeven en Gert-Jan Euverink. We hebben regelmatig besprekingen gehad en het team werd gemotiveerd door de gepresenteerde resultaten en door de discussies werd ik weer gemotiveerd om verder te gaan. Een ideale manier van samenwerken.

Louis, wij hebben het meest contact gehad en ik wil je ontzettend bedanken voor je geduld en de altijd positieve steun. Je hebt me meerdere malen opgepept, alle stukken kritisch doorgelezen, inzichten gegeven, geïnspireerd en ik heb het ontzettend leuk gevonden om met je samen te werken. Heel erg bedankt hiervoor. Paul heeft heel veel wegen voor mij binnen Unilever open gemaakt. Ik heb ontzettend veel van je geleerd en heb met volle teugen genoten van de reizen naar India. Paul heeft het mede mogelijk gemaakt dat we de uiteindelijke prototypen konden testen in India: de kroon op mijn werk! Flip, onze zeer ervaren adviseur, bedankt voor jouw ideeën, enthousiasme en al je wijze woorden. Bij Gert-Jan ben ik vaak langs geweest voor advies of om samen experimentele resultaten te bespreken. Bedankt dat je deur altijd open stond en het feit dat je een andere wetenschappelijke achtergrond hebt, heeft vaak tot andere, zeer nuttige inzichten geleid.

Natuurlijk wil ik ook mijn studenten bedanken: Adeline Cognard, Stephanie Tournie, Wilco Faber, Tineke van der Brink en Lucy Tosh thank you for your interest and effort in the project. Your input, energy and questions helped me a lot in completing this thesis.

Alle Wetsus promovendi komen uit alle hoeken van het land en zelfs alle hoeken van de wereld, samen in Leeuwarden. Omdat we allemaal in hetzelfde schuitje zaten en veel met elkaar optrokken, krijg je automatisch een hechte band met je collega's. Ronald, Guillo, Ellen, Rene, Maxime en Perry, bedankt dat jullie het begin bij Wetsus zo gemakkelijk hebben gemaakt.

In het begin (september 2004) stond er nog helemaal niets bij Wetsus. Bob, Janneke en Jelmer, jullie hebben het lab fantastisch opgebouwd. Het is een ongelofelijke luxe dat we zoveel verschillende analyses kunnen laten doen. Wim, Harry en Harm, jullie hebben de experimenteerhal, de werkplaats en nog zoveel meer geweldig opgebouwd. Mijn dag begon ook altijd met een bakkie koffie om acht uur met de mannen, dat was altijd een goed begin van de dag. Mannen, ik was echt niet degene die altijd met vieze praat begon, hoor!

Ik heb Wetsus mogen zien groeien van 6 promovendi naar de 37. Ik ben ontzettend trots op iedereen die daarbij heeft geholpen. Cees Buisman en Johannes Boonstra, ik heb veel respect voor jullie, zoals jullie Wetsus hebben doen groeien tot een "Centre of Excellence". Ik zal Wetsus met zeer veel interesse blijven volgen: op naar Europa!

Gelukkig was er ook veel tijd voor ontspanning. De grappen en grollen in het lab, het hooghouden met de bal (zie de Wereld Draait Door), meidenavondjes, Sinterklaas, films, stappen en nog veel meer, ik heb er enorm van genoten. Veronique en Marthe, ik heb altijd zo ontzettend genoten van onze fietstochten door het prachtige Friese land. Petra en Rene, ik heb weer wat tips en tricks (nodig), wanneer gaan we weer eten? Rene, in het begin mijn steun en toeverlaat, kom maar weer terug uit Australië, want we missen je hier. Bas, Meike, Leontien en Josephine het was altijd heerlijk thuiskomen bij jullie. Het spelen met de meiden, lekker eten en de gezelligheid heeft de tijd in Leeuwarden mede tot een heerlijke tijd gemaakt.

Zullen ze deze herriemaker wel gaan missen in het kantoor? Ingo en Bart bedankt voor de discussies over het modelleren (fijn dat ik soms even kon nerden met jullie), Sandra bedankt voor je advies over de Engelse taal en de gezellig momentjes op kantoor. Een andere kamergenoot op afstand Paul Willems, bedankt dat je me hebt geholpen met het modelleren en het nalezen van hoofdstukken en papers. Goed voorbeeld doet goed volgen, zullen we maar zeggen! Ik ben ontzettend blij dat jij en Alisia bij mijn promotie aanwezig zullen zijn.

Ik ben heel blij en trots dat ik twee geweldige paranimfen naast me heb staan. Petra, thanks for your incredible friendship, your friendship is very rare and it is really precious to me. Adriaan mijn idool op de saxofoon, ik hoop dat ik later net zo weg kan toeteren als jij. Bedankt voor jouw bijzondere vriendschap. Helena bedankt voor de avondjes samen eten, met wie moet ik nu lekker chillen, ff rustig aan doen en de dag doornemen? Paula, jij was een van de mensen die veel van de uitjes (werk gerelateerd en niet-werk gerelateerd) regelde, bedankt daarvoor en succes met het afronden van je promotie. Piotr, thanks for your smile and jokes to cheer me up. En natuurlijk onze Wetsus band: Loes, Ingo, Bob, Jelmer, Marthe, Luewton, Adriaan en Johannes jullie

hebben me gewoon weer aan het dwarsfluiten gekregen! Dat is wel een ontzettend wonder na al die jaren. Ik heb ontzettend genoten van jullie muzikale talent en ik hoop dat de band nog lang mag bestaan.

Wetsus is zo ontzettend gegroeid: Ludmila, Hans, Astrid, Tom, Jan, Joost, Nienke, Agatha, Martijn, Tim, Phillip, Lucia, Kamuran, Elsemiek, Luciaan, Marko, Urania, Geke, Trienke, Nynke, Linda, Aleid, Martijn, Nelleke, Heleen, Hester, Hellen, Ime, Maarten, Arie, Sybrand, Mateo, Jos, Jan M., Jan de G., Agatha en Albert. Ik wens jullie allemaal veel succes en plezier en voor de promovendi veel succes met afronden van je promotie!

Ook kan ik natuurlijk de groep in Eindhoven niet vergeten, Marjet en Ferdy bedankt dat jullie van mijn bezoeken in Enschede en Eindhoven altijd een thuiskomst hebben gemaakt. Alle mensen van de Separation Technolgy Group in Enschede en de Process Systems Engineering in Eindhoven, ook al zat ik op afstand, bedankt voor jullie gastvrijheid tijdens mijn bezoeken.

Wie had ooit gedacht dat ik dit allemaal zou schrijven, dat ik mijn proefschrift heb afgerond? Lieve pap, mam en Galina, ik kan hier geen woorden schrijven die mijn dankbaarheid helemaal beschrijft. Bedankt voor jullie steun, jullie geloof in mij door alle jaren heen, want de basis ligt al veel langer terug. Lieve Tim, ik heb je van tevoren gewaarschuwd, een relatie met een promovendus in haar laatste jaar valt niet mee. Maar met jouw liefde, geduld en relatieveringsvermogen heb je ons door deze tijd gesleept, bedankt!

Natasja

november 2008

List of publications

Schouten, N., van der Ham, A.G.J., Euverink, G.J., de Haan, A.B.
Adsorbent selection for the removal of anionic surfactants from laundry rinsing water (2006) Proceedings of 2nd International conference on Environmental Science and Technology (ICEST2006) held in Houston in August 2006
ISBN 0-9768853-6-0 © 2006 American Science Press, Volume 1, Pages 308-312

Schouten, N., van der Ham, A.G.J., Euverink, G.J., de Haan, A.B.
Selection and evaluation of adsorbents for the removal of anionic surfactants from laundry rinsing water
(2007) Water Research, 41, Pages 4233-4241

Schouten, N., van der Ham, A.G.J., Euverink, G.J., de Haan, A.B.
Optimization of layered double hydroxide stability and adsorption capacity for anionic surfactants
(2007) Adsorption, 13, Pages 523-532

Schouten, N., van der Ham, A.G.J., Euverink, G.J., de Haan, A.B.
Kinetic analysis of anionic surfactant (LAS) adsorption from aqueous solution onto activated carbon and layered double hydroxide with the zero length column method
(2008) Separation and Purification Technology, *Submitted*

Schouten, N., van der Ham, A.G.J., Euverink, G.J., de Haan, A.B.
Re-use of laundry rinsing water in India
(2008) NPT Procestechnologie, 4, September 2008 Pages 38-39

About the author

Natasja Schouten was born 20th of September 1980 in Amsterdam, the Netherlands. After finishing secondary school (HAVO) at the Alkwin College in Uithoorn in 1997, she studied Chemical Engineering at the Hogeschool van Amsterdam. She finished her bachelor degree in 2001 and subsequently started her Master degree at the University of Twente in Enschede, both degrees are specialized in Process Technology. Her graduation took place at the Separation Technology Group of prof. dr. ir. André de Haan on "Expression of Oilseeds" and she finished her graduation in June 2004. In September 2004, Natasja joined Wetsus, Centre of Excellence for Sustainable Water Technology and worked on the project "Re-use of laundry rinsing water by low cost adsorption technology" under supervision of prof. dr. ir. André de Haan at the Separation Technology group, University of Twente and the Process Systems Engineering group, Eindhoven University of Technology. She completed her thesis in September 2008 and will defend her thesis in February 2009. She started working as a Researcher Iron Making at Corus R&D, IJmuiden from October 2008.